

University of Groningen

Biobased furanics from sugars

Soetedjo, Jenny Novianti Muliarahayu

IMPORTANT NOTE: You are advised to consult the publisher's version (publisher's PDF) if you wish to cite from it. Please check the document version below.

Document Version

Publisher's PDF, also known as Version of record

Publication date:

2017

[Link to publication in University of Groningen/UMCG research database](#)

Citation for published version (APA):

Soetedjo, J. N. M. (2017). *Biobased furanics from sugars*. [Thesis fully internal (DIV), University of Groningen]. University of Groningen.

Copyright

Other than for strictly personal use, it is not permitted to download or to forward/distribute the text or part of it without the consent of the author(s) and/or copyright holder(s), unless the work is under an open content license (like Creative Commons).

The publication may also be distributed here under the terms of Article 25fa of the Dutch Copyright Act, indicated by the "Taverne" license. More information can be found on the University of Groningen website: <https://www.rug.nl/library/open-access/self-archiving-pure/taverne-amendment>.

Take-down policy

If you believe that this document breaches copyright please contact us providing details, and we will remove access to the work immediately and investigate your claim.

Downloaded from the University of Groningen/UMCG research database (Pure): <http://www.rug.nl/research/portal>. For technical reasons the number of authors shown on this cover page is limited to 10 maximum.

BIOBASED FURANICS FROM SUGARS

Jenny Novianti Muliarahayu Tan-Soetedjo

Biobased Furanics from Sugars

Jenny Novianti Muliarahayu Tan-Soetedjo

Doctoral thesis
University of Groningen
The Netherlands

The work described in this dissertation was conducted at the Department of Chemical Engineering of the University of Groningen.

This doctoral project was financially supported by the Directorate General of Higher Education of the Republic of Indonesia and Parahyangan Catholic University, Bandung, Indonesia.

Cover design, layout and printing by  Lovebird design.
www.lovebird-design.com

ISBN: 978-94-034-0150-8

ISBN: 978-94-034-0149-2 (electronic version)



university of
 groningen

Biobased Furanics from Sugars

PhD thesis

to obtain the degree of PhD at the
University of Groningen
on the authority of the
Rector Magnificus Prof. E. Sterken
and in accordance with
the decision by the College of Deans.

This thesis will be defended in public on

Friday 8 December 2017 at 09.00 hours

by

Jenny Novianti Muliarahayu Soetedjo

born on 22 November 1978
in Bandung, Indonesia

Supervisor

Prof. H. J. Heeres

Assessment committee

Prof. A.A. Broekhuis

Prof. F. Picchioni

Prof. A.M. Raspolli Galletti

**Dedicated to my beloved:
parents and husband**

*After climbing a great hill,
one only finds that there are many more hills to climb.*
(Nelson Mandela)

TABLE OF CONTENTS

Chapter 1	Introduction	1
Chapter 2	Experimental and Kinetic Modeling Studies on the Conversion of Sucrose to Levulinic Acid and 5-Hydroxymethylfurfural using Sulphuric Acid in Water	39
Chapter 3	Reactivity studies on the acid-catalysed dehydration of 2-ketohexoses to 5-hydroxymethylfurfural in water	73
Chapter 4	Biobased Furanics: Kinetic Studies on the Acid Catalysed Decomposition of 2-Hydroxyacetyl Furan in Water using Brønsted Acid Catalysts	91
Chapter 5	Remarkable Solvent Effects on The Dehydration of Xylose to Furfural in Ethanol/Water Mixtures Using Homogeneous and Heterogeneous Brønsted Acid Catalysts	117
	Summary	155
	Samenvatting	161
	Acknowledgements	165
	List of Publications	169



CHAPTER 1.

Introduction



1. GENERAL OVERVIEW ON RENEWABLES AND BIOMASS

The search for techno-economically viable renewable resources for heat and power generation, transportation fuels and chemicals is ongoing since the early 1970's and impressive results have been obtained¹. Major drivers for these developments are the projected increase in the world energy consumption and the negative effects associated with the use of fossil resources. According to the International Energy Outlook 2016, the total world energy consumption will increase by 48% in the period of 2012 to 2040². Renewables including solar, wind, wave, tidal, geothermal, hydropower and biomass are among the fastest growing source with an average annual increase of 2.6% (Figure 1).

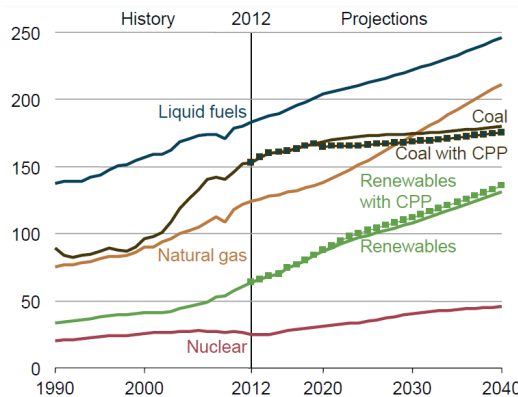


Figure 1. World energy consumption by source (in quadrillion Btu), taken from [2] with permission; dotted lines for coal and renewables show projected effects of the U.S. Clean Power Plan

For electricity generation, 5.9 trillion kWh of new renewables is projected in 2040, with hydropower and wind contributing each for 1.9 trillion kWh (33%), solar energy for 859 billion kWh (15%), and other renewables (mostly biomass and waste) for 856 billion kWh (14%) (Figure 2). In fact, for the industrial sector, biomass currently provides most of the renewable energy (excluding hydroelectricity) and is projected to do so until 2040.

Biomass is a special renewable resource. Among the renewable resources, it is the only carbon-based one. As such, it is expected to play a major role in

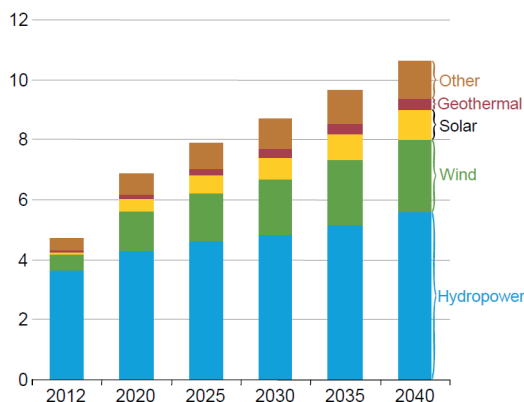


Figure 2. World electricity generation from renewables (trillion kilowatthours), taken from [2] with permission; other resources include biomass, waste and energy from tide/wave/ocean

the future transporation sector, and particularly for aviation and long range heavy weight land transportation, as well as for the chemical industry to make for instance carbon based polymers³.

2. BIOMASS: DEFINITIONS, COMPOSITION AND SOURCES

Biomass is defined as “any organic matter that is available on a renewable basis, including dedicated energy crops and trees, agricultural food and feed crop residues, aquatic plants, wood and wood residues, animal wastes and other waste materials”³. Biomass is abundantly available on earth with an estimated potential of $170\text{--}200 \times 10^9$ MT on annual basis¹. Biomass typically consists of lipids (fats, waxes, oils), carbohydrates (starch, cellulose, and hemicellulose), proteins, lignin (an aromatic rich thermoset) beside a large number of minor constituents (vitamins, dyes, flavors and aromatic essences)³, see Figure 3 for details.

Particularly the use of lignocellulosic biomass is currently receiving high attention. Examples of lignocellulosic biomass are wood, straw and grasses. From a chemical point of view, lignocellulosic biomass consists mainly of cellulose, hemicellulose and lignin with small amount of proteins and ash. The actual composition is a function of the biomass source, see Table 1 for details.

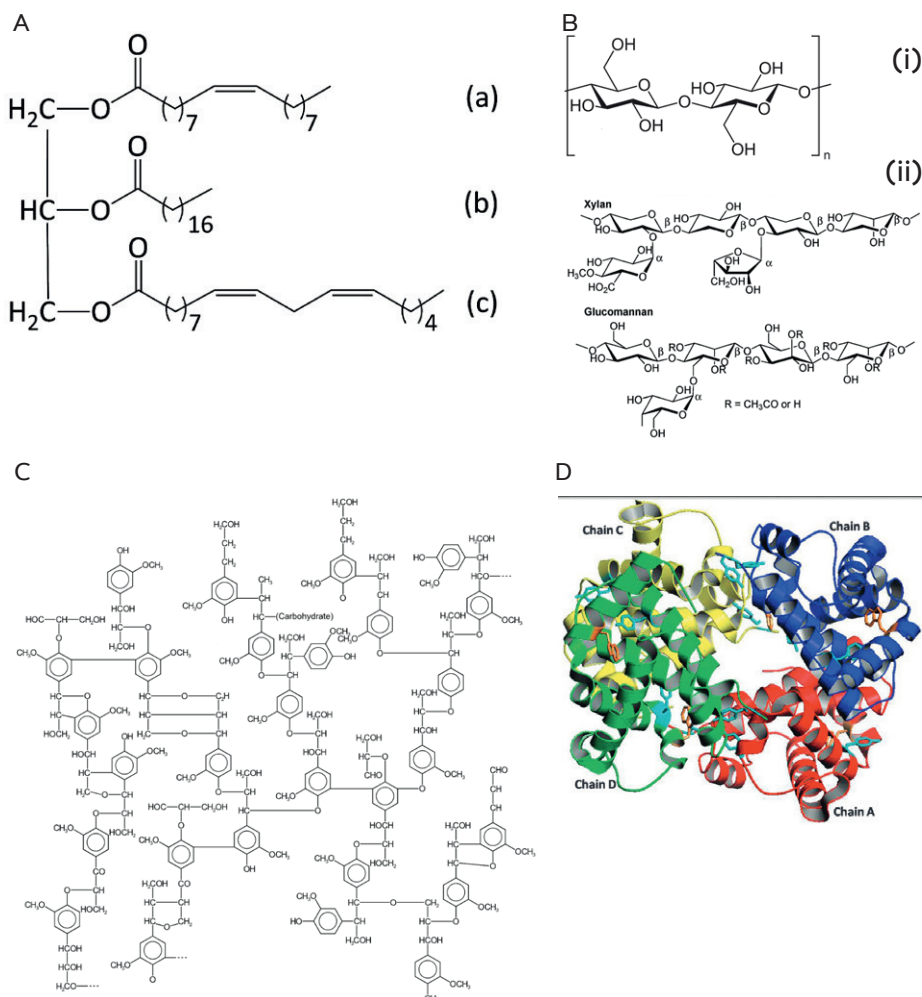


Figure 3. Representative structures of biomass fractions A. Lipids: (a) oleate, (b) stearate and (c) linoleate; B. (i) cellulose [4] and (ii) hemicellulose [5]; C. lignin [6] and D. proteins [7]. All images are reproduced with permission.

Table 1. The composition of several lignocellulosic feedstocks

Source	Composition (weight-%)				Ref
	Cellulose	Hemi-cellulose	Lignin	Ash	
<i>Miscanthus giganteus</i> (perennial grass)	37–45	17–21	19–25	1–3	8
Pine (softwood tree)	25–42	18–26	21–30	0.3–2	8
Poplar (hardwood tree)	4–55	18–25	24–40	1–4	8
<i>Agave tequilana</i> (arid climate succulent)	31–55	7–12	8–17	3–7	8
Corn stover	37–42	20–28	18–22	n.d.	9
Sugarcane bagasse	26–50	24–34	10–26	n.d.	9
Wheat straw	31–44	22–24	16–24	n.d.	9
Hardwood stems	40–45	18–40	18–28	n.d.	9
Softwood stems	34–50	21–35	28–35	n.d.	9
Rice straw	32–41	15–24	10–18	n.d.	9
Barley straw	33–40	20–35	8–17	n.d.	9
Switch grass	33–46	22–32	12–23	n.d.	9
Energy crops	43–45	24–31	19–12	n.d.	9
Grasses (average) e.g. reed canary grass, smooth brome grass, tall fescue etc.	25–40	25–50	10–30	n.d.	9
Manure solid fibers	8–27	12–22	2–13	n.d.	9
Municipal organic waste	21–64	5–22	3–28	n.d.	9

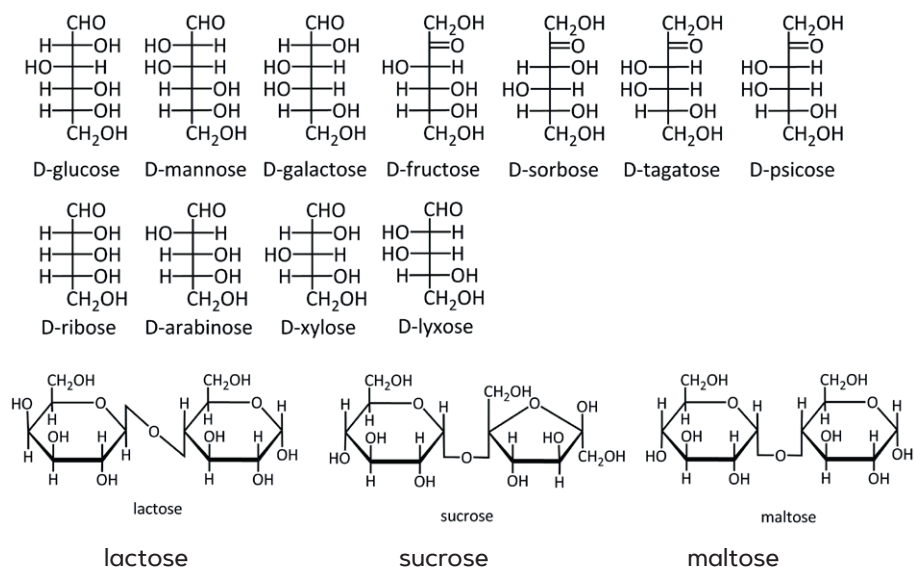


Figure 4. Structures of C5 and C6 sugar building blocks from carbohydrates

Cellulose and starch are composed of glucose, whereas the sugars in the hemicellulose fraction are more diverse and consist of a both C6 and C5 sugars (pentoses). Examples of sugars present in biomass are given in Figure 4. The molecular structure of lignin is complex and diverse, see Figure 3 for details. It is a thermoset and consists of (substituted) aromatic rings connected with various types of linkages.

Possible chemicals and materials derived from the major lignocellulosic biomass constituent are presented in Table 2.

Table 2. Potential chemicals and materials derived from the main ligno-cellulosic biomass constituents [10]

Feedstock	Building block chemicals	Performance materials
Lipids	fatty- acids, esters, alcohols and amines, epoxide, polyols, α -olefins, diacids, hydro-carbons	surfactants, lubricants, hydraulic fluids, fabric softeners
Carbohydrates	succinic acid, furanics, hydroxypropionic acid, glycerol, sorbitol, xylitol, levulinic acid, biohydro-carbons, lactic acid, ethanol, butanol	starch esters and esters for thickeners, suspension agents, protective colloids, building and packaging materials. Cellulose ethers for films and fiber materials, coatings, oil-well drilling muds, paints, detergents, adhesives. Cellulosic nanomaterials and composites for fiber reinforcements, packaging materials, optically transparent materials for electronic devices.
Lignin	aromatics (BTX, styrene), benzoic acid, phenolics, cyclo-hexane, isophthalic acid	lignosulphonates, road-dust suppressants, pellet binders, rubber formulations
Proteins	styrene, isobutyraldehyde, caprolactam	adhesives, coatings, surfactants

3. BIOREFINING AND CASCADING

3.1 Biorefining

Biorefining is defined as “the sustainable and integrated processing of low-value biomass into marketable products (energy, fuels, chemicals, materials) using optimum resources with minimum use of energy and low amounts of waste”^{11,12}. In biorefineries, various processes are coupled to convert biomass feeds into industrial intermediates and final products (Figure 5).

In fact, the biorefinery concept is comparable to today’s crude oil refineries, the only difference being the feedstock of the refinery (biomass versus fossil resources). Kamm et al.¹³ have classified biorefineries into four categories i.e. the whole crop biorefinery (WC-BR), the green biorefinery (G-BR), the lignocellulose feedstock biorefinery (LCF-BR), and the two platform concept as shown in Figure 6.

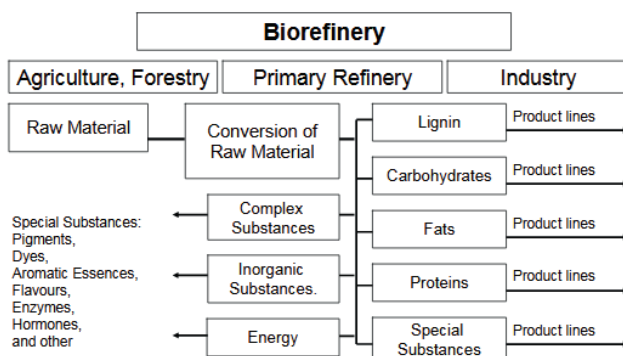


Figure 5. General overview of the biorefinery principle [3]

3.2 The Biomass Value Pyramid

The main products of biorefineries are energy, transportation fuels and biobased products. An essential question is the choice of the optimal product slate of a biorefinery. Should the focus be on energy only, or solely on biobased chemicals? In this respect, it is useful to consider the biomass value pyramid (Figure 7). It classifies the possible product classes into value and volume, with high value low volume products at the top and low value, high volume products at the base of the pyramid. As such, several different product classes can be categorised, from heat and power generation at the base to pharmaceutical products at the top¹⁴. When considering that the total amount of biomass generated on earth is not sufficient for the global heat and power demand as well as for all transportation fuels, it is best to use the biomass for particularly high value, low volume applications. As such, the use of biomass for the production of biobased chemicals is of high interest, also considering the fact that biomass is the only renewable resources containing carbon.

4. BIOBASED CHEMICALS

4.1 Biomass Value Chains

A number of approaches can be discriminated when aiming for biobased chemicals from biomass. The first involves slight modification of natural biopolymers (starch, cellulose, lignin etc.) with minimum molecular

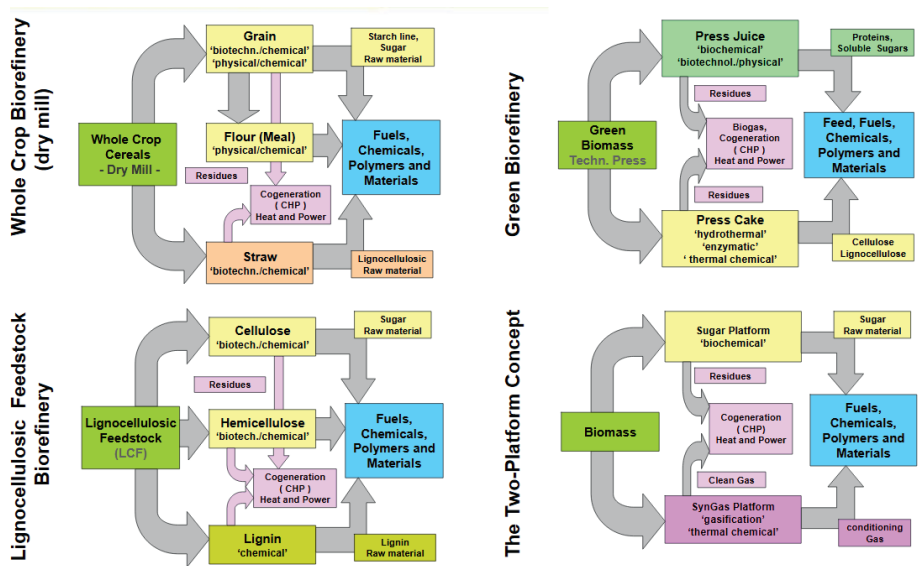


Figure 6. Examples of biorefinery concepts. Reproduced with permission from [13].

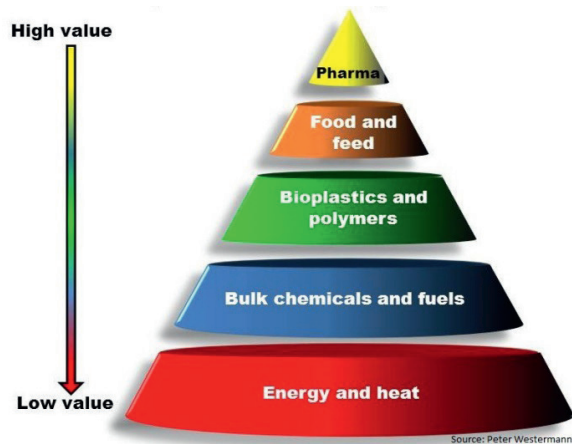


Figure 7. Value pyramid for biomass, taken from [14] with permission

weights reduction, for instance starch modification by chemical reactions like acetylation, carboxymethylation, to produce high added value end-products such as oil recovery chemicals, additives and biodegradable plastics¹⁵. The second approach applies the concept of the so called “platform

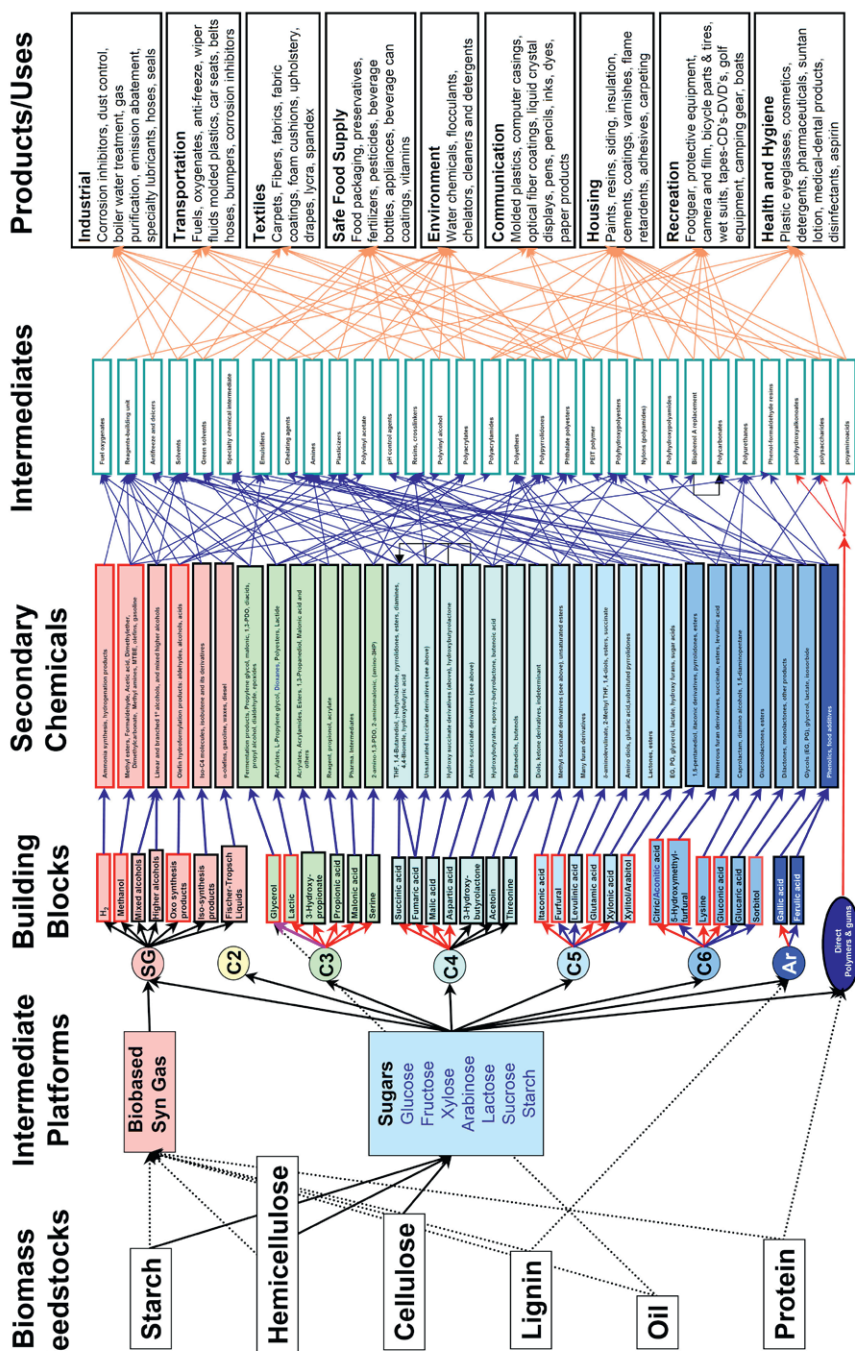
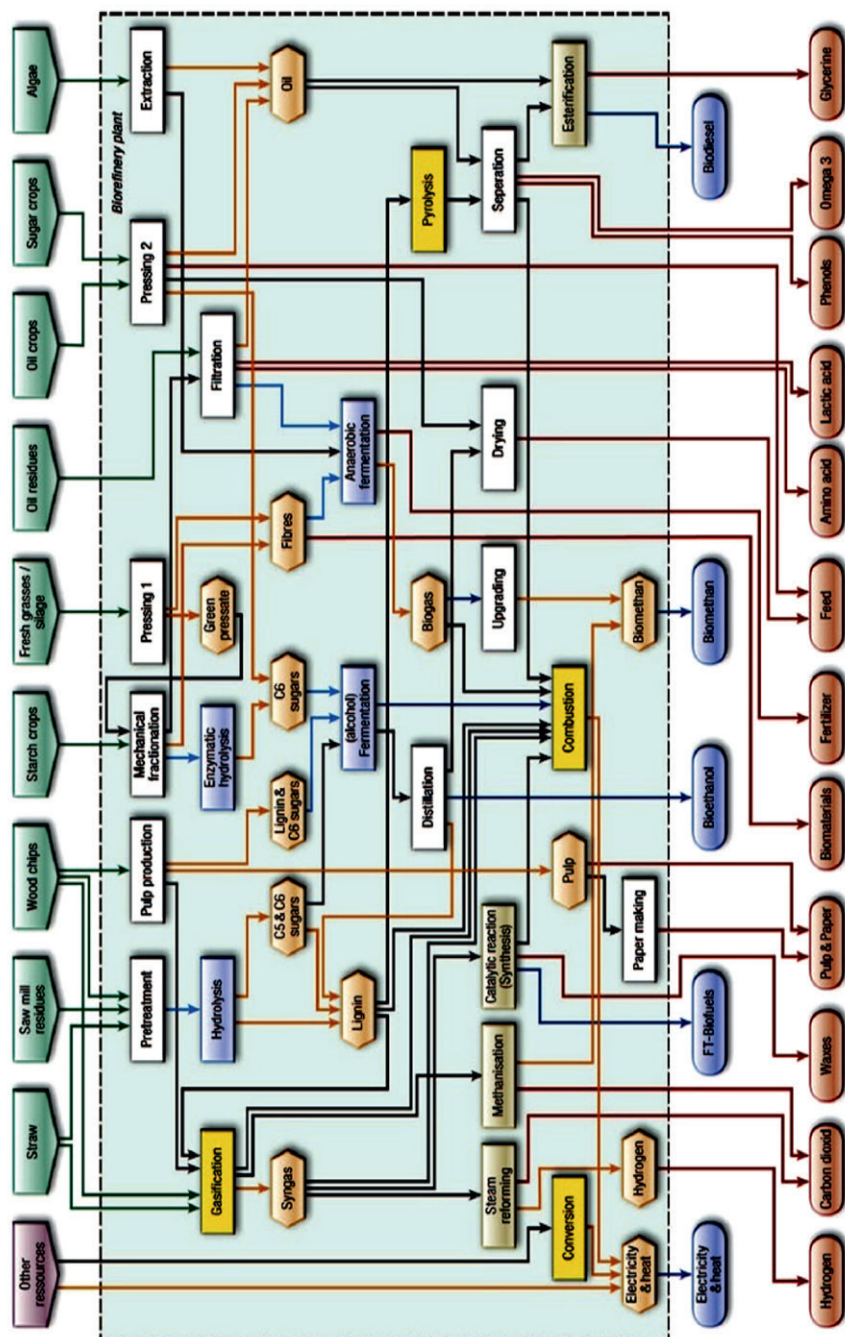


Figure 8. Platform chemicals from several biomass resources [16].



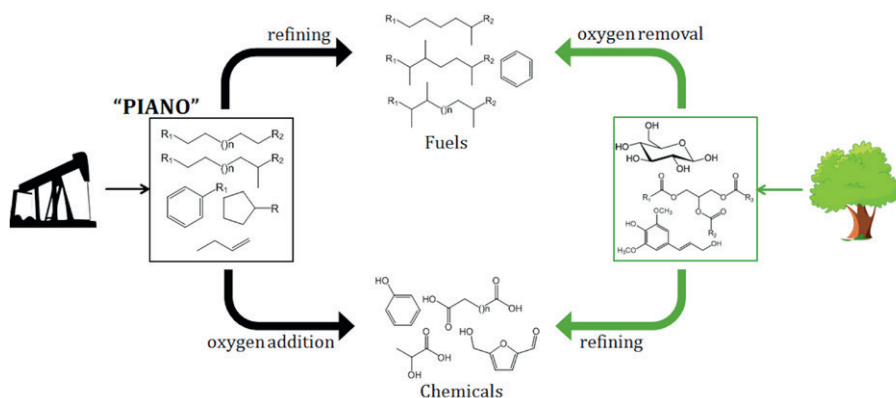


Figure 10. Similarities between petroleum and biorefinery, courtesy of Louis Daniel [17]

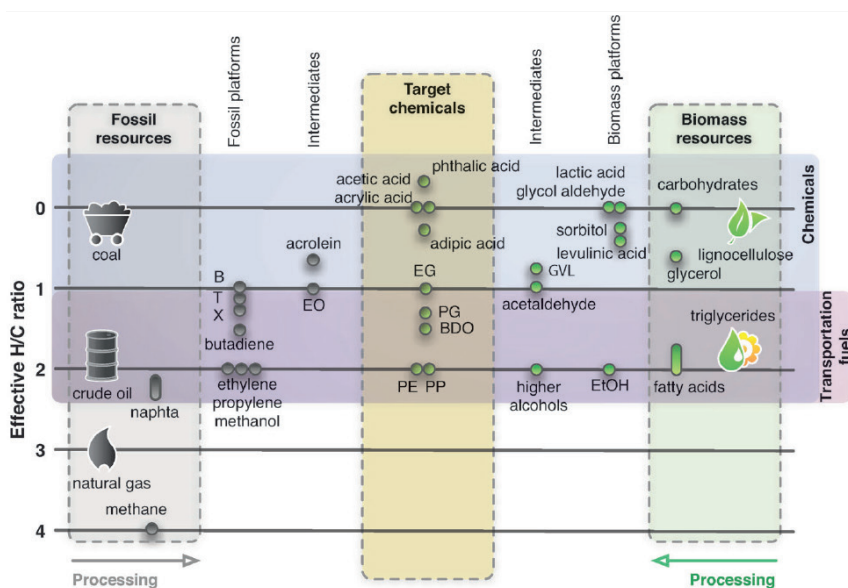


Figure 11. Effective H/C ratio map of current and future bulk chemicals as well as feedstocks with a qualitative indication of the degree of processing. B = benzene, BDO = 1,4-butanediol, EG = ethylene glycol, EO = ethylene oxide, GVL = g-valerolactone, PE = polyethylene, PG = propylene glycol, PP = polypropylene, T = toluene, X = xylenes, taken from [18] with permission

chemicals”, which involves breakdown of the biopolymers to low molecular weight building blocks (platform chemicals) for further conversion and usage, see Figure 8 for details.

A wide range of biobased chemicals and products can be made from biomass. A number of studies have been performed with the objective to categorize the various biomass value chains. Typical examples are given in Figure 8 and Figure 9¹⁶. Werpy et al.¹⁶ considered six biomass feedstocks i.e. starch, hemicellulose, cellulose, lignin, oil, and protein, and used these as input for two intermediate platforms (biobased syn gas and sugars, see Figure 8). These platforms generate building block chemicals that can be converted to secondary chemicals and/or intermediates followed by their use in complex products.

In 2008, the IEA Bioenergy Task 42 also investigated various biomass value chains, see Figure 9 for details¹².

4.2 Biomass versus Fossil Resources

The chemical composition of biomass and particularly lignocellulosic biomass differ considerably from fossil resources. For instance, crude oil consists (mainly) of hydrocarbons like paraffins, naphthenes and aromatics, which have a low oxygen content, high energy density, limited number of functional groups and high thermal stability. On the other hand, lignocellulosic biomass consists of carbohydrates and lignin which have many different functional groups. As such, biomass is more oxygenated than fossil resources¹¹.

However, when considering biobased chemicals, the presence of bound oxygen is not necessary a disadvantage for the use of biomass for chemical products. Most of the carbon-based intermediates in the petrochemical industry are actually oxygenated, see Figure 10 for details. As such, fossil resources need to be oxidised, which is not necessary when using biomass. This is also supported by an extensive study by Vennestrom et al.¹⁸, see Figure 11 for details.

An example why biomass is a better feedstock for (oxygenated) chemicals production than hydrocarbon feeds is given in Figure 12. It shows the comparison in synthesis pathway of terephthalic acid (TPA, $C_8H_6O_4$) between sugar conversion routes ($C_6H_{12}O_6$) via oxygenates such as 5-Hydroxymethylfurfural (HMF, $C_6H_6O_3$) or 2,5-Furandicarboxylic acid (FDCA, $C_6H_4O_5$) and conventional petroleum routes with para-xylene (pX, C_8H_{10}) as intermediate. The graph shows the number of carbon and oxygen in the feedstock, intermediate

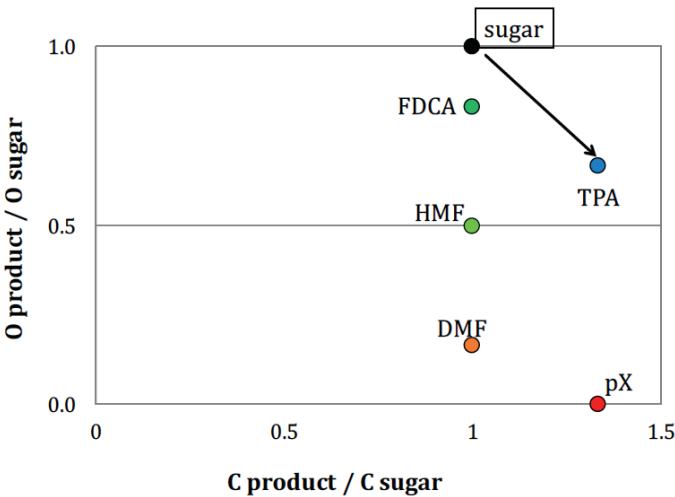


Figure 12. Comparison of the number of carbon and oxygen in feedstock, intermediate products and final product for the synthesis of TPA from sugar, courtesy of Louis Daniel [17]



Figure 13. An overview of current and planned biobased product facilities in the United States in 2016, taken from [24] with permission

products, and the final products. When using sugars as the feed, the production of TPA via HMF and FDCA proceeds a shorter route compared to pX. In fact, the latter is produced by a complete oxygen removal while adding carbons through conventional petroleum route which then later needed to be subsequently oxidised all the way to produce TPA. The difference in process efficiency resulted in the difference on yield gained from each pathway. The theoretical pX and TPA yields of the conventional route, following five steps using naphta as the feedstock, range in between 32–62%^{19,20} and 30–58%^{21,22}, respectively, depending on the reaction routes chosen. Meanwhile, the theoretical TPA yield for the former process (via HMF and FDCA), following only four steps using sugars as the feedstock, reaches up to 61%²².

4.3 Commercial Status of Biobased Products: Examples

A number of processes for biobased chemicals have been commercialised in the last decade. An example is polyethylene furanoate (PEF), a biomass-derived polymer which is aimed to replace polyethylene terephthalate (PET), due to its better gas barrier performance compared to PET²³. Some other examples of (close to) commercial processes for biobased chemicals are²⁴:

- Genomatica: biobased 1,4-butanediol from lignocellulosic sugars
- INVISTA and LanzaTech: fermentation of syngas to 2,3-butanediol
- A number of companies: furfural from bagasse and cobs.
- Archer Daniels Midland (ADM) and others: glycerol from natural lipids.
- Amyris (expected): bio-isoprene from sugarcane.
- NatureWorks and Purac: lactic acid from biomass.
- Cellulac: lactic acid and ethyl lactate from agricultural residues.
- BioAmber with licensing agreements from Cargill: adoption of yeast microorganism to utilize a range of lignocellulosic feedstocks.
- Anellotech: renewable para-xylene via a thermochemical catalytic fast pyrolysis route which can utilize a range of cellulosic convertible feedstocks.

An overview of recently commercially introduced biobased chemicals in the United States is given in Figure 13.

5. PLATFORM CHEMICALS

5.1. Definition of Platform Chemicals

Platform chemicals are defined as “building blocks which can be converted to a wide range of chemicals or materials”²⁵. Biobased platform chemicals offer great potential to produce everyday products, from clothes to plastics and car parts, in a green and sustainable manner. In 2004, the US National Renewable Energy Laboratory issued a list of top 12 value added chemicals derived from carbohydrates¹⁶. In 2010, a new list was published with some changes compared to the original list¹⁰. Recently, an updated list was issued, with the technology readiness level (TRL) as a major selection criterium. As such, biohydrocarbons like 1,3-butadiene, p-xylene, and isoprene, all existing petrochemicals produced in large quantities, are more prominently present. Moreover, fatty alcohols, also existing biobased products derived from natural oils and fats are added to the list. An overview of the various top platform chemicals lists is given in Table 3.

The estimated price and volumes of the emerging near term deployment of biobased chemicals is presented in Table 4. *para*-Xylene is considered a very attractive option, both when considering volume and price levels.

Table 3. Top platform chemicals from biomass published in the period of 2004–2016

Top 12 platform chemicals from carbohydrates — original list, data 2004 ¹⁶	Top 12 revisited, data 2010 ¹⁰	Emerging near-term deployment biobased chemicals, data 2016 ²⁴
1,4-diacids (succinic, fumaric, malic)	Succinic acid	Succinic acid
2,5-furan dicarboxylic acid	Furanics	Furfural
3-hydroxy propionic acid	Hydroxy propionic acid / aldehyde	(1,3-) Propanediol
Glycerol	Glycerol and derivatives	Glycerol
Sorbitol	Sorbitol	1,4-butanediol
Xylitol/arabinitol	Xylitol	1,3-butadiene
Levulinic acid	Levulinic acid	Propylene glycol
Aspartic acid	Lactic acid	Lactic acid
Glucaric acid	Biohydrocarbons	Ethyl lactate
Glutamic acid	Ethanol	(para-) Xylene
Itaconic acid	-	Isoprene
3-hydroxy butyrolactone	-	Fatty alcohols

Table 4. Estimated price and volumes of the emerging near-term deployment biobased chemicals

Product	Price (\$/t)	Volume (ktpa)	Sales (m\$/y)	% of total existing market	Year	Ref
Furfural	1,000–1,450	300–700	300–1,015	assumed 100%	2013–2014	26
Succinic acid	2,940	38	111	49%		
Lactic acid	1,450	472	684	100%		
1,3-propanediol		60	157	n.a.	2012	27
		150	560		2019	
glycerol	500	1,200	600	88%	2010	28
1,4-butanediol	2,100–2,300	>2,360	5,000–5,500	n.a.	2012	29
1,3-butadiene	1300–1578 ^a	10,200		n.a.	2010	30 ^a
					2017 ^a	31
Propylene glycol	1500–2000 ^b	2180		n.a.	2013	32 ^b
					2014 ^b	33
Ethyl lactate	2000–3750	3500–4500		n.a.	2017	34
pX	1,300	30,000	39,000	n.a.	2010	35
(para-xylene)	2,035	57,000	116,000	n.a.	2020	
Isoprene		>1,000	4,000	n.a.	2014	36
Fatty alcohols		2,200		assumed 100%	2012	37

6. PLATFORM CHEMICALS: FURANICS (FURFURAL, 5-HYDROXYMETHYLFURFURAL) AND LA

6.1 Potential of Furanics (Furfural, HMF) and LA to Replace Fossil-Based Chemicals

Lignocellulosic biomass is a very important resource for the production of chemicals and materials. From the carbohydrates fraction, three important platform chemicals can be obtained using chemo-catalytic methodologies, viz. furfural (FF), 5-hydroxymethylfurfural (5-HMF), and levulinic acid (LA, Figure 14). This has led to a high research interest in the last 15 years, expressed by an exponential increase in publications in peer reviewed journals³⁸.

Furfural

Furfural or furan-2-carbaldehyde (FF), for the first time isolated by Doebernier in 1821³⁹, is an important commercially available renewable, non-petroleum

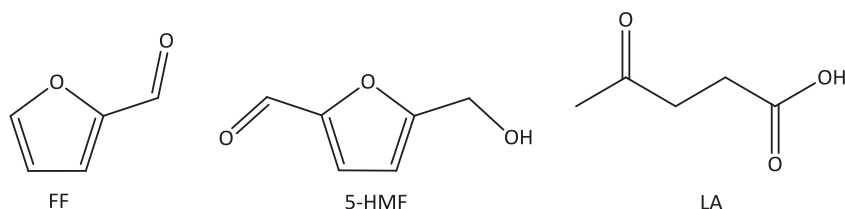


Figure 14. Molecular structure of furfural (FF), 5-hydroxymethylfurfural (5-HMF), and levulinic acid (LA)

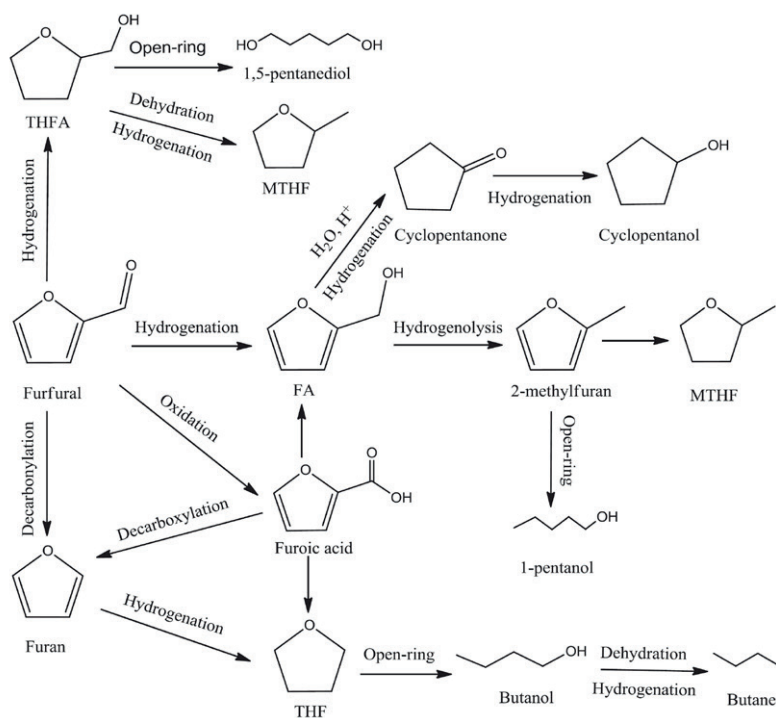


Figure 15. Potential of FF for the production of chemicals and fuels, taken from [46] with permission

based chemical building block and used for the production of amongst others furfuryl alcohol, furoic acid and furans^{39–44}.

Furfural has been produced commercially since the 1920s^{43,44}. It is formed by the conversion of the C5 sugars (mainly xylose) present in the biomass feed. Sugarcane bagasse and corncobs are typically used as the biomass feed.

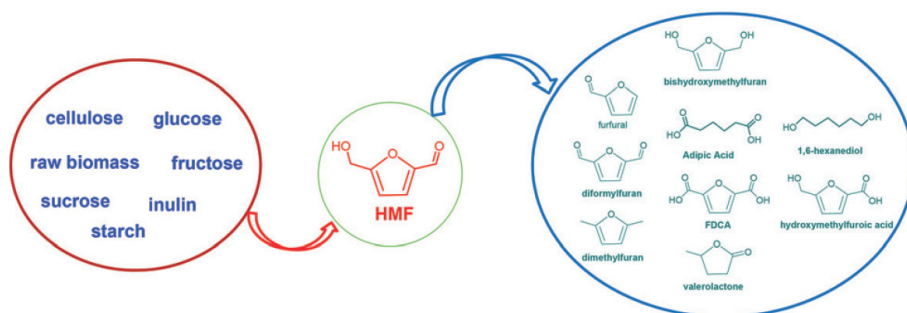


Figure 16. 5-HMF as an important biomass derivative for various chemicals, taken from [48] with permission

The global production capacity was about 800,000 tons in 2012, mainly in South Africa and the Dominican Republic⁹. A number of process concepts have been commercialised (Quacker, Agrifurane, Rosenlew, Escher Wyss), though all suffer from relatively low FF yields (50% range)⁴⁴.

Recent studies have shown that the application range of FF can be extended considerably and new derivatives and outlets have been identified, see Figure 15 for details⁴⁵. As such, FF has been classified as a top 12 chemical from biomass¹⁰.

HMF

HMF (or 5-HMF) is considered a very versatile platform chemical and can be made from various carbohydrates and particularly from the C6 sugars. HMF yields are a strong function of the C6 sugar used and best results have been reported with ketohexoses like fructose and psicose⁴⁷. The yields from aldohexoses like glucose are by far lower and typically below 10 mol%.

Some important derivatives from 5-HMF with high application potential are provided in Figure 16⁴⁸. Well known examples are the conversion to 2,5-dimethylfuran (DMF), 2,5-furandicarboxylic acid (FDCA) and adipic acid. DMF is a promising biofuel (additive) which has an energy density 40% larger than ethanol⁴⁹. FDCA is an important polymer precursor for the production of polyethylenefuranoate (PEF). PEF is considered as a promising replacement for either petro- as well as biobased PET, which has a market of 22.26 MT/year in 2015 with a 6.1% projected yearly growth for the next 5 years⁵⁰. Adipic acid is

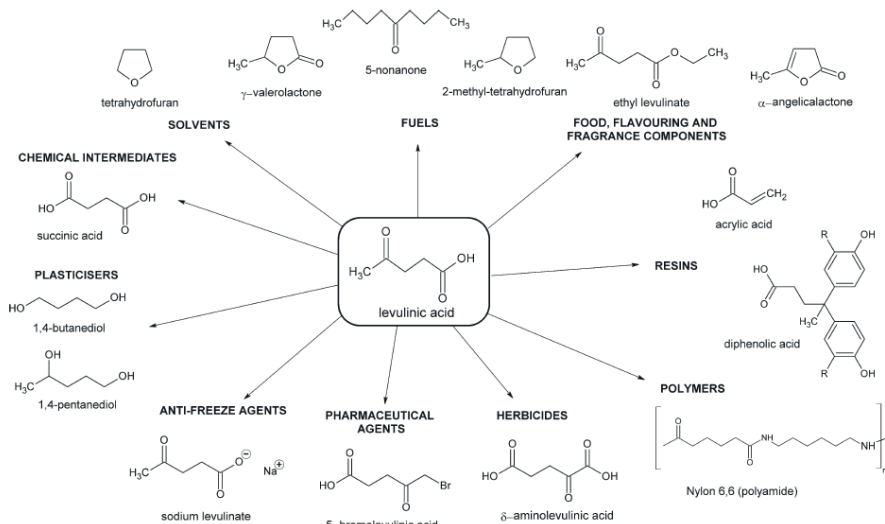


Figure 17. Overview of LA derivatives [57,65]

an existing petrochemical used for polyester production with a global market valued at 4.56 MT/year (2014) with a 4.4% projected growth per year between 2015–2022⁵¹.

Another important derivative is caprolactam which is used for over 98% of the total world production of nylon 6 fibers and nylon 6 resins⁵². The production of caprolactam was reported to be about 6.5 MT/year in 2015 with a projected annual 3% increase in demand⁵³.

Levulinic Acid

Levulinic acid (4-oxopentanoic acid, LA) is considered a very important biobased platform chemical with a wide derivatization and application range^{10,24,54}. It is accessible by the acid catalysed hydrolysis of the

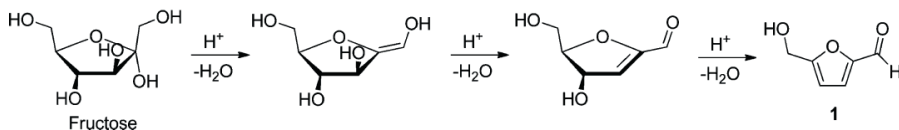


Figure 18. HMF synthesis from fructose

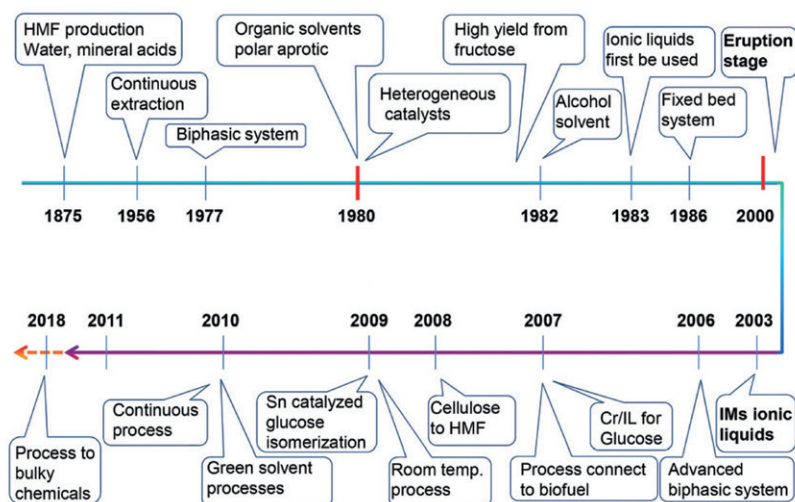


Figure 19. Landmarks in HMF synthesis, taken from [48] with permission

C6-sugars in various biomass sources^{55–65} and furfural when C5 sugars are present in the feed.

LA has high derivatization potential, see Figure 17 for details. Examples are γ -valerolactone (gVL), succinic acid, tetrahydrofuran (THF) and acrylic acid^{57,65}. GVL may be converted to bulk chemicals like methylpentenoates and adipic acid, as well as intermediates in fine chemicals synthesis and for fuel (additives)⁶⁶, commonly referred to as “valeric biofuels”⁶⁷.

6.2 Synthetic Methodology for Furfural, 5-hydroxymethyl-furfural, and Levulinic Acid

HMF Synthesis

HMF is typically obtained from fructose by an acid-catalysed dehydration (Figure 18). First reports on the synthesis of HMF already are from 1875⁴⁸, see Figure 19 for milestones in HMF synthesis. Various reviews on HMF synthesis have been published the last decade (see van Putten⁶⁸ and Teong⁴⁸). As such, only some highlights regarding 5-HMF synthesis will be given here.

HMF was produced by acid dehydration of sugar for the first time in 1875⁴⁸. Since then, the research and development in HMF production was in

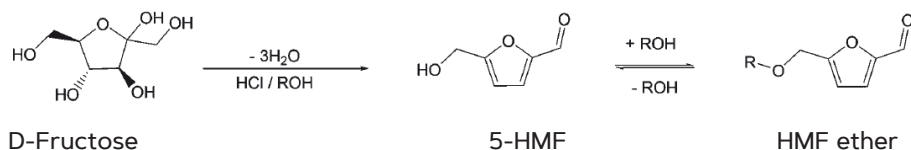


Figure 20. Production of HMF ether from fructose in alcohol media under acidic conditions

stagnancy and only focused on the mineral acid systems in aqueous solvent. It is well known that this system is unfavourable due to low selectivity to HMF as well as difficulties in product recovery from the solution. Typical yields of HMF were less than 50% from fructose^{48,68}. Later, it was demonstrated that HMF is unstable in water under acidic conditions to give solid product, recently known as humins, as byproduct.

To overcome this issue, Peniston developed a biphasic liquid-liquid system using *n*-butanol and water to transfer HMF from the aqueous to the organic phase once it is formed⁶⁹. Using this method, a HMF yield of 68% was obtained after 8 minutes at 170 °C. Later, in 1977, Kuster et al. employed a biphasic liquid-liquid system using water and methyl isobutyl ketone (MIBK) as solvents, and obtained 69% yield of HMF from 1 M fructose using 0.1 M H₃PO₄ as catalyst after 5 min at 190 °C⁷⁰. The use of organic solvents such as DMSO was also employed to give an HMF yield of 90% using a solid resin (Diaion PK-216) as the catalyst⁷¹. The development continued using ionic liquids as solvent and an HMF yield of 70% was obtained from fructose after 30 minutes at 120 °C⁷². The search for greener solvent with a lower boiling point than DMSO or ionic liquids led to the use of alcohol as solvent, and in 1982 Brown et al.⁷³ employed various alcohols such methanol, ethanol, iso-propanol and *n*-butanol as solvents for fructose dehydration. Under this condition, HMF is produced in the ether form, as shown in Figure 20. HMF ether yields of 19–55% were obtained after 20 h at 100 °C. Further, the biphasic liquid-liquid systems also continued to be developed, mostly are using a water-MIBK solvent combination and various solid acid catalysts in combination with a wide range of carbohydrate feedstocks. After 2000, major achievements were made by the Dumesic group, who studied biphasic liquid-liquid systems extensively using various solvents, homogeneous and heterogeneous catalysts, as well as the use of mineral salts^{74–78}.

Further advances in HMF synthesis are the large scale demonstration of HMF synthesis as well as its derivatives in a one-pot system and the use of

ionic liquids in combination with mineral salts as catalyst⁷⁹. Using [EMIM] Cl and CrCl₂ catalyst, a substantially higher yield of HMF was obtained from fructose and glucose, being 65% and 68%, respectively, after 3 h at 100 °C⁸⁰. Further improvement of HMF yields from fructose and glucose were obtained when the reactions were performed in imidazolium ionic liquid using chromium chloride catalysts in combination with N-heterocyclic carbene ligands. Using this system, HMF yields of 96% and 81% were obtained from fructose and glucose, respectively⁸¹. Since then, chromium-based catalysts, either as salts, nanoparticles, or other catalysts have been widely used in carbohydrates dehydration reactions, including polysaccharides such as pine wood, cellobiose, starch, and sucrose^{82–85}.

Conversion of C5 Sugars to Furfural

Furfural, also known as 2-furaldehyde or furfuraldehyde, is an important chemical derived from C5 sugars. It is the starting material for the production of important value-added chemicals such as 2-methylfuran, 2-methyltetrahydrofuran, furfuryl alcohol, tetrahydrofurfuryl alcohol, furan, tetrahydrofuran, as well as various cyclo-products (cyclopentanol, cyclopentanone)⁴⁶, which may serve as building blocks for the production of fuels, solvents, fertilisers, plastics, and paints.

Furfural was produced for the first time in large amounts by the Quaker Oats company in 1921⁴³. The production of furfural involves hydrolysis of the hemicellulose fraction of the biomass source into pentosans and monomeric pentoses and their subsequent acid hydrolysis. The process employs aqueous sulphuric acid, is typically operated in batch mode at 443–458 K to achieve 40–50% yield of furfural. Further process improvements always involved the use of mineral acids, which give difficulties in product recovery as well as operational issues such as corrosion and handling of corrosive mineral acids. In 2010, Binder, et al.⁸⁶ found that the combination of Cr (II) or Cr (III) salts with HCl in organic solvents resulted in moderate furfural yields. Further improvements were reported by Zhao, et al.⁸⁷, reporting 63% furfural yield when converting xylan using a CrCl₃ catalyst in ionic liquids under microwave assisted heating at 200 °C. The application of heterogeneous catalysts has also received considerable attention due to the ease of product recovery. Solid catalysts such as zeolites, microporous and mesoporous niobium silicalites, micro/mesoporous sulphonic acids, layered titanates, niobates and

titanoniobates, delaminated aluminosilicates, cesium salts of 12-tungstophosphoric acid and mesoporous silica-supported 12-tungstophosphoric acid, bulk and mesostructured sulphated zirconia, Nafion® 117, and a combination of different acidic and basic solid catalysts have been employed⁴⁶. Table 5 gives a number of representative examples for the synthesis of furfural.

A major breakthrough in furfural synthesis involved the use of a biphasic water-organic solvent. In this approach, furfural is, once formed, transferred to the organic phase where the stability is higher than in the water phase (Figure 21).

Table 5. Representative examples for furfural production from xylose⁴⁶

No	Catalyst	Reaction conditions	Conversion	Yield of FF	Ref
1	MCM-41-SO ₃ H	140 °C, 24h in water/toluene	91	75.5	88
2	ZSM5 zeolite	200 °C, 3h, in water solvent	n.d.	46	89
3	PSZ-MCM-41	160 °C, 4h in water/toluene	95		90
4	Nafion® 117	150 °C, 2h in DMSO	91	60	91
5	Dealuminated HNu-6(2)	170 °C, 4h in water/toluene	40–90	47	92
6	H-mordenite13	260 °C, 0.05h in water/toluene	98	98	93
7	Zeolite beta	170 °C, 4h in water	100	77	94
8	SO ₄ ²⁻ /ZrO ₂ – Al ₂ O ₃ /SBA-15	160 °C, 4h, water/toluene solvent	98.7	52	95
9	Amberlyst® 15 / Hydrotalcite	100 °C, 3h, DMF	72	36	96
10	HCl	170 °C, 15 min, biphasic reactor system	92	76	97
11	HCl	170 °C, 20 min, biphasic reactor system	98	78	97
12	HCl	170 °C, 30 min, biphasic reactor system	100	71	97
13	ChCl-citric acid	90 °C, 30 min	53.4 ± 0.8	08.3 ± 0.2	98
14	ChCl-citric acid	90 °C, 30 min, co-catalyst (AlCl ₃ ·6H ₂ O)	64.3 ± 0.3	15.3 ± 0.2	98
15	ChCl-citric acid	100 °C, 30 min, co-catalyst (AlCl ₃ ·6H ₂ O)	69.8 ± 1.2	22.8 ± 0.4	98
16	ChCl-citric acid	120 °C, 25 min, co-catalyst (AlCl ₃ ·6H ₂ O)	86.1 ± 0.3	36.5 ± 0.3	98
17	ChCl-citric acid	140 °C, 10 min, co-catalyst (AlCl ₃ ·6H ₂ O)	90.5 ± 0.7	49.8 ± 0.4	98
18	ChCl-citric acid	140 °C, 15 min, co-catalyst (CrCl ₃ ·6H ₂ O)	82.1 ± 0.9	44.6 ± 0.2	98
19	ChCl-citric acid	140 °C, 25 min, co-catalyst (FeCl ₃ ·6H ₂ O)	96.1 ± 0.4	58.5 ± 0.1	98
20	ChCl-citric acid	140 °C, 25 min, biphasic reactor system, co-catalyst (AlCl ₃ ·6H ₂ O)	99.8	73.1	98
21	ChCl-citric acid	140 °C, 35 min, biphasic reactor system, co-catalyst (FeCl ₃ ·6H ₂ O)	99.7	71.4	98
22	MCM-41	170 °C, water/1-butanol solvent	96.9	44.1	99
23	MCM-41	200 °C, water/1-butanol solvent	98.9	39.8	99
24	Arenesulphonic SBA-15	160 °C, water/toluene solvent	99.0	86	100

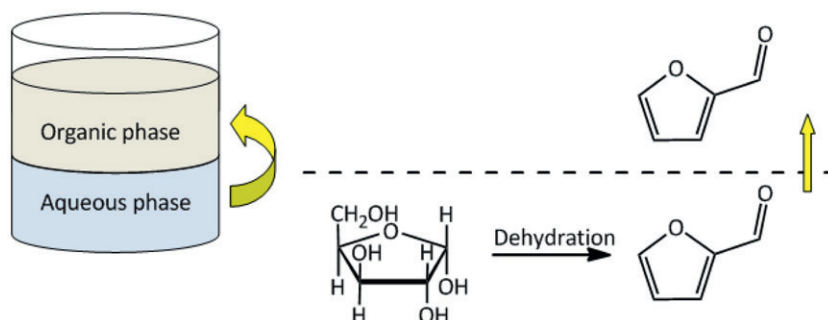


Figure 21. Biphase liquid-liquid system for direct removal of furfural from the aqueous phase.

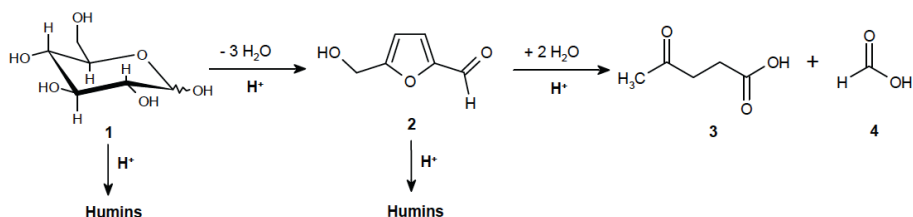


Figure 22. LA synthesis from C6 sugars (hexoses)

Conversion of C5 and C6 Sugars to Levulinic Acid

Conventionally, LA is produced by the dehydration of C6 sugars (hexoses) to HMF and further hydration to form LA (Figure 22). A comprehensive review of laboratory scale production of LA derived from various C6 sugars feedstocks has recently been published¹⁰¹. To convert glucose to LA, Choudhary et al.¹⁰² suggested that a combination of Lewis and Brønsted acids is beneficial. Here, the Lewis acid catalyses the isomerisation of glucose to fructose, while the Brønsted acid catalyses the subsequent conversion of fructose to LA. Solid acid catalysts based on transition metals like Cr and Zr give LA yields comparable to those obtained by mineral acids with the advantages of ease of product recovery and catalyst recyclability¹⁰¹. Solvent effects are also profound and for instance a mixture of gVL and water was shown to be beneficial for LA synthesis from cellulose¹⁰³.

C5 sugars (pentoses) can also be used as the feed for LA synthesis by using a hydrolysis/hydrogenation approach (Figure 23). The yield of the FF

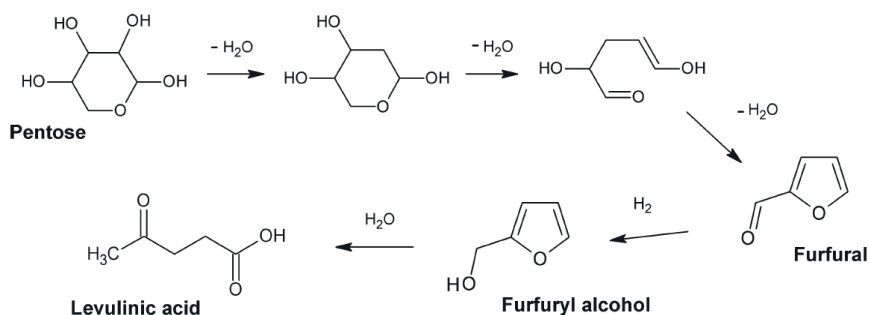


Figure 23. Synthesis of LA from C5 sugars, taken from [65] with permission

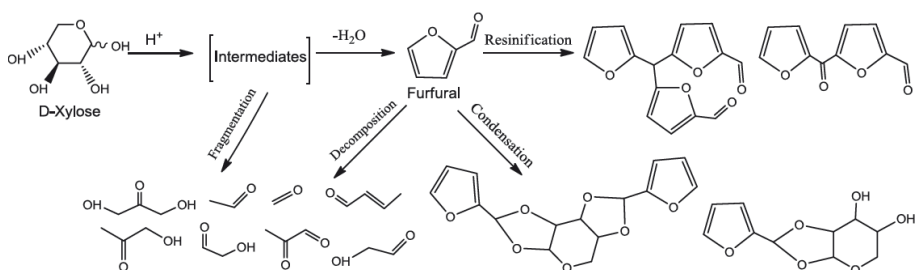


Figure 24. Pathways to humins formation during FF synthesis, taken from [46] with permission

intermediate is in the range reported in the literature. Furfuryl alcohol can be obtained with a yield exceeding 95% using a hydrogenation protocol⁶⁵. Further acid hydrolysis of furfuryl alcohol gave LA in yields up to 93% mol⁶⁵.

6.3 Challenges: Humins Formation

During the synthesis of biobased chemicals from sugars, inevitably solid by-products are formed, which are known as humin^{56–58,68,104–107}. These not only reduce the product yields but also create operational issues like clogging. The last decade, a number of groups have reported on the chemical structure of the humins and have proposed possible reaction pathways for humins as well as the methods/reaction conditions to reduce/avoid humins formation.

Humins formation during FF synthesis from C5 sugars is explained by considering the involvement of a reactive intermediates and subsequent

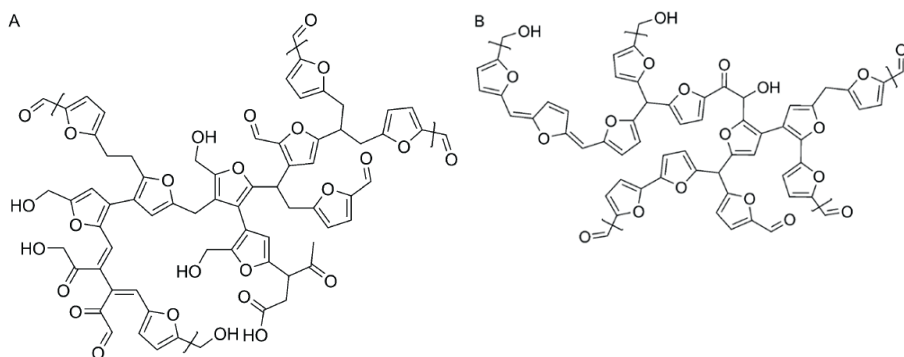


Figure 25. Model representing humins fragments for: A) glucose-derived humins and B) xylose derived humin¹⁰⁴

reactions of FF. The decomposition of FF may involve, among others, fragmentation, condensation, and resinification, as shown in Figure 24.

Sumerskii and co-workers¹⁰⁸ investigated the pathways for humins formation by analysis of humins formed when converting a range of mono- and di-saccharides and HMF using reaction conditions typically applied for the acid hydrolysis of wood (0.5% H_2SO_4 , 175–180 °C, 2 h). After thorough separation and purification, the solid produced was analysed by several analytical techniques, among others, NMR and pyrolytic GC-MS. The results suggest that the solid consists of about 60% of furan rings and 20% aliphatic fragments. A mechanism for humins formation was proposed, with a strong involvement of 5-hydroxymethylfurfural.

A different reaction pathway for humins formation was proposed by the group of Lund^{109,110}. It involves hydration of HMF to form 2,5-dioxo-6-hydroxyhexanal (DHH) which polymerises via aldol condensations with HMF to give humins.

Weckhuysen and co-workers¹⁰⁴ studied the acid catalysed conversion of glucose, fructose, xylose and mixtures thereof both individually as well as in the presence of HMF or 1,2,4-trihydroxybenzene (TB) at standard reaction conditions (180 °C, 1 M solution of sugar, and 0.01 M of H_2SO_4). They concluded that for C6 sugars, humins are derived mainly from 5-HMF. Further, inclusion of re-hydration products such as DHH and to a very limited extent, LA, occurs through aldol condensations. For C5-sugar-derived humins, the structure resembles poly-furfural as a result of poly-self-condensation to give furan units linked by CH and CH_2 units. Further, it was shown that HMF

is more reactive and prone to polymerisation than furfural. In contrary to the results of Sumerskii, the humins produced here were more dehydrated and do not contain acetal bonds. Figure 25 shows the proposed structure of glucose- and xylose-derived humins as suggested by Weckhuysen and co-workers.

7. THESIS OUTLINE

In this thesis, experimental studies are reported on the synthesis of biobased furanics from sugars. The main objective of the research was to develop efficient synthetic methodology for the conversion of sugars to HMF and FF by exploring the effects of i) process conditions (temperature, concentrations, type of solvent), ii) sugar feedstock and iii) the use of catalysts.

In Chapter 1, a general overview on biorefineries and platform chemicals is provided, with an emphasis on biobased furanics. Synthetic methodology for HMF and FF will be provided and reviewed.

In Chapter 2, experimental and kinetic modeling studies on the conversion of sucrose to HMF and LA in water using sulphuric acid as the catalyst are reported. Several reaction networks are proposed based on earlier proposals developed for the individual sugars (glucose and fructose). The kinetic parameters and their standard deviations were determined using a MATLAB optimization routine. The best fit kinetic model was then used to determine the optimum reaction conditions for HMF and LA production from sucrose in a batch reactor set-up.

In Chapter 3, the use of the four possible ketohexoses (fructose, tagatose, sorbose and psicose) for 5-HMF synthesis in water using sulphuric acid as the catalyst is reported. HMF yields were determined and the best ketohexose regarding HMF yield was determined.

In Chapter 4, the stability of 2-HAF (2-hydroxyacetylfuran), a well-known side product from the acid catalysed dehydration of C6 sugars to 5-HMF in water in the presence of Brønsted acid catalysts was studied. The main goal of this study was to determine rate of decomposition of 2-HAF and its possible involvement in LA formation. A number of experiments was performed at different process conditions and the decomposition rate was modeled using a Matlab optimization routine. Additionally, the effect of mineral acids (sulphuric and hydrochloric acid) on the rate of the hydrolysis reaction was studied.

In Chapter 5, experimental studies on solvent effects on the conversion of xylose to furfural in ethanol/water mixtures both using homogeneous and

heterogeneous Brønsted acid catalysts are provided. A reaction pathway is proposed to explain the experimentally observed solvent effect on FF yield, supported by studies with FF.

REFERENCES

1. Zoebelein, H. *Dictionary of Renewable Resources*; WILEY-VCH Verlag GmbH: Weinheim, 2001.
2. EIA. *Annual Energy Outlook 2016: With Projections to 2040*; U.S. Energy Information Administration: Washington DC, 2016.
3. Kamm, B.; Kamm, M. Principles of Biorefineries. *Appl. Microbiol. Biotechnol.* **2004**, *64*, 137–145.
4. Nishiyama, Y.; Langan, P.; Chanzy, H. Crystal Structure and Hydrogen-Bonding System in Cellulose I β from Synchrotron X-ray and Neutron Fiber Diffraction. *J. Am. Chem. Soc.* **2002**, *124* (31), 9074–9082.
5. Dutta, S.; De, S.; Saha, B.; Alam, M. I. Advances in conversion of hemi-cellulosic biomass to furfural and upgrading to biofuels. *Catal. Sci. Technol.* **2012**, *2*, 2025–2036.
6. Christopher, L. P.; Yao, B.; Ji, Y. Lignin Biodegradation with Laccase-mediator Systems. *Front. Energy Res.* **2014**.
7. Jha, I.; Attri, P.; Venkatesu, P. Unexpected Effects Of The Alteration Of Structure And Stability Of Myoglobin And Hemoglobin In Ammonium-Based Ionic Liquids. *Phys. Chem. Chem. Phys.* **2014**, *16*, 5514–5526.
8. Sorek, N.; Yeats, T. H.; Szemenyei, H.; Youngs, H.; Somerville, C. R. The Implications of Lignocellulosic Biomass Chemical Composition for the Production of Advanced Biofuels. *BioSci.* **2014**, *64* (3), 192–201.
9. Biswas, R.; Uellendahl, H.; Ahring, B. K. Wet Explosion: a Universal and Efficient Pretreatment Process for Lignocellulosic Biorefineries. *BioEnergy Res.* **2015**, *8* (3), 1101–1116.
10. Bozell, J. J.; Petersen, G. R. Technology development for the production of biobased products from biorefinery carbohydrates - the US Department of Energy's "Top 10" revisited. *Green Chemistry* **2010**, *12* (4), 539–554.
11. Cherubini, F.; Strømman, A. H. Chemicals from Lignocellulosic Biomass: Opportunities, Perspectives and Potential of Biorefinery Systems. *Biofuels, Bioprod. Biorefin.* **2011**, *5*, 548–561.
12. de Jong, E.; Jungmeier, G. Chapter1. Biorefinery Concepts in Comparison to Petrochemical Refineries. In *Industrial Biorefineries and White*

- Biotechnology*; Pandey, A., Höfer, R., Larroche, C., Taherzadeh, M., Nampoothiri, T. M., Eds.; Elsevier: Waltham, WA, USA, 2015; pp 3–33.
13. Kamm, B.; Gruber, P. R.; Kamm, M. Biorefineries – Industrial Processes and Products. In *Ullmann's Encyclopedia of Industrial Chemistry*; Wiley-VCH Verlag GmbH & Co. KGaA: Weinheim, Germany, 2002; Vol. 5, pp 659–688.
 14. Lene, L. The Importance of Fungi and Mycology for Addressing Major Global Challenges. *IMA Fungus*. **2014**, 5 (2), 463–471.
 15. Clark, J. H.; Deswarte, F. E. I.; Farmer, T. J. The Integration Of Green Chemistry into Future Biorefineries. *Biofuels, Bioprod. Bioref.* **2009**, 3, 72–90.
 16. Werpy, T.; Petersen, G. *Top Value Added Chemicals from Biomass: Volume I - Results of Screening for Potential Candidates from Sugars and Synthesis Gas*; National Renewable Energy Laboratory: Springfield, VA, 2004.
 17. Daniel, L. *Green is The New Black: Conversions of Biomass to "Drop" in Chemicals and Materials. Presented for Lux Research Inc.*; Presentation for Lux Research Inc.; Amsterdam, June 10, 2016.
 18. Vennestrom, P. N. R.; Osmundsen, C. M.; Christensen, C. H.; Taarning, E. Beyond Petrochemicals: The Renewable Chemicals Industry. *Angew. Chem. Int. Ed* **2011**, 50 (2), 10502–10509.
 19. Tsai, T.-C.; Liu, S.-B.; Wang, I. Disproportionation and Transalkylation of Alkylbenzenes over Zeolite Catalysts. *Appl. Catal., A* **1999**, 181, 355–398.
 20. Ashraf, M. T.; Chebbi, R.; Darwish, N. A. Process of p-Xylene Production by Highly Selective Methylation of Toluene. *Ind. Eng. Chem. Res.* **2013**, 52, 13730–13737.
 21. Tomas, R. A. F.; Bordado, J. C. M.; Gomes, J. F. P. p-Xylene Oxidation to Terephthalic Acid: A Literature Review Oriented toward Process Optimization and Development. *Chem. Rev.* **2013**, 113, 7421–7469.
 22. Collias, D. I.; Harris, A. M.; Nagpal, V.; Cottrell, I. W.; Schultheis, M. W. Biobased Terephthalic Acid Technologies: A Literature Review. *Ind. Biotechnol.* **2014**, 10, 91–105.
 23. Burgess, S. K.; Kriegel, R. M.; Koros, W. J. Carbon Dioxide Sorption and Transport in Amorphous Poly(ethylene furanoate). *Macromolecules* **2015**, 48, 2184–2193.
 24. Biddy, M. J.; Scarlata, C.; Kinchin, C. *Chemicals from Biomass: A Market Assessment of Bioproducts with Near-Term Potential*; National Renewable Energy Laboratory (NREL): Denver West Parkway, Golden, CO, U.S.A., 2016.
 25. Kläusli, T. Green Chemistry: The Nexus Blog. communities.acs.org/community/science/sustainability/green-chemistry-nexus-blog/

- blog/2014/07/17/bio-based-platform-chemicals-and-alternative-feed-stocks (accessed July 27, 2017).
26. E4tech; RE-CORD; WUR. *From the Sugar Platform to Biofuels and Biochemicals*; Final report for the European Commission, contract No. ENER/C2/423–2012/SI2.673791; European Union: London, 2015.
 27. Lee, C. S.; Aroua, M. K.; Daud, W. M. A. W.; Cognet, P.; Pérès-Lucchese, Y.; Fabre, P.-L.; Reynes, O.; Latapie, L. A Review: Conversion of Bioglycerol into 1,3-propanediol via Biological and Chemical Method. *Renewable Sustainable Energy Rev.* **2015**, *42*, 963–972.
 28. Tan, H. W.; AbdulAziz, A. R.; Aroua, M. K. Glycerol Production and Its Applications as a Raw Material: A Review. *Renewable Sustainable Energy Rev* **2013**, *27*, 118–127.
 29. Merchant Research&Consulting, L. World Butanediol (BDO) Production Volume to Go Beyond 2.49 Mln Tonnes in 2017. <https://mcgroup.co.uk/news/20140516/butanediol-bdo-production-volume-249-mln-tonnes.html> (accessed July 27, 2017).
 30. Massey, R.; Jacobs, M. Chapter I: Trends and Indicators. In *Global Chemicals Outlook - Towards Sound Management of Chemicals*; Kemf, E., Ed.; United Nations Environment Programme, 2013; p 19.
 31. Chohan, D. European Butadiene Prices Fall on Bearish Sentiment, Asia Drop. www.platts.com/latest-news/petrochemicals/london/european-butadiene-prices-fall-on-bearish-sentiment-26715011 (accessed July 27, 2017).
 32. Merchant Research and Consulting, L. World Propylene Glycol Market to Reach Supply-Demand Balance in 2015. <https://mcgroup.co.uk/news/20140418/propylene-glycol-market-reach-supplydemand-balance-2015.html> (accessed July 27, 2017).
 33. George, M. Acrylic Acid Overview: Global Propylene and Derivatives Summit. www.propylene-propane-markets-2014.com/media/downloads/15-day-two-matthew-george-head-of-exports-indian-oil.pdf (accessed July 27, 2017).
 34. Cellulac. Ethyl Lactate. cellulac.co.uk/en/ethyl-lactate/ (accessed July 27, 2017).
 35. Furlong, K. Bio-Based Paraxylene for PET: Bringing BioBased Paraxylene Through the PET Supply Chain with Key Partnerships. *4th Annual Info-cast Biobased Chemicals Summit, January 29th 2013, Del Mar, California, United States*, 2013.
 36. Syngip. Isoprene. syngip.com/isoprene/ (accessed July 27, 2017).
 37. Oleoline. The production capacity of fatty alcohols in Asia may grow by more than 30% in 2013. www.oleoline.com/index.php/news/the-

- production-capacity-of-fatty-alcohols-in-asia-may-grow-by-more-than-30-in-2013/ (accessed July 2017, 2017).
38. Fusaro, M. B.; Chagnault, V.; Postel, D. Reactivity of D-Fructose and D-Xylose in Acidic Media in Homogeneous Phases. *Carbohydr. Res.* **2015**, *409*, 9–19.
 39. Döbereiner, J. Ueber die medicinische und chemische Anwendung und die vortheilhafte Darstellung der Ameisensäure. *Annalen der Pharmacie* **1832**, *3* (2), 141–146.
 40. Corma, A.; Iborra, S.; Velty, A. Chemical Routes for the Transformation of Biomass into Chemicals. *Chemical Reviews* **2007**, *107* (6), 2411–2502.
 41. Zeitsch, K. J. *The Chemistry and Technology of Furfural and Its Many By-Products*; Elsevier: Koln, Germany, 2000; Vol. 13, 1 vols..
 42. Sain, B.; Chaudhuri, A.; Borgohain, J. N.; Baruah, B. P.; Ghose, J. L. Furfural And Furfural-Based Industrial-Chemicals. *J. Sci. Ind. Res.* **1982**, *41* (7), 431–438.
 43. Brownlee, H. J.; Miner, C. S. Industrial Development of Furfural. *Industrial And Engineering Chemistry* **1948**, *40* (2), 201–204.
 44. Hoydonckx, H. E.; van Rhijn, W. M.; van Rhijn, W.; de Vos, D. E.; Jacobs, P. A. Furfural and Derivatives. In *Ullmann's Encyclopedia of Industrial Chemistry*; Wiley-VCH Verlag GmbH & Co. KGaA: Weinheim, 2002; pp 285–309.
 45. Xing, R.; Subrahmanyam, A. V.; Olcay, H.; Qi, W.; van Walsum, G. P.; Pendse, H.; Huber, G. W. Production of Jet and Diesel Fuel Range Alkanes from Waste Hemicellulose-Derived Aqueous Solutions. *Green Chem.* **2010**, *12*, 1933–1946.
 46. Yan, K.; Wu, G.; Lafleur, T.; Jarvis, C. Production, Properties and Catalytic Hydrogenation of Furfural to Fuel Additives and Value-Added Chemicals. *Renewable Sustainable Energy Rev.* **2014**, *38*, 663–676.
 47. van Putten, R.-J.; Soetedjo, J. N. M.; Pidko, E. A.; van der Waal, J. C.; Hensen, E. J. M.; de Jong, E.; Heeres, H. J. Dehydration of Different Ketoses and Aldoses to 5-Hydroxymethylfurfural. *Chemsuschem* **2013**, *6* (9), 1682–1687.
 48. Teong, S. P.; Yia, G.; Zhang, Y. Hydroxymethylfurfural production from biore-sources: past, present and future. *Green Chem.* **2014**, *16* (4), 2015–2026.
 49. Caes, B. R.; Teixeira, R. E.; Knapp, K. G.; Raines, R. T. Biomass to Furanics: Renewable Routes to Chemicals and Fuels. *ACS Sustainable Chem. Eng.* **2015**, *3*, 2591–2605.
 50. Mordor Intelligence. Polyethylene Teraphtalate (PET) Market — Segmented by Product type, Industry and Geography — Trends and Fore-casts (2016–2022). www.mordorintelligence.com/industry-reports/global-polyethylene-teraphtalate-market-industry?gclid=CJacw9ykrdUCFawp-0wodNnkCnw (accessed July 29, 2017).

51. Credence Research. Adipic Acid Market (Nylon 66 Fibers, Engineering Plastics (Nylon 66 Resin), Polyurethanes, Adipic/Adipate Esters (Plasticizers), Others)—Growth, Share, Opportunities, Competitive Analysis, and Forecast 2015–2022”. technorati.com/global-adipic-acid-market-is-estimated-to-expand-with-a-cagr-of-4-4-from-2015-to-2022/ (accessed July 29, 2017).
52. Buntara, T.; Noel, S.; Phua, P. H.; Cabrera, I. M.; de Vries, J. G.; Heeres, H. J. Caprolactam from Renewable Resources: Catalytic Conversion of 5-Hydroxymethylfurfural into Caprolactone. *Angew. Chem. Int. Ed.* **2011**, *50*, 7083.
53. AdvanSix. *Caprolactame in AdvanSix Analyst Presentation - September 15, 2016*; AdvanSix: New York, 2016.
54. Bozell, J. J.; Moens, L.; Elliott, D. C.; Wang, Y.; Neuenschwander, G. G.; Fitzpatrick, S. W.; Bilski, R. J.; Jarnefeld, J. L. Production of Levulinic Acid and Use as a Platform Chemical for Derived Products. *Resour., Conserv. Recycl.* **2000**, *28* (3), 227–239.
55. Girisuta, B.; Janssen, L. P. B. M.; Heeres, H. J. Kinetic study on the acid-catalyzed hydrolysis of cellulose to levulinic acid. *Industrial Engineering, Chemistry Research* **2007**, *46*, 1969–1708.
56. Girisuta, B.; Janssen, L. P. B. M.; Heeres, H. J. A kinetic study on the decomposition of 5-hydroxymethylfurfural into levulinic acid. *Green Chemistry* **2006**, *8*, 701–709.
57. Girisuta, B.; Janssen, L. P. B. M.; Heeres, H. J. Green chemicals: A kinetic study on the conversion of glucose to levulinic acid. *Chemical Engineering Research and Design* **2006**, *84* (A5), 339–349.
58. Hayes, D. J.; Fitzpatrick, S. W.; Hayes, M. H.; Ross, J. R. The Biofine process — Production of Levulinic acid, furfural and formic acid from lignocellulosic feedstocks. In *Biorefineries - Industrial Processes and Products: Status Quo and Future Directions*; Kamm, B., Gruber, P. R., Kamm, M., Eds.; John Wiley & Sons: Weinheim Germany, 2006; Chapter 7, Vol. 1, pp 136–163.
59. Grote, A. F.; Tollens, B. Formation of levulinic acid from dextrose. *Justus Liebigs Annalen der Chemie* **1881**, *206* (1–2), 226–231.
60. Rodewald, H.; Tollens, B. The formation of levulinic acid from lactose. *Justus Liebigs Annalen der Chemie* **1881**, *206* (1–2).
61. Kent, W. H.; Tollens, B. Studies on lactose and galactose. *Justus Liebigs Annalen der Chemie* **1885**, *227* (1–2), 221–232.
62. Rischbiet, P.; Tollens, B. Experiments with molasses and cotton raffinose. *Justus Liebigs Annalen der Chemie* **1886**, *232* (2), 172–201.

63. Wehmer, C.; Tollens, B. The formation of levulinic acid, the reactions from all carbohydrates. *Justus Liebigs Annalen der Chemie* **1888**, 243 (3), 314–334.
64. Fischer, E.; Hirschberger, J. The Mannose II. *Berichte der deutschen chemischen Gesellschaft* **1889**, 22 (1), 365–376.
65. Rackemann, D. W.; Doherty; S., W. O. The Conversion of Lignocellulosics to Levulinic Acid. *Biofuels, Bioprod. Bioref.* **2011**, 5, 198–214.
66. Horvath, I. T.; Mehdi, H.; Fabos, V.; Boda, L.; Mika, L. T. Gamma-Valerolactone – a Sustainable Liquid for Energy and Carbon-Based Chemicals. *Green Chem.* **2008**, 10, 238–242.
67. Piskun, A. S.; de Haan, J. E.; Wilbers, E.; van de Bovenkamp, H. H.; Tang, Z.; Heeres, H. J. Hydrogenation of Levulinic Acid to γ -Valerolactone in Water Using Millimeter Sized Supported Ru Catalysts in a Packed Bed Reactor. *ACS Sustainable Chem. Eng.* **2016**, 4 (6), 2939–2950.
68. van Putten, R.-J.; van der Waal, J. C.; de Jong, E.; Rasrendra, C. B.; Hero, H. J.; de Vries, J. G. Hydroxymethylfurfural, A Versatile Platform Chemical Made from Renewable Resources. *Chem. Rev.* **2013**, 113, 1499–1597.
69. Peniston, Q. P. Manufacture of 5-Hydroxymethyl 2-Furfural. US 2,750,394, June 12, 1956.
70. Kuster, B. F. M.; van der Steen, H. J. C. Starch/Staerke. *Preparation of 5-Hydroxymethylfurfural Part I. Dehydration of Fructose in a Continuous Stirred Tank Reactor* **1977**, 29, 99–103.
71. Y. Nakamura and S. Morikawa, B. C. S. J. . 1. The Dehydration of D-Fructose to 5-Hydroxymethyl-2-furaldehyde. *Bull. Chem. Soc. Jpn.* **1980**, 53 (12), 3705–3706.
72. Fayet, C.; Gelas, J. Nouvelle Méthode de Preparation du 5-Hydroxymethyl-2-Furaldéhyde par Action de Sels D'Ammonium ou D'Immonium Sur Les Mono-, Oligo- et Polysaccarides. Accès Direct aux 5-Halogénométhyl-2-Furaldéhydes. *Carbohydr. Res.* **1983**, 122, 59–68.
73. Brown, D. W.; Floyd, A. J.; Kinsma, R. G.; Roshan-Ali, Y. Dehydration Reactions of Fructose in Non-Aqueous Media. *J. Chem. Tech. Biotechnol.* **1982**, 32, 920–924.
74. Román-Leshkov, Y.; Chheda, J. N.; Dumesic, J. A. Phase Modifiers Promote Efficient Production of Hydroxymethylfurfural from Fructose. *Science* **2006**, 312, 1933–1937.
75. Chheda, J. N.; Roman-Leshkov, Y.; Dumesic, J. A. Production of 5-hydroxymethylfurfural and furfural by dehydration of biomass-derived mono- and poly-saccharides. *Green Chemistry* **2007**, 9 (4), 342–350.

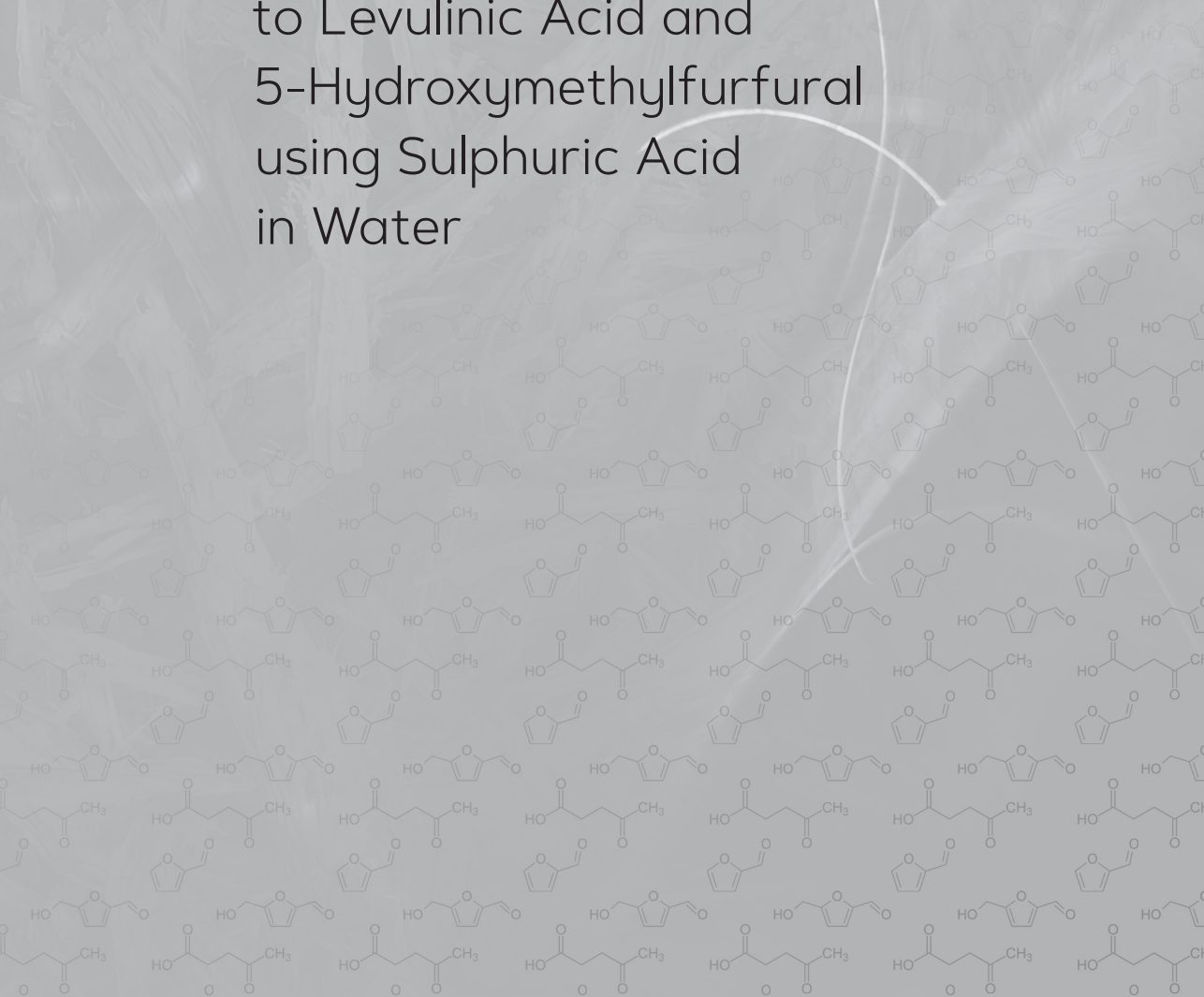
76. Román-Leshkov, Y.; Dumesic, J. A. Solvent Effects on Fructose Dehydration to 5-Hydroxymethylfurfural in Biphasic Systems Saturated with Inorganic Salts. *Top. Catal.* **2009**, *52* (3), 297–303.
77. Crisci, A. J.; Tucker, M. H.; Dumesic, J. A.; Scott, S. L. Bifunctional Solid Catalysts for the Selective Conversion of Fructose to 5-Hydroxymethylfurfural. *Top. Catal.* **2010**, *53*, 1185–1192.
78. Chheda, J. N.; Dumesic, J. A. An overview of dehydration, aldol-condensation and hydrogenation processes for production of liquid alkanes from biomass-derived carbohydrates. *Catalysis Today* **2007**, *123* (1–4), 59–70.
79. Kroger, M.; Prusse, U.; Vorlop, K. D. A New Approach for The Production Of 2,5-Furandicarboxylic Acid by In Situ Oxidation of 5-Hydroxymethylfurfural Starting from Fructose. *Top. Catal.* **2000**, *13*, 237–242.
80. Zhao, H.; Holladay, J. E.; Brown, H.; Zhang, Z. C. Metal Chlorides in Ionic Liquid Solvents Convert Sugars to 5-Hydroxymethylfurfural. *Science* **2007**, *316* (5831), 1597–1600.
81. Yong, G.; Zhang, Y.; Ying, J. Y. Efficient Catalytic System for the Selective Production of 5-Hydroxymethylfurfural from Glucose and Fructose. *Angew. Chem., Int. Ed.* **2008**, *47*, 9345–9348.
82. Jadhav, H.; Taarning, E.; Pedersen, C. M.; Bols, M. Conversion of D-Glucose into 5-Hydroxymethylfurfural (HMF) using Zeolite in [Bmim]Cl or Tetrabutylammonium Chloride (TBAC)/CrCl₃. *Tetrahedron Lett.* **2012**, *53*, 983–985.
83. Zhang, Y.; Pidko, E. A.; Hensen, E. J. M. Molecular Aspects of Glucose Dehydration by Chromium Chlorides in Ionic Liquids. *Chem.–Eur. J.* **2011**, *17*, 5281–5288.
84. Qi, X.; Watanabe, M.; Aida, T. M.; Smith Jr., R. L. Fast Transformation of Glucose and Di-/Polysaccharides into 5-Hydroxymethylfurfural by Microwave Heating in an Ionic Liquid/Catalyst System. *ChemSusChem* **2010**, *3*, 1071–1077.
85. Hu, L.; Sun, Y.; Lin, L. Efficient Conversion of Glucose into 5-Hydroxymethylfurfural by Chromium(III) Chloride in Inexpensive Ionic Liquid. *Ind. Eng. Chem. Res.* **2012**, *51*, 1099–1104.
86. Binder, J. B.; Raines, R. T. J. Simple Chemical Transformation of Lignocellulosic Biomass into Furans for Fuels and Chemicals. *J. Am. Chem. Soc.* **2009**, *131*, 1979–1985.
87. Zhang, Z.; Zhao, Z. K. Microwave-Assisted Conversion of Lignocellulosic Biomass into Furans in Ionic Liquid. *Bioresour. Technol.* **2010**, *101*, 1111–1114.
88. Dias, A. S.; Pillinger, M.; Valente, A. A. Dehydration of Xylose Into Furfural over Micro-Mesoporous Sulfonic Acid Catalysts. *Journal of Catalysis* **2005**, *229* (2), 414–423.

89. Neill, R.; Ahmad, M. N. . V. L.; Aiouache, F. Kinetics of aqueous phase dehydration of xylose into furfural catalysed by ZSM-5 zeolite. *Ind. Chem. Eng. Res* **2009**, *48*, 4300–4306.
90. Dias, A. S.; Lima, S.; Pillinger, M.; Valente, A. A. Modified Versions of Sulfated Zirconia as Catalysts for The Conversion of Xylose to Furfural. *Catal. Lett.* **2007**, *114*, 151–160.
91. Lam, E.; Majid, E.; Leung, A. C. W.; Chong, J. H.; Mahmoud, K. A.; T., L. J. H. Synthesis of Furfural from Xylose by Heterogeneous and Reusable Nafion® Catalysts. *ChemSusChem* **2011**, *4*, 535–541.
92. Lima, S.; Pillinger, M.; Valente, A. A. Dehydration of D-xylose into furfural catalysed by solid acids derived from the layered zeolite Nu-6(1). *Catal. Commun.* **2008**, *9*, 2144–2148.
93. Lessard, J.; Morin, J. F.; Wehrung, J. F.; Magnin, D.; Chornet, E. High Yield Conversion of Residual Pentoses into Furfural via Zeolite Catalysis and Catalytic Hydrogenation of Furfural to 2-Methylfuran. *Top. Catal.* **2010**, *53*, 1231–1234.
94. Ferreira, L. R. . L. S.; Neves, P.; Antunes, M. M.; Rocha, S. M.; Pillinger, M.; al., e. Aqueous Phase Reactions of Pentoses in The Presence of Nanocrystalline Zeolite Beta: Identification of By-Products and Kinetic Modeling. *Chem. Eng. J.* **2013**, *215–216*, 772–783.
95. Shi, X.; Wu, Y.; Li, P.; Yi, H.; Yang, M.; Wang, G. Catalytic Conversion of Xylose to Furfural over The Solid Acid SO₄²⁻/ZrO₂–Al₂O₃/SBA-15 catalysts. *Carbohydr. Res.* **2011**, *346*, 480–487.
96. Tarabanko, V. E.; Smirnova, M. A.; Chernyak, M. Y. Investigation of Acid-Catalytic Conversion of Carbohydrates in the Presence of Aliphatic Alcohols at Mild Temperatures. *Chemistry for Sustainable Development* **2005**, *13*, 551–558.
97. Gürbüz, E. *Strategies for The Catalytic Conversion of Lignocellulose-Derived Carbohydrates to Chemicals and Fuels (Ph.D Thesis)*; University of Wisconsin - Madison: Madison, Wisconsin, 2012.
98. Zhang, L.; Yu, H. B. Conversion of Xylan and Xylose Into Furfural in Biorenewable Deep Eutectic Solvent with Trivalent Metal Chloride Added. *Bioresources* **2013**, *8*, 6014–6025.
99. Zhang, J.; Zhuang, J.; L., L.; Liu, S.; Zhang, Z. Conversion of D-Xylose into Furfural with Mesoporous Molecular Sieve MCM-41 as Catalyst and Butanol as The Extraction Phase. *Biomass Bioenerg.* **2012**, *39*, 73–77.
100. Agirrezabal-Telleria, I.; Requies, J.; B., G. M.; L., A. P. Dehydration of D-Xylose to Furfural using Selective and Hydrothermally Stable Arenesulfonic SBA-15 Catalysts. *Appl. Catal. B.* **2014**, *145*, 34.

101. Mukherjee, A.; Dumont, M.-J.; Raghavan, V. Review: Sustainable Production of Hydroxymethylfurfural and Levulinic Acid: Challenges and Opportunities. *Biomass Bioenergy* **2015**, *72*, 143–183.
102. Choudhary, V.; Mushrif, S. H.; Ho, C.; Anderko, A.; Nikolakis, V.; Marinkovic, N. S.; Frenkel, A. I.; Sandler, S. I.; Vlachos, D. G. Insights Into The Interplay of Lewis and Brønsted Acid Catalysts in Glucose and Fructose Conversion to 5-(Hydroxymethyl)Furfural and Levulinic Acid in Aqueous Media. *J. Am. Chem. Soc.* **2013**, *135* (10), 3997–4006.
103. Alonso, D. M.; Gallo, J. M. R.; Mellmer, M. A.; Wettstein, S. G.; Dumesic, J. A. Direct Conversion of Cellulose to Levulinic Acid and Gamma-Valerolactone using Solid Acid Catalysts. *Catal. Sci. Technol.* **2013**, *3* (4), 927–931.
104. van Zandvoort, I.; Wang, Y.; Rasrendra, C. B.; Eck, E. R. H.; Bruijninx, P. C. A.; Heeres, H. J.; Weckhuysen, B. M. Formation, Molecular Structure, and Morphology of Humins in Biomass Conversion: Influence of Feedstock and Processing Conditions. *ChemSusChem* **2013**, *6* (9), 1745–1758.
105. Kuster, B. F. M. 5-Hydroxymethylfurfural (HMF). A Review Focusing on its Manufacture. *Starch/Starke* **1990**, *42*, 314–321.
106. Root, D. F.; Saeman, J. F.; Harris, J. F. Chemical Conversion of Wood Residues Part II: Kinetics of The Acid-Catalysed Conversion of Xylose to Furfural. *Forest Products Journal* **1959**, *9* (5), 158–165.
107. Lange, J.-P.; van der Heide, E.; van Buijtenen, J.; Price, R. Furfural—A Promising Platform for Lignocellulosic Biofuels. *ChemSusChem* **2012**, *5* (1), 150–166.
108. Sumerskii, I. V.; Krutov, S. M.; Zarubin, M. Y. Humin-Like Substances Formed under the Conditions of Industrial Hydrolysis of Wood. *Russian Journal of Applied Chemistry* **2010**, *83* (2), 320–327.
109. Patil, S. K. R.; Lund, C. R. F. Formation and Growth of Humins via Aldol Addition and Condensation during Acid-Catalyzed Conversion of 5-Hydroxymethylfurfural. *Energy Fuels* **2011**, *25*, 4745–4755.
110. Patil, S. K. R.; Heltzel, J.; Lund, C. R. F. Comparison of Structural Features of Humins Formed Catalytically from Glucose, Fructose, and 5-Hydroxymethylfurfuraldehyde. *Energy Fuels* **2012**, *26*, 5281–5293.

CHAPTER 2.

Experimental and
Kinetic Modeling Studies on
the Conversion of Sucrose
to Levulinic Acid and
5-Hydroxymethylfurfural
using Sulphuric Acid
in Water



ABSTRACT

We here report experimental and kinetic modeling studies on the conversion of sucrose to levulinic acid (LA) and 5-hydroxymethylfurfural (HMF) in water using sulphuric acid as the catalyst. Both compounds are versatile building blocks for the synthesis of various biobased (bulk) chemicals. A total of 24 experiments were performed in a temperature window of 80–180 °C, a sulphuric acid concentration between 0.005 and 0.5 M, and an initial sucrose concentration between 0.05 and 0.5 M. Glucose, fructose and HMF were detected as the intermediate products. The maximum LA yield was 61 mol%, obtained at 160 °C, an initial sucrose concentration of 0.05 M and an acid concentration of 0.2 M. The maximum HMF yield (22 mol%) was found for an acid concentration of 0.05 M, an initial sucrose concentration of 0.05 M and a temperature of 140 °C. The experimental data were modeled using a number of possible reaction networks. The best model was obtained when using a first order approach in substrates (except for the reversion of glucose) and agreement between experiment and model was satisfactorily. The implication of the model regarding batch optimization is also discussed.

The research described in this Chapter is published in:

Tan-Soetedjo, J. N. M.; van de Bovenkamp, H. H.; Abdilla, R. M.; Rasrendra, C. B.; van Ginkel, J.; Heeres, H. J., Experimental and Kinetic Modelling Studies on the Conversion of Sucrose to Levulinic Acid and 5-Hydroxymethylfurfural Using Sulphuric Acid in Water, *Ind. Eng. Chem. Res.*, **2017**.

1. INTRODUCTION

Levulinic acid (4-oxopentanoic acid, LA) is considered as a very important biobased platform chemical with a wide derivatization and application range¹⁻⁹. It is accessible by the acid catalysed hydrolysis of the C6-sugars in various biomass sources^{1-4,10-18}. Typical byproducts are formic acid and humins. The latter are oligomeric/polymeric substances that are either soluble or insoluble in the reaction mixture. HMF, also a very versatile platform chemical, is an intermediate in the conversion of C6 sugars to LA. HMF yields are a strong function of the C6 sugar used and best results have been reported with ketohexoses like fructose and psicose¹⁹. The yields from aldohexoses like glucose are by far lower and typically below 10 mol%.

The Biofine company has been actively involved in the conversion of lignocellulosic biomass to LA in the last 15 years²⁰. In their process, the lignocellulosic biomass and sulphuric acid catalyst are mixed in water, and the resulting slurry is supplied to the reactor section. The reaction conditions, typically 180–210 °C, are such that formic acid and furfural, the two major low molecular weight byproducts, are vaporised and collected separately. The liquid phase with the LA and solids (humins, lignins) is filtered to obtain an aqueous LA solution, which is neutralised and further purified to obtain LA. Typical yields of LA are between 15 and 41 wt% on feed, the exact value being a function of the reaction conditions and biomass source. GFBiochemicals recently reported a Biofine derived process to produce LA from a wide range of biomass feeds. Yield improvements were reported based on further optimization/modification of the reactor and work-up section, though details are to the best of our knowledge not reported yet. Commercial production in Casserta, Italy started in the summer of 2015. The unit will be scaled up to a full capacity of 10,000 MT/a by 2017²¹.

A wide range of biomass feeds has been reported for LA synthesis, including both monomeric and dimeric sugars as well as complex biomass sources such as *Mischantus*²², starch²³, wood cellulose^{24,25} and waterhyacinth²⁶. Among them, sucrose has also been studied^{1-3,18,27-32}. It is easily hydrolysable to its monomers, D-glucose and D-fructose, which both can be converted to LA in good yields. Sucrose is present in high amounts in sugar-cane and beets. Waste streams of the sugar industry contain significant amounts of sucrose and this justifies a detailed study on the use of sucrose for LA synthesis.

The first studies on the conversion of sucrose to LA have already been reported in 1873 by Grote and Tollens¹⁰. Later studies reported the use of various

Table 1. Selected examples for LA and HMF synthesis from sucrose in water using homogeneous Brønsted acid catalysts

No	Sucrose concentration	Catalyst	Catalyst concentration	Time	T (°C)	P (atm)	HMF yield ^a (mol%)	LA yield ^a (mol%)	Ref.
1	0.66 M		1.80 M	8 h	140		n.d.	40–50 ^b	32
2	0.05 M		0.001 M	32 s	250	341	25	n.d.	34
3	0.18 M		1 M	16 h	125		n.d.	42 ^b	28
4	1.17 M		2 M	24 h	100		n.d.	21–22	27
5	0.86 M		2 M	1 h	162	7	n.d.	42–43	18
6	0.18 M		3 M	16 h	125		n.d.	60 ^b	28
7	0.29 M		6 M	5 h	108		n.d.	62	29
8	0.33 M		3.84 M	1 h	98		n.d.	50 ^b	31
9	0.18 M		1 M	16 h	125		n.d.	70 ^b	28
10	25 wt%	Oxalic acid	0.03 M	2.5 h	145, 15 min then 125		27	n.d.	35
11	23 wt%	Oxalic acid	0.23 wt%	3 h	200	3	25	n.d.	36

^a Yields are based on monosaccharide concentration ^b Not clear whether yields are based on mol% or wt%, or on monosaccharide or sucrose concentration

mineral acids such as hydrochloric acid, sulphuric acid, hydrobromic acid as well as heterogeneous catalysts^{18,27,28,30,31}. Table 1 summarizes a number of representative studies on the acid-catalysed conversion of sucrose to HMF and LA using homogeneous Brønsted acid catalysts. The highest reported LA yield is about 70 mol%, whereas the maximum HMF yield is limited to about 27%.

Kinetic studies on the conversion of sucrose to HMF/LA using simple homogeneous Brønsted acids like sulphuric acid in water have to the best of our knowledge not been reported in the literature. Recently, Woodley et al. published a kinetic study on the conversion of glucose-fructose mixtures using HCl as the catalyst in an acetone-water mixture³⁷. Kinetic studies are of prime importance for a proper design of the reactor section of LA processes and also allow selection of the best operating conditions to achieve maximum yields and volumetric production rates of LA.

In this paper, the kinetics of the conversion of sucrose to LA using a batch set-up is studied in a broad range of process conditions (80–180 °C, sulphuric acid concentrations between 0.005–0.50 M. and initial sucrose concentrations between 0.05–0.50 M). The concentrations of the intermediates (glucose, fructose and HMF) were also determined and these components were included in the kinetic analysis. Based on the experimental data, a reaction network is proposed and the experimental data were modeled using a kinetic scheme in line with this proposal. Furthermore, a number of alternative kinetic networks

were evaluated and the results are compared with the original scheme. Finally, the optimum conditions for batch processing to obtain highest LA/HMF yields were determined on the basis of the model and will be discussed.

2. METHODS AND ANALYSIS

2

2.1 Chemicals

All chemicals were of analytical grade and used without further purification. Concentrated sulphuric acid (95–97 wt% [7664-93-9]) and formic acid (98–100 wt% [64-18-6]) were purchased from Merck KGaA (Darmstadt, Germany). Sucrose (> 95 wt% [57-50-1]) and fructose (> 95 wt% [57-48-7]) were acquired from Fisher Scientific UK (Leicestershire, Great Britain); glucose (> 99.5 wt% [14431-43-7]), 5-HMF (> 99 wt% [67-47-0]) and levulinic acid (98 wt% [123-76-2]) were obtained from Sigma-Aldrich Chemie GmbH (Steinheim, Germany). Deionised water was used to prepare the various solutions.

2.2 Experimental Procedures

All reactions were carried out in glass ampoules with an internal diameter of 3 mm, a wall thickness of 1.5 mm, and a length of 15 cm. These were filled at room temperature with a solution of sucrose and sulphuric acid (total liquid volume of 0.5 cm³) and then sealed with a torch. A series of ampoules was placed in a rack and placed in a constant temperature oven (± 1 °C) which was pre-set at the desired reaction temperature. At different reaction times, an ampoule was taken from the oven and directly quenched into a cold water bath. The liquid content was then filtered using a PTFE syringe filter (0.45 μ m, VWR, the Netherlands). The particle free aliquot was then diluted 7–8 times with water prior to HPLC analysis.

2.3 Analytical Methods

The composition of the liquid phase was determined using two different HPLC systems. An Agilent 1200 HPLC consisting of a Hewlett Packard 1200 pump and a Bio-Rad organic acid column (Aminex HPX-87H) was used for

glucose, fructose, HMF and LA analysis. A typical example of a chromatogram is given in Figure S1 (Supplementary Information). For glucose, fructose and LA, quantification was performed using an RID detector whereas a UV detector was used for HMF. An aqueous sulphuric acid (5 mM) solution was used as the mobile phase at a flow rate of 0.55 cm³ per minute. The column was operated at 60 °C. The analysis of a sample was complete within 60 min.

An Agilent 1050 HPLC consisting of a Hewlett Packard 1050 pump, a Bio-Rad sugar column (Aminex HPX-87P), and a Waters 410 refractive index detector was used for sucrose quantification. Double distilled water was used as the mobile phase at a flow rate of 0.55 cm³ per minute. The column was operated at 80 °C. The analysis of a sample was complete within 30 min.

The concentrations of each compound in the product mixture were determined using calibration curves obtained by analysing standard solutions of known concentrations.

2.4 Definitions

The conversion of sucrose (X_{SUC}) and the yields of HMF (Y_{HMF}) and LA (Y_{LA}) are defined in eq. 1–3.

$$X_{SUC} = \frac{(C_{Suc,0} - C_{Suc})}{C_{Suc,0}} \quad (1)$$

$$Y_{HMF} = \frac{(C_{HMF})}{2 \times C_{Suc,0}} \quad (2)$$

$$Y_{LA} = \frac{(C_{LA})}{2 \times C_{Suc,0}} \quad (3)$$

Here, $C_{Suc,0}$ is the initial concentration of sucrose. All definitions are on a molar basis.

2.5 Determination of the Kinetic Parameters

The kinetic parameters were determined using a nonlinear least squares approach using the MATLAB function *lsqnonlin*, which is based on an Trust-Region-Reflective algorithm, and involves minimization of the errors between the experimental data and the kinetic model. Details about this procedure can be found in the literature^{38,39}.

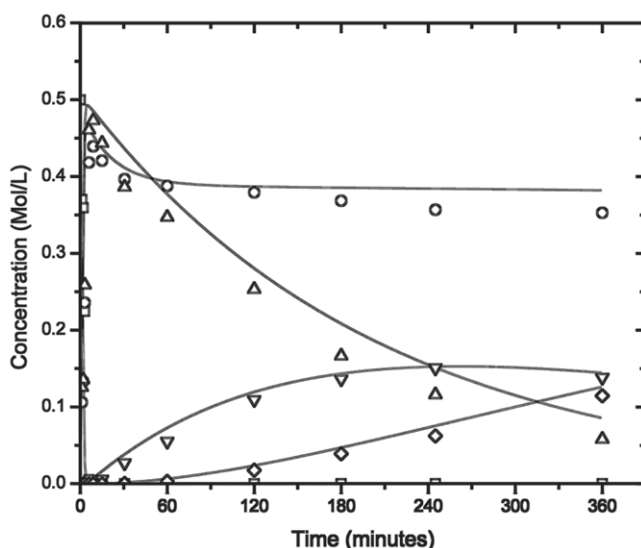


Figure 1. Typical time-concentration profile of the products of the acid-catalysed hydrolysis of sucrose at 120 °C, $C_{H_2SO_4} = 0.05$ M, $C_{Suc,0} = 0.5$ M (markers: experimental (□-sucrose, ○-glucose, △-fructose, ▽-HMF, ◇-LA, lines: model).

3. RESULTS AND DISCUSSION

3.1 Experimental Studies

A total of 24 experiments were performed in a temperature window of 80–180 °C, a sulphuric acid concentration between 0.005 and 0.5 M, and an initial sucrose concentration between 0.05 and 0.5 M. Main products (HPLC) i.e. fructose, glucose, HMF, LA and formic acid (FA) are in line with earlier studies^{1–3,8,32}. The latter was not quantified in detail. Upon reaction, the colour of the reaction mixtures changed from transparent to yellowish-brown and in some cases solid dark brown byproducts (humins) were formed. These are formed by condensation reactions of products and intermediates, and were not quantified. In addition, soluble humins may be formed as well.

The concentrations of the main products as a function of the batch time were determined (HPLC) and the results for two representative experiments are given in Figure 1 (120 °C) and 2 (180 °C).

The conversion rate of sucrose is a strong function of temperature and acid concentration. The time for quantitative conversion is typically less

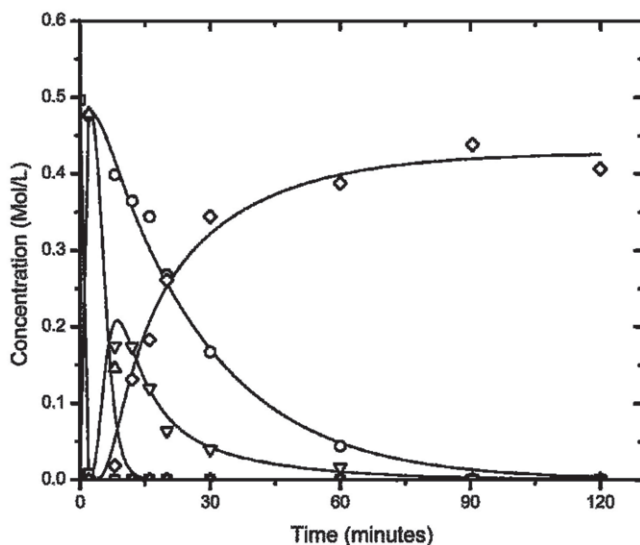


Figure 2. Typical time-concentration profile of the products of the acid-catalysed hydrolysis of sucrose at 180 °C, $C_{H_2SO_4} = 0.05$ M, $C_{Suc,0} = 0.5$ M (markers: experimental (\square -sucrose, \circ -glucose, \triangle -fructose, ∇ -HMF, \diamond -LA, lines: model).

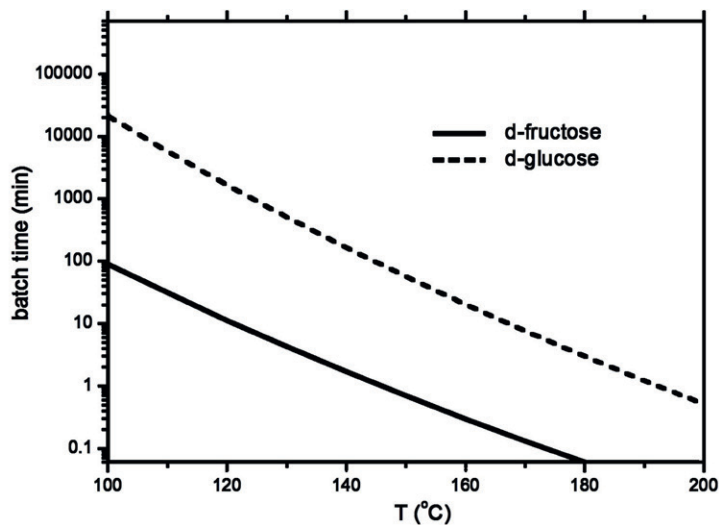


Figure 3. Required batch time for 90% C6-sugar conversion (fructose and glucose) versus temperature in water using sulphuric acid as the catalyst (1 M). Reproduced with permission from [40].

than 1 min at temperatures exceeding 120 °C and as such sucrose is not observed in most reaction mixtures (Figure 2). At low temperatures (80 and 100 °C) and low acid concentrations, sucrose is detected in the reaction mixtures for up to 20 min (100 °C, 0.005 M H₂SO₄). As expected, glucose and fructose are the initial products and are derived from the acid catalysed hydrolysis (inversion) of sucrose. The glucose and fructose yields are around 100%, indicating that sucrose inversion is very selective in the experimental window of process conditions.

Glucose, fructose and HMF are typical intermediates and in some cases (particularly at higher severity) show a clear maximum, whereas LA is formed in significant amounts upon prolonged batch times. Glucose is by far less reactive than fructose. These findings are in line with earlier kinetic studies from our group on the conversion of the individual sugars (Figure 3)⁴⁰. Here, it was demonstrated that on average, fructose is about 100 times more reactive than glucose in the temperature window employed in this study.

LA is stable under the experimental conditions employed as is evident from a constant concentration level at prolonged reaction times (up to 900 min, data not shown for brevity). The maximum experimental LA yield was 61 mol%, obtained at 160 °C, an initial sucrose concentration of 0.05 M and an acid concentration of 0.2 M. The maximum LA yield in this study is higher than reported in the literature for sucrose when using sulphuric acid as the catalyst (40–50 mol%)³². It is also of interest to compare the experimental LA yields with previous studies using the individual sugars (glucose, fructose) in water with sulphuric acid as the catalyst. For fructose alone, the highest experimental yield was 74 mol% (fructose concentration of 0.1 M, a sulphuric acid concentration of 1 M and a temperature of 140 °C)⁴⁰ whereas the best yields for glucose were somewhat lower (60%, 140 °C, C_{GLC,0}: 0.1 M, C_{acid}: 1 M)⁸. Though the experimental conditions are different, the data imply that the experimentally observed highest LA yield for sucrose in this study is in line with the values obtained for experiments with the individual sugars.

The maximum HMF yield within the experimental window of process conditions was 22 mol% (0.05 M sulphuric acid, 0.05 M sucrose, 140 °C). This value is slightly lower than reported in the literature for sucrose in water using sulphuric acid as the catalyst (25 mol%, see Table 1), though comparison is hampered as the experimental conditions are different. For fructose alone, the highest reported HMF yield in water using sulphuric acid is 53 mol% (initial fructose concentration of 0.1 M, a sulphuric acid concentration of 0.01 M and a temperature of 180 °C)⁴⁰. For glucose, the HMF yield is

considerably lower and for instance Girisuta et al. reported a maximum yield of 5 mol% in water using sulphuric acid as the catalyst in a similar window of process conditions⁸. As such, the value of 22 mol% for sucrose is in line with the literature, particularly when considering that the initial inversion of sucrose to fructose and glucose is fast and essentially quantitative.

Glucose can be isomerised to fructose, though the reaction is known to be slow in the absence of catalysts and equilibrium limited in water. At 150 °C, the equilibrium constant in water is about 1⁴¹. In this study, the rate of glucose-fructose isomerization appears to be slow compared to the timescale of the other reactions, particularly at low temperatures. This is illustrated by Figure 1, showing that the glucose concentration is about constant after its initial formation from sucrose whereas the fructose concentration is dropping more rapidly. In case of the occurrence of a rapid isomerization reaction, a different profile is expected with a constant fructose to glucose ratio.

Of interest is the observation of a small drop in the glucose concentration directly after its formation from sucrose, see Figure 1 for a representative example. This effect is particularly evident for experiments carried out in the lower temperature range. A possible explanation is the formation of reversion products of glucose, mostly dimers, as also proposed by Johnson et al.⁴². These reactions are known to be relatively fast and equilibrium limited (*vide infra*). For fructose, this trend is not observed, likely due to the fact that fructose is by far more reactive than glucose and already converted to a significant extent directly after its formation.

3.2 Kinetic Modeling Studies

Reaction Network Development

The experimental data were initially modeled (model 1) with a global reaction network given in Figure 4. The reaction network is based on earlier reaction networks proposed for experimental and kinetic modeling studies for glucose and fructose individually^{8,40}. The latter is justified as it was shown experimentally that sucrose is rapidly hydrolysed and inverted to a 1 to 1 molar mixture of fructose and glucose.

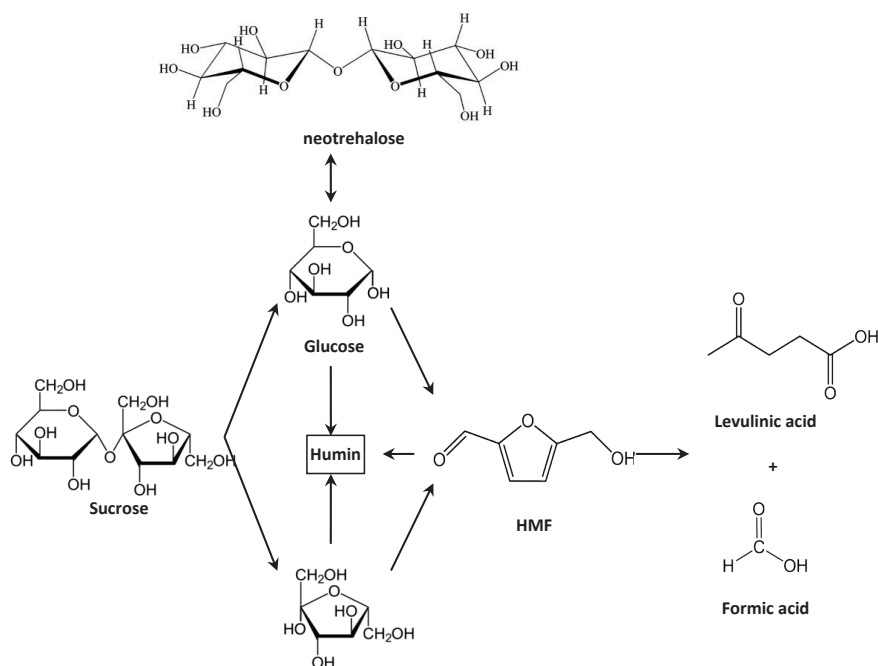


Figure 4. Proposed reaction network (model 1) for the conversion of sucrose to LA and HMF

In acidic media, glucose may dehydrate inter- and intra-molecularly to form glucose oligomers and anhydroglucoses (mainly levoglucosan, LG), respectively⁴². Literature studies revealed that up to 12 wt% of the glucose is converted into reversion products at high sugar loadings (200 mg.cm⁻³). The reversion products are mainly disaccharides and larger oligosaccharides were not reported to be formed in significant amounts. In Figure 4, only one (neotrehalose) of the possible reversion dimers is shown. Disaccharide formation was modeled using a second-order dependency in glucose. In addition, the dimerization reaction is known to be reversible and this was also assumed in our model. Johnson et al.⁴² also reported the formation of levoglucosan (LG) from glucose, though only in significant amounts at low glucose concentrations (< 10 mg.cm⁻³). LG was also not detected in this study, and as such this reversion product was not included in the kinetic models.

The equilibrium reaction between glucose and fructose was also not included in the first model. This reaction is known to be catalysed by (inorganic) bases and enzymes. Acids are known to be less effective and the acid

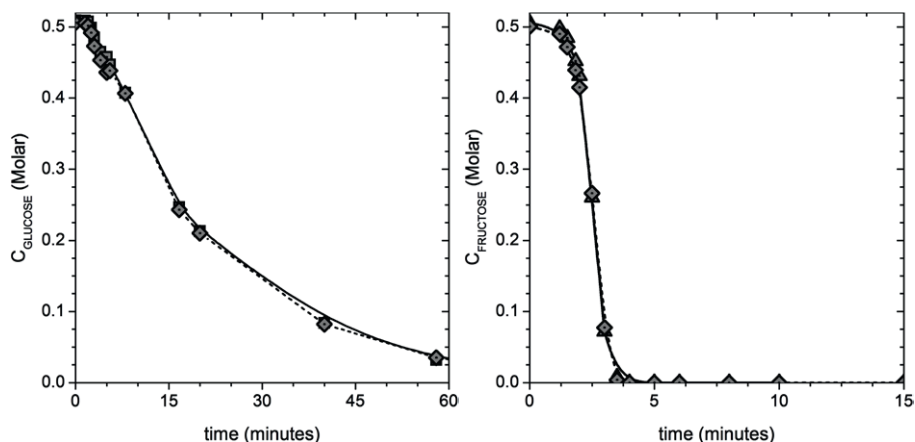


Figure 5. Concentration-time profiles for glucose and a mixture of glucose and fructose (1 to 1 molar ratio, left) and fructose and a mixture of fructose and glucose (1 to 1 molar ratio, right). $C_{\text{GLU},0} = C_{\text{FRU},0} = 0.50 \text{ M}$, 180°C , $C_{\text{H}_2\text{SO}_4} = 0.05 \text{ M}$

catalysed isomerization reaction is known to be by far slower than the base catalysed isomerization. For instance, Watanabe et al. showed that fructose reacts in acidic aqueous media to HMF with negligible glucose formation⁴³. However, when starting with glucose, some fructose besides HMF and LA were observed. As such, glucose-fructose isomerization was included in subsequent kinetic models (*vide infra*).

Furthermore, model 1 assumes that both fructose and glucose react independently to HMF. This assumption is based on literature evidence for kinetic studies using glucose⁸ only and recent studies by Woodley et al. for fructose-glucose mixtures in water-acetone as the solvent³⁷. In the latter, the reaction of glucose to HMF was required to obtain a better model description of the experimental data.

Finally, it is assumed that glucose, fructose and HMF individually react to soluble and insoluble humins, as proposed for studies with the individual sugars. This is a simplification as cross condensations between the various intermediates (fructose, glucose, HMF) cannot be excluded beforehand. The possibility of cross condensations between glucose and fructose to form humins was investigated independently. For this purpose, the concentration-time profile for the individual sugar was compared to that of a mixture of both sugars in a 1 to 1 ratio. The results for two representative experiments are given in Figure 5. It shows that the concentration-time profiles for the

individual sugars are not affected in the presence of the other sugar, implying that cross condensation reactions between the two sugars do not take place to a considerable extent.

Model Development

The first kinetic model (model 1) was developed based on the reaction network given in Figure 4 and assumes first order reactions in most substrates. As the timescale of sucrose inversion to glucose and fructose is much faster than for the consecutive reactions, the inversion of sucrose was modeled independently. In a later stage, extended reaction networks (including glucose-fructose isomerization) were modeled and the results will be provided in a separate paragraph.

Kinetic Modeling of Sucrose Conversion to Glucose and Fructose

The kinetic model for the conversion of sucrose to glucose and fructose was developed using 8 experiments from the dataset with in total 29 datapoints. Only this limited dataset could be used as, sucrose is converted on the timescale of less than a minute at the higher temperatures within the temperature window.

The inversion of sucrose to fructose and glucose is typically modeled in the literature using a first order approach in acid and sucrose (Table 2) and a similar approach was used in this study.

For a batch reactor, the mass balance for sucrose is given in eq. 4.

$$\frac{dC_{Suc}}{dt} = -R_{1S} \quad (4)$$

When assuming first order reactions for the sucrose, R_{1S} is given by eq. 5.

$$R_{1S} = k_{1S}(C_{SUC})(C_{H^+}) \quad (5)$$

The temperature dependence of the kinetic constant was considered using a modified Arrhenius equation as given in eq. 6.

$$k_{1S} = k_{1RS} \exp\left[\frac{E_{a1S}}{R}\left(\frac{T - T_R}{T_R T}\right)\right] \quad (6)$$

Table 2. Overview of kinetic studies on sucrose hydrolysis to glucose and fructose

No	C_{SUCO} [M]	C_{acid} [M]	Conditions	T [°C]	t [h]	R_{SUC} / mol L ⁻¹ min ⁻¹ ^a	Ref
1	0-2.63	$C_{H^+} = 3 \times 10^{-7} - 0.1$	Isothermal operation	20-130	n.a.	$R_{SUC} = 2.8 \times 10^{16} \exp \left[-\frac{108,570}{RT} \right] C_H + C_{SUC}$	44
2	0.01-0.1	$C_{H_2SO_4} = 0.10 - 1.0$	Isothermal operation	45-55	0.50	$R_{SUC} = 2.8 \times 10^{15} \exp \left[\frac{-99,160}{RT} \right] C_H + C_{SUC}$	45
3	0.07	$C_{H_2SO_4} = 0.01 - 0.20$	Isothermal operation	160-200	0.05-0.20	Too fast, not observable	46
4	0.06	$C_{HCl} = 5 \times 10^{-4}$	Non-isothermal, linear gradient	70-98	15	$R_{SUC} = 3.5 \times 10^{12} \exp \left[\frac{-102,330}{RT} \right] C_H + C_{SUC}$	47
				60-98	16	$R_{SUC} = 1.7 \times 10^{13} \exp \left[\frac{-105,970}{RT} \right] C_H + C_{SUC}$	
				60-90	15	$R_{SUC} = 7.8 \times 10^{12} \exp \left[\frac{-103,720}{RT} \right] C_H + C_{SUC}$	
5	0.03	$C_{HCl} = 0.25$	Continuous flow non-isothermal, ramp time of 2.5 seconds, flowrate of 450 mL/min	$T_{set} = 151$ (151-155) $T_{set} = 144$ (144-150) $T_{set} = 139$ (139-146)	0.0125 0.0125 0.0125	$R_{SUC} = 1.4 \times 10^{14} \exp \left[\frac{-112,700}{RT} \right] C_H + C_{SUC}$ $R_{SUC} = 7.2 \times 10^{14} \exp \left[\frac{-117,700}{RT} \right] C_H + C_{SUC}$ $R_{SUC} = 4.2 \times 10^{12} \exp \left[\frac{-100,200}{RT} \right] C_H + C_{SUC}$	48
6	0.015, 0.15, 0.73	$C_{HCl} = 10^{-4} - 10^{-8}$	pressure of 10 MPa, sub-critical water	160-200	1-4 minutes	$R_{SUC} = 3.8 \times 10^{11} \exp \left[\frac{-98,000}{RT} \right] C_H + C_{SUC}$	49
7	3×10^{-3}	$C_{HNO_3} = 0.5 - 2.5$	Non-isothermal method	50-90	0.83	$R_{SUC} = 2.9 \times 10^{15} \exp \left[\frac{-99,000}{RT} \right] C_H + C_{SUC}$	50
8	0.26	$C_{H^+} = 0.34$ (>1.70 Na ⁺ eq/L, 800g/L)	Microwave, Amberlite 200C	40-80	500	$R_{SUC} = 3.8 \times 10^{12} \exp \left[\frac{-92,800}{RT} \right] C_H + C_{SUC}$	51

^a T in K

where T_R is the reference temperature (140 °C), k_{1RS} is the rate constant at the reference temperature and E_{a1S} is the activation energy.

At the start-up of the reaction, the reaction takes place non-isothermally due to heating-up of the contents of the ampoule from room temperature to the oven temperature. The experimental profiles at different temperatures were modeled using a heat balance for the contents in an ampoule using eq. 7 and 8.

$$\frac{d(MC_pT)}{dt} = U \cdot A_t \cdot (T_{oven} - T) \quad (7)$$

$$T = T_{oven} - (T_{oven} - T_i) \exp^{-ht} \quad (8)$$

The value of h was shown to be a function of the set-point of the oven. This temperature dependence was determined by fitting the calculated h -values at different set points of the oven (80–180 °C) and was found to be described properly using a simple linear relation (eq. 9):

$$h(T) = 0.00128 \cdot T \text{ (K)} \quad (9)$$

The actual H^+ concentration was calculated using eq. 10.

$$C_{H^+} = C_{H_2SO_4} + \frac{1}{2} \left(-K_{a,HSO_4^-} - C_{H_2SO_4} + \sqrt{(K_{a,HSO_4^-} + C_{H_2SO_4})^2 + 4C_{H_2SO_4}K_{a,HSO_4^-}} \right) \quad (10)$$

Here K_{a,HSO_4^-} represents the dissociation constant of HSO_4^- . The temperature dependence of this dissociation constant is given in eq. 11 (T in K)⁵².

$$pK_{a,HSO_4^-} = 0.0152 \cdot T - 2.636 \quad (11)$$

The kinetic constants and the activation energies were determined using the MATLAB software package by simultaneous modeling of the 8 selected experiments. Good agreement between model and experimental data was obtained, as is evident from a parity plot and the time concentration graph of a selected experiment (Figure 6). The estimated value for k_{1RS} was $730 \pm 290 \text{ L mol}^{-1} \text{ min}^{-1}$ and $110 \pm 10 \text{ kJ.mol}^{-1}$ for the activation energy. The experimentally determined activation energy for the reaction is within the 93–118 kJ.mol^{-1} range as reported in the literature (Table 2).

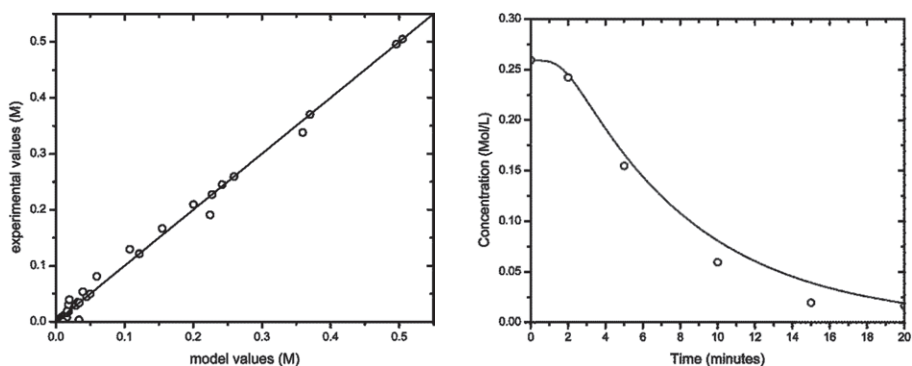


Figure 6. Parity plot for experimental and model data (left) and a representative concentration-time curve (right) for the reaction of sucrose to glucose and fructose. Conditions (right), $T = 100\text{ }^{\circ}\text{C}$, $C_{\text{suc}(0)} = 0.26\text{ M}$, $C_{\text{acid}} = 0.005\text{ M}$.

Kinetic Modeling Using Network 1

A simplified representation of the reaction network of model 1 (Figure 4) including a labeling scheme of the individual reactions is given in Figure 7. For all reactions, a first order approach in reactants was applied, the only exception being the reaction of glucose to glucose dimers, which was assumed to be second order. The kinetic constants for sucrose (SUC) inversion to fructose (FRC) and glucose (GLC) were fixed to the model values obtained in the previous paragraph.

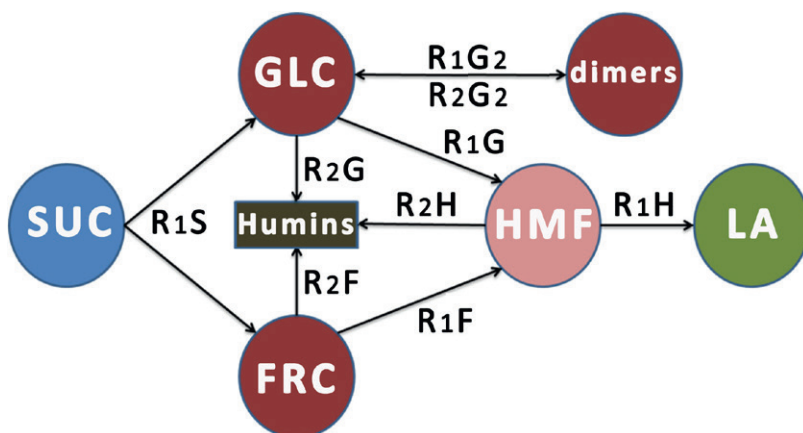


Figure 7. Schematic representation of the reaction network for kinetic model 1.

The individual reaction rates are defined in eq. 12–19.

$$R_{1F} = k_{1F}(C_{FRC})(C_{H^+}) \quad (12)$$

$$R_{2F} = k_{2F}(C_{FRC})(C_{H^+}) \quad (13)$$

$$R_{1G} = k_{1G}(C_{GLC})(C_{H^+}) \quad (14)$$

$$R_{2G} = k_{2G}(C_{GLC})(C_{H^+}) \quad (15)$$

$$R_{1H} = k_{1H}(C_{HMF})(C_{H^+}) \quad (16)$$

$$R_{2H} = k_{2H}(C_{HMF})(C_{H^+}) \quad (17)$$

$$R_{1G2} = k_{1G2}(C_{GLC})^2(C_{H^+}) \quad (18)$$

$$R_{2G2} = k_{2G2}(C_{G2})(C_{H^+}) \quad (19)$$

The temperature dependencies of the kinetic rate constants were defined in term of modified Arrhenius equation like the one given in eq. 6, and a reference temperature of 140 °C was used.

For a batch reactor set-up, the concentrations of the individual species are a function of time. When using the proposed kinetic model as given in Figure 7, these are represented by the following differential equations:

$$\frac{dC_{FRC}}{dt} = R_{1S} - R_{1F} - R_{2F} \quad (20)$$

$$\frac{dC_{GLC}}{dt} = R_{1S} - R_{1G} - R_{2G} - R_{1G2} + 2R_{2G2} \quad (21)$$

$$\frac{dC_{HMF}}{dt} = R_{1F} + R_{1G} - R_{1H} - R_{2H} \quad (22)$$

$$\frac{dC_{LA}}{dt} = R_{1H} \quad (23)$$

$$\frac{dC_{G2}}{dt} = \frac{1}{2}R_{1G2} - R_{2G2} \quad (24)$$

Modeling Results for Model 1

A total of 24 experiments with 884 experimental datapoints, being the concentrations of glucose, fructose, HMF and LA at different reaction times, was used for the development of the kinetic model. The best estimation of the kinetic parameters and their standard deviations were determined using a MATLAB optimization routine and the results are given in Table 3.

Table 3. Model results for model 1 (Figure 7)

k value at 140 °C	Model result	±	Dimension
k_{1G}	0.009	0.002	$L \text{ mol}^{-1} \text{ min}^{-1}$
k_{2G}	0.005	0.002	$L \text{ mol}^{-1} \text{ min}^{-1}$
k_{1F}	0.361	0.016	$L \text{ mol}^{-1} \text{ min}^{-1}$
k_{2F}	0.200	0.020	$L \text{ mol}^{-1} \text{ min}^{-1}$
k_{1HMF}	0.225	0.010	$L \text{ mol}^{-1} \text{ min}^{-1}$
k_{2HMF}	0.026	0.019	$L \text{ mol}^{-1} \text{ min}^{-1}$
k_{1G2}	0.227	0.057	$L^2 \text{ mol}^{-2} \text{ min}^{-1}$
k_{2G2}	1.427	0.394	$L \text{ mol}^{-1} \text{ min}^{-1}$
Ea_{1G}	153	14	kJ mol^{-1}
Ea_{2G}	172	19	kJ mol^{-1}
Ea_{1F}	116	3	kJ mol^{-1}
Ea_{2F}	122	5	kJ mol^{-1}
Ea_{1HMF}	92	3	kJ mol^{-1}
Ea_{2HMF}	146	43	kJ mol^{-1}
Ea_{1G2}	55	14	kJ mol^{-1}
Ea_{2G2}	99	17	kJ mol^{-1}

Agreement between model and experiment is good, as illustrated by the overall parity plot, the parity plot for LA (Figure 8) and a number of modeled profiles in Figure 9.

Inspection of the kinetic constants at reference temperature in Table 3 show that the sucrose inversion to fructose and glucose is by far the fastest reaction in the network followed by the glucose dimerization equilibrium reaction, which is in line with the experimental findings (Figure 1). In addition, the kinetic constant for the reaction of glucose to HMF is about 40 times lower than for the reaction of fructose to HMF, which is also in agreement with studies for the individual sugars⁴⁰.

It is of interest to compare the activation energies for the main reactions with those provided in the literature for aqueous systems using homogeneous

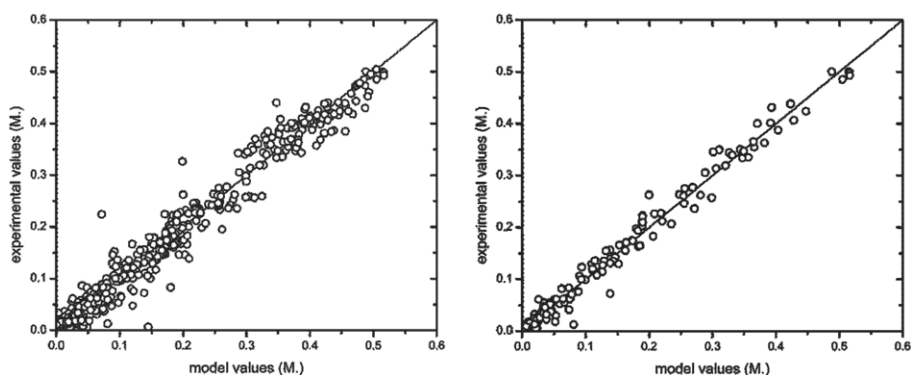


Figure 8. Parity plot including the concentrations of all components (left) and only LA (right).

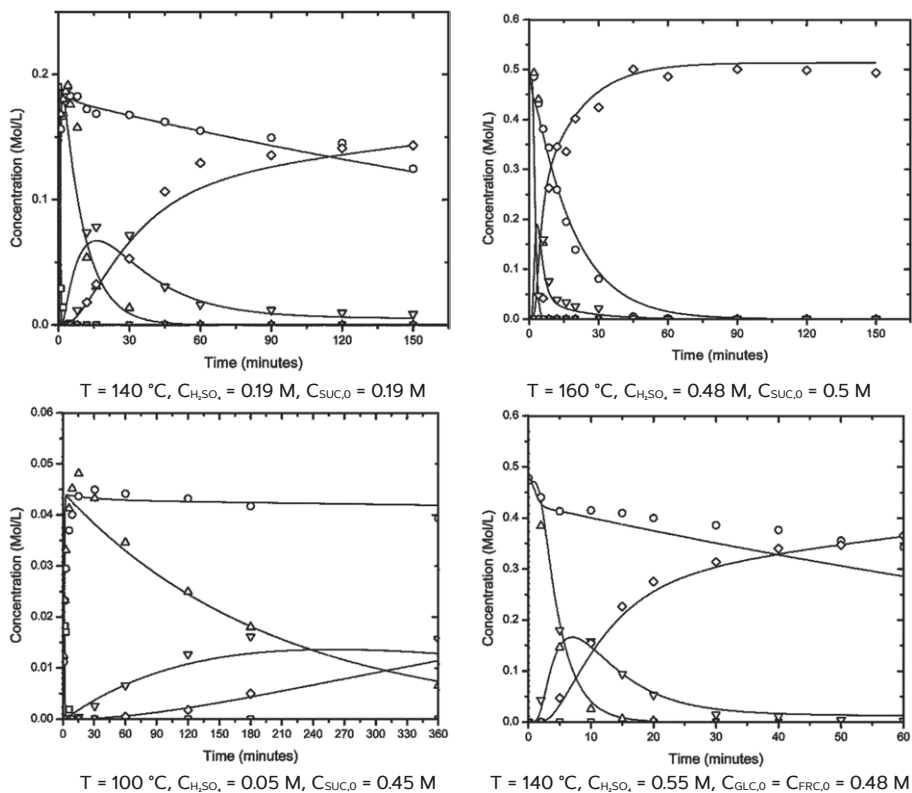


Figure 9. Experimental data points and model lines (model 1) for a number of representative batch experiments (markers: experimental (\square -sucrose, \circ -glucose, \triangle -fructose, ∇ -HMF, \diamond -LA, lines: model 1))

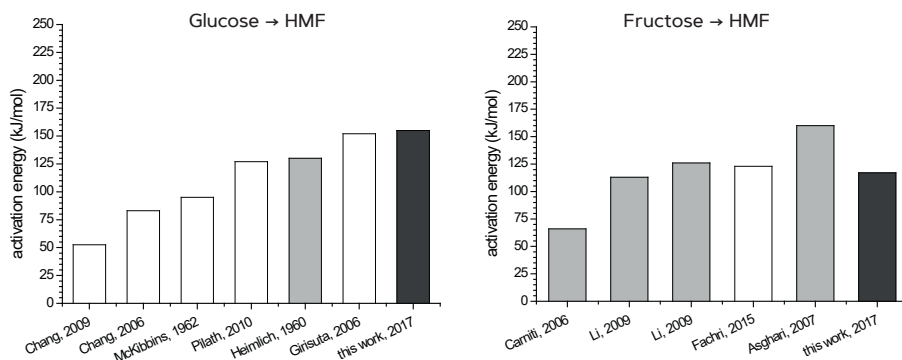


Figure 10. Overview of activation energies for the Brønsted acid catalysed conversion of glucose (left) and fructose (right) to HMF in water. White bars: using sulphuric acid catalyst, grey bars: other acid catalysts, black bars: this study

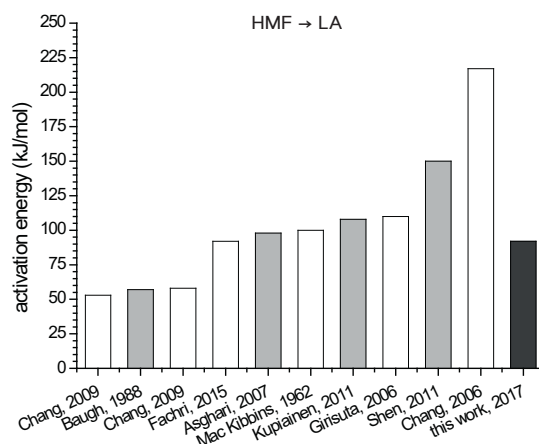


Figure 11. Overview of activation energies for the Brønsted acid catalysed conversion of HMF to LA in water. White bars: using sulphuric acid catalyst, grey bars: other acid catalysts, black bars: this study.

catalysts (glucose^{43,53–57} and fructose to HMF^{40,58–60} and HMF to LA^{40,53–56,58,60–63}). The results are provided in Figure 10 and Figure 11.

The activation energy for glucose to HMF found in this study ($153 \pm 14 \text{ kJ mol}^{-1}$) is equal within the confidence interval to the value reported for the reaction using the individual sugar as the starting material ($152 \pm 1 \text{ kJ mol}^{-1}$) and sulphuric acid as the catalyst by Girisuta et al.⁸ For fructose, a broad range of activation

energies has been reported (Figure 10, right). The value of $116 \pm 3 \text{ kJ mol}^{-1}$ is close to that reported for fructose only studies ($123 \pm 5 \text{ kJ mol}^{-1}$) using sulphuric acid as the catalyst by Fachri et al.⁴⁰. The activation energies reported in the literature for the conversion of HMF to LA show a large spread (Figure 11). However, the value found here ($92 \pm 3 \text{ kJ mol}^{-1}$) is within the range and close to those found previously for kinetic modeling studies in our group for fructose and glucose only (111 ± 1 and $92 \pm 5 \text{ kJ mol}^{-1}$)^{8,40} using sulphuric acid as the catalyst.

In the reaction network of model 1, all intermediates (glucose, fructose and HMF) may either react to desired products or to humins. The activation energies for the desired reactions are all lower than for those forming humins (Table 3). This suggests that LA formation will be favoured when the reaction is carried out at lower temperatures (*vide infra*).

Alternative Kinetic Models

A number of kinetic models derived from alternative reaction networks were explored and the results were compared with those for model 1. The alternative reaction networks (2 and 3) are schematically given in Table 4.

The reaction network for model 2 is similar to that for 1, the only difference is the use of a power law approach to describe the kinetics of humins formation (eq. 25–27) instead of a first order approach. This approach was selected as previous studies with the individual sugars showed that an order higher than 1 gave a better model fit, rationalised by considering that humins forming reactions are intermolecular condensation reactions which are likely not first order reactions^{8,40}.

$$R_{2F} = k_{2F}(C_{FRC})^{aF}(C_{H^+}) \quad (25)$$

$$R_{2G} = k_{2G}(C_{GLC})^{aG}(C_{H^+}) \quad (26)$$

$$R_{2H} = k_{2H}(C_{HMF})^{aH}(C_{H^+}) \quad (27)$$

The data set was modeled including the three additional parameters representing the orders in humins formation (aF, aG, aH). The values for the three parameters were 1.6 ± 0.2 , 1.5 ± 1 and 0.94 ± 0.1 for aF, aG and aH, respectively (Table S1, Supplementary information). The quality of the model as expressed

Table 4: Reaction networks tested for kinetic modeling

Model	Reaction network	R ²	AIC ⁶²
1		<p>Overall 0.97782</p> <p>LA 0.98456</p> <p>Sucrose 0.99379</p> <p>Glucose 0.98150</p> <p>Fructose 0.96038</p> <p>HMF 0.89693</p>	-6951.9
2	Model 1 with a power law approach for the orders in humins formation	<p>Overall 0.97771</p> <p>LA 0.98414</p> <p>Sucrose 0.99379</p> <p>Glucose 0.98131</p> <p>Fructose 0.96072</p> <p>HMF 0.89628</p>	-6947.5
3		<p>Overall 0.97771</p> <p>LA 0.98409</p> <p>Sucrose 0.99379</p> <p>Glucose 0.98137</p> <p>Fructose 0.96038</p> <p>HMF 0.89789</p>	-6947.6

in terms of R² and the AIC criterion⁶⁴ was not much better than model 1 (Table 4). In addition, the value for aH is close to 1 and the value for aG has a large confidence interval including 1. As such, and also considering the fact that a model with the lowest number of parameters is preferred, model 2 does not provide a considerable improvement.

In model 1, glucose-fructose isomerization is not included, rationalised by the observation that the acid catalysed reaction is known to be by much slower than the base catalysed isomerization reaction⁴³. To assess the importance of isomerization, the glucose-fructose isomerization reaction is included in model 3, see Table 4 for details.

$$R_{1eq} = k_{1eq} \left((C_{GLC}) - \left(\frac{C_{FRC}}{K} \right) \right) (C_{H^+}) \quad (28)$$

Table 5. Model results for model 3 (including glucose-fructose isomerization, see Table 4)

k value at 140 °C	Model result	±	Dimension
k1G	0.010	0.002	L mol ⁻¹ min ⁻¹
k2G	0.004	0.002	L mol ⁻¹ min ⁻¹
k1F	0.363	0.015	L mol ⁻¹ min ⁻¹
k2F	0.196	0.020	L mol ⁻¹ min ⁻¹
k1HMF	0.226	0.009	L mol ⁻¹ min ⁻¹
k2HMF	0.030	0.020	L mol ⁻¹ min ⁻¹
k1G2	1.004	0.231	L ² mol ⁻² min ⁻¹
k2G2	3.095	0.814	L mol ⁻¹ min ⁻¹
k1eq	1.7E-04	1.0E-03	L mol ⁻¹ min ⁻¹
Ea1G	156	16	kJ mol ⁻¹
Ea2G	167	31	kJ mol ⁻¹
Ea1F	117	3	kJ mol ⁻¹
Ea2F	119	6	kJ mol ⁻¹
Ea1HMF	92	3	kJ mol ⁻¹
Ea2HMF	138	30	kJ mol ⁻¹
Ea1G2	48	11	kJ mol ⁻¹
Ea2G2	89	15	kJ mol ⁻¹
Eaeq	2	2	kJ mol ⁻¹

The reaction was modeled as an equilibrium reaction (eq. 28) with a first order dependency in both glucose and fructose. The value of the equilibrium constant (about 1 in the temperature window of this study) was taken from the literature^{41,65} and as such only the rate of one of the reactions was fitted. The model quality, expressed by the R²-value and the AIC criterion, were close to those for model 1 (Table 4). The modeled value of k_{1eq} was $1.7 \times 10^{-4} \pm 1.0 \times 10^{-3}$ L mol⁻¹ min⁻¹, which is a factor of 10 lower than all other rate constants (Table 5). As such, this confirms that the rate of the isomerization reaction is relatively slow compared to the timescale of all other reactions. In addition, the confidence interval is larger than the modeled value of the kinetic constant, also an indication that the kinetic constant may actually be close to zero and thus has limited value. Thus, we can conclude that a reaction network involving glucose-fructose isomerization provides a good representation of the experimental dataset, though that the model predicts that the contribution of the isomerization reaction is very limited under the prevailing reaction conditions, in line with experimental findings (*vide supra*).

3.3 Model Implications

Determination of Optimum Conditions for LA and HMF Yield in Batch

The model implication calculations were all carried out using model 1, thus assuming that all reactions in the model are first order in reactants and acid concentration, except for glucose reversion. Figure 12 shows the yield of LA as a function of time for different temperatures, at a sucrose starting concentration of 0.1 M and an acid concentration of 0.5 M.

The model predicts that the LA yield is highest at the lowest temperature in the range, viz. 70 mol% at 100 °C. This may be rationalised by considering that the reactions leading to humins all have higher activation energies than the reactions forming LA. Therefore, lowering the temperature will lead to higher LA yields. However, the batch times at lower temperatures are excessively longer than at the highest temperature (up to 70,000 min for maximum LA yield at 100 °C), leading to very unrealistically low reactor productivities ($\text{mol LA} \cdot \text{m}^{-3} \text{reactor} \cdot \text{h}^{-1}$). As such, the optimum temperature for LA synthesis will be a compromise between LA yield and batch time.

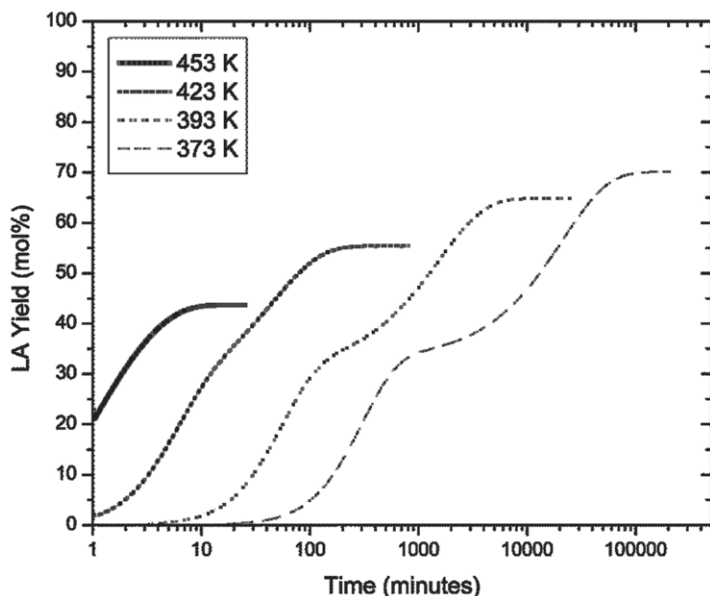


Figure 12. Modeled LA yield as function of batch time at different temperatures (initial sucrose concentration of 0.1 M, sulphuric acid concentration of 0.5 M).

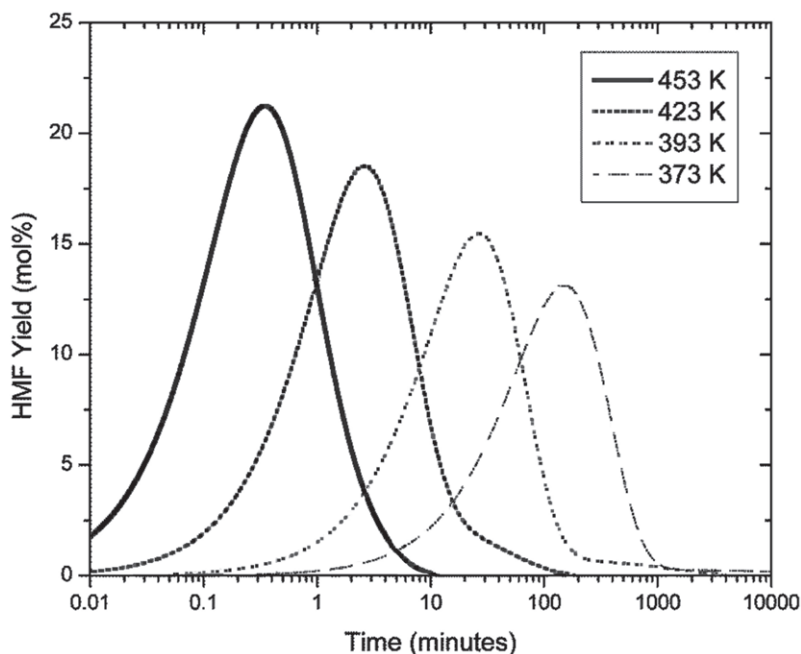


Figure 13. Modeled HMF yield as a function of time at different temperatures (initial sucrose concentration of 0.1 M, sulphuric acid concentration of 0.5 M).

The highest experimental value for the yield of LA was 61 mol% at 160 °C, in line with model predictions using the experimental conditions as input. LA yields at lower temperatures were, in contrast to model predictions, lower, which is due to incomplete conversion of particularly glucose, the least reactive sugar, and as such the maximum LA yields were not attained.

The modelled HMF yield versus the temperature is given in Figure 13. The highest modeled HMF yield is 21 mol%, obtained at the highest temperature in the range.

4. CONCLUSIONS

An experimental and kinetic modeling study on the conversion of sucrose to LA and HMF in water using sulphuric acid as the catalyst is reported. The maximum experimental LA yield was 61 mol% (160 °C, an initial sucrose concentration of 0.05 M and an acid concentration of 0.2 M), whereas the

maximum HMF yield was 22 mol% (140 °C, an initial sucrose concentration of 0.05 M and an acid concentration of 0.05 M). The experimental data were modeled using a number of possible reaction networks and the best model when considering model quality indicators (R-squared of parity plots, AIC criterion and number of model parameters) was obtained when using a first order approach in substrates (except for the reversion of glucose). The model was used to determine optimum conditions regarding LA and HMF yields in batch and predicts that highest LA yields are possible at the lowest temperature in the range, though this goes at the expense of reactor productivity ($\text{mol LA} \cdot \text{m}^{-3}_{\text{reactor}} \cdot \text{h}^{-1}$) due to considerable reductions in reaction rates. Highest HMF yields are predicted for the highest temperature in the range.

This information may be used to develop efficient processes for the conversion of sucrose solutions to biobased building blocks like HMF and LA. In addition, it may also be the starting point for the development of such processes using waste streams from sugar industries, though experimental studies with such real feeds will be required to assess the effects of impurities (salts, proteins, bases,) on rates of the individual reactions.

5. ACKNOWLEDGEMENT

One of the authors (J.N.M. Tan-Soetedjo) would like to thank DIKTI (Directorate General of Indonesia Higher Education) and the Parahyangan Catholic University for financial support by a personal scholarship. We also acknowledge Jan Henk Marsman and Léon Rohrbach for analytical support and Marcel de Vries, Anne Appeldoorn and Erwin Wilbers for technical support.

REFERENCES

- (1) Licursi, C. A. D.; Fulignati, S.; Valentini, G.; Raspoli Galetti, A.M. New frontiers in the catalytic synthesis of levulinic acid: from sugars to raw and waste biomass as starting feedstock. *Catalysts* **2016**, *6*, 196.
- (2) Zheng, X.; Gu, X.; Ren, Y.; Zhi, Z.; Lu, X. Production of 5-hydroxymethylfurfural and levulinic acid from lignocellulose in aqueous solution and different solvents. *Biofuels, Bioprod. Bioref.* **2016**, *10*, 917.
- (3) Pileidis, F. D.; Titirici, M.M. Levulinic acid biorefineries: new challenges for efficient utilization of biomass. *ChemSusChem* **2016**, *9*, 562.
- (4) Mulder, G. J. Untersuchungen über die Humussubstanzen. *Journal für praktische Chemie* **1840**, *21*, 230.
- (5) Conrad, M. Acetopropionic Acid and Its Identity with levulinic acid. *Berichte der Deutschen Chemischen Gesellschaft* **1878**, *11*, 2177.
- (6) Bozell, J. J.; Petersen, G. R. Technology development for the production of biobased products from biorefinery carbohydrates — the US Department of Energy's "Top 10" revisited. *Green Chem.* **2010**, *12*, 539–554.
- (7) Bozell, J. J.; Elliot, D. C.; Wang, Y.; Neuenschwander, G. G.; Fitzpatrick, S. W. Production of levulinic acid and use as a platform chemical for derived products. *Resour. Conserv. Recy.* **2000**, *28*, 227.
- (8) Girisuta, B.; Janssen, L. P. B. M.; Heeres, H. J. Green chemicals: A kinetic study on the conversion of glucose to levulinic acid. *Chem. Eng. Res. Des.* **2006**, *84*, 339.
- (9) Hayes, D. J.; Fitzpatrick, S. W.; Hayes, M. H.; Ross, J. R. The Biofine process - Production of Levulinic acid, furfural and formic acid from lignocellulosic feedstocks. In *Biorefineries - Industrial Processes and Products: Status Quo and Future Directions*; John Wiley & Sons: Weinheim, 2006; Vol. 1, 136.
- (10) Grote, A. F. v.; Tollens, B. The effect of sulfuric acid on sugar in producing levulinic acid. *Berichte der deutschen chemischen Gesellschaft* **1874**, *VII*, 1375.
- (11) Grote, A. F. v.; Kehler, D. E.; Tollens, B. Preparation and properties of Levulinic acid. *Justus Liebigs Ann. Chem.* **1881**, *206*, 207.
- (12) Grote, A. F.; Tollens, B. Formation of levulinic acid from dextrose. *Justus Liebigs Ann. Chem.* **1881**, *206*, 226.
- (13) Rodewald, H.; Tollens, B. The formation of levulinic acid from lactose. *Justus Liebigs Ann. Chem.* **1881**, *206*, 231.
- (14) Kent, W. H.; Tollens, B. Studies on lactose and galactose. *Justus Liebigs Ann. Chem.* **1885**, *227*, 221.

- (15) Rischbiet, P.; Tollens, B. Experiments with molasses and cotton raffinose. *Justus Liebigs Ann. Chem.* **1886**, 232, 172.
- (16) Wehmer, C.; Tollens, B. The formation of levulinic acid, the reactions from all carbohydrates. *Justus Liebigs Ann. Chem.* **1888**, 243, 314.
- (17) Fischer, E.; Hirschberger, J. The Mannose II. *Berichte der Deutschen Chemischen Gesellschaft* **1889**, 22, 365.
- (18) Thomas, R. W.; Schuete, H. A. Studies on levulinic acid, I. Its preparation from carbohydrates by digestion with hydrochloric acid under pressure. *J. Am. Chem. Soc.* **1931**, 53, 2324.
- (19) van Putten, R.-J.; Soetedjo, J. N. M.; Pidko, E. A.; van der Waal, J. C.; Hensen, E. J. M.; de Jong, E.; Heeres, H. J. Dehydration of Different Ketoses and Aldoses to 5-Hydroxymethylfurfural. *Chemsuschem* **2013**, 6, 1682.
- (20) Fitzpatrick, S. W. Production of levulinic acid from carbohydrate-containing materials. U.S. Patent 5608105A, June, 7, 1995.
- (21) GFBiochemicals, L. Making Levulinic Acid Happen. www.gfbiochemicals.com/company/ (accessed April 12, 2017).
- (22) Dussan, K.; Girisuta, B.; Haverty, D.; Leahy, J. J.; Hayes, M. H. B. Kinetics of levulinic acid and furfural production from *Miscanthus x giganteus*. *Bioresour. Technol.* **2013**, 149, 216–224.
- (23) Hands, C. H. G.; Whitt, F. R. The Preparation of levulinic acid on a semi-technical scale. *J. Soc. Chem. Ind.* **1947**, 66, 415.
- (24) Frost, T. R.; Kurth, E. F. Levulinic acid from wood cellulose. *TAPPI* **1951**, 34, 80.
- (25) Saeman, J. F. Kinetics of wood saccharification - hydrolysis of cellulose and decomposition of sugars in dilute acid at high temperature. *Ind. Eng. Chem.* **1945**, 37, 43.
- (26) Girisuta, B.; Danon, B.; Manurung, R.; Janssen, L. P. B. M.; Heeres, H. J. Experimental and kinetic modelling studies on the acid-catalysed hydrolysis of the water hyacinth plant to levulinic acid. *Bioresour. Technol.* **2008**, 99, 8367.
- (27) McKenzie, B. F. Levulinic acid. *Org. Synth.* **1929**, IX, 50.
- (28) Wiggins, L. F. The utilization of sucrose. *Adv. Carbohydr. Chem. Biochem.* **1949**, 4, 293–336.
- (29) Dahlmann, J. Preparation of Levulinic Acid. *Chem. Ber.* **1968**, 101, 4251.
- (30) Schraufnagel, A.; Rase, H. F. Levulinic Acid from Sucrose Using Acidic Ion-Exchange Resins. *Ind. Eng. Chem. Prod. Res. Dev.* **1975**, 14, 40.
- (31) Tarabanko, V. E.; Chernyak, M. Y.; Aralova, S. V.; Kuznetsov, B. N. Kinetics of levulinic acid formation from carbohydrates at moderate temperatures. *React. Kinet. Catal. Lett.* **2002**, 75, 117.

- (32) Mehdi, H.; Fabos, V.; Tuba, R.; Bodor, A. Integration of Homogeneous and Heterogeneous Catalytic Processes for a Multi-step Conversion of Bio-mass: From Sucrose to Levulinic Acid, γ -Valerolactone, 1,4-Pentanediol, 2-Methyl-tetrahydrofuran, and Alkanes. *Top. Catal.* **2008**, *48*, 49.
- (33) Barnett, J. W.; O' Connor, J. Solvent effects on the acid-catalysed inversion of sucrose. *J. Chem. Soc. B.* **1971**, 1163.
- (34) Antal, J. . M. J.; Mok, W. S. L.; Richards, G. N. Mechanism of formation of S(hydroxymethyl)-2-furaldehyde from D-fructose and sucrose. *Carbo-hydr. Res.* **1990**, *199*, 91.
- (35) Haworth, W. N.; Jones, W. G. M. 183. The conversion of sucrose into fu-ran compounds. Part I. 5-Hydroxymethylfurfuraldehyde and some deriv-atives. *J. Chem. Soc.* **1944**, 667.
- (36) Middendorp, J. A. Sur l'oxyméthylfurfurol. *Recl. Trav. Chim. Pays-Bas et de la Belgique.* **1919**, *38*, 1.
- (37) Pedersen, A. T.; Ringborg, R.; Grotkjær, T.; Pedersen, S.; Woodley, J. M. Synthesis of 5-hydroxymethylfurfural (HMF) by acid catalyzed dehydra-tion of glucose–fructose mixtures. *Chem. Eng. J.* **2015**, *273*, 455.
- (38) Bard, Y. *Nonlinear parameter estimation*; Academic Press: New York, 1974; 61.
- (39) Knightes, C. D.; Peters, C. A. Statistical Analysis of Nonlinear Parameter Estimation for Monod Biodegradation Kinetics Using Bivariate Data. *Bio-technol. Bioeng.* **2000**, *69*, 160.
- (40) Fachri, B. A.; Abdilla, R. M.; van de Bovenkamp, H. H.; Rasrendra, C. B.; Heeres, H. J. Experimental and Kinetic Modeling Studies on the Sulfuric Acid Catalyzed Conversion of DFructose to 5Hydroxymethylfurfural and Levulinic Acid in Water. *ACS Sustain. Chem. Eng.* **2015**, *3*, 3024.
- (41) Tewari, Y. B.; Goldberg, R. N. Thermodynamics of the conversion of aque-ous glucose to fructose. *J. Solution Chem.* **1984**, *13*, 523.
- (42) Pilath, H. M.; Nimlos, M. R.; Mittal, A.; Himmel, M. E.; Johnson, D. K. Glucose Reversion Reaction Kinetics. *J. Agric. Food Chem.* **2010**, *58*, 6131.
- (43) Watanabe, M.; Aizawa, Y.; Iida, T.; Aida, T. M.; Levy, C.; Su, K.; Inomata, H. Glucose reactions with acid and base catalysts in hot compressed water at 473 K. *Carbohydr. Res.* **2005**, *340*, 1925.
- (44) Vukov, K. Kinetic aspects of sucrose hydrolysis. *Int. Sugar J.* **1965**, *67*, 798.
- (45) Hartofylax, V. H.; Efstathiou, C. E.; Hadjiioanno, T. P. Kinetic study of the acid hydrolysis of sucrose and lactose and kinetic determination of sucrose using a periodate-selective electrode. *Anal. Chim. Acta.* **1989**, *224*, 159.

- (46) Bower, S.; Wickramasinghe, R.; Nagle, N. J.; Schell, D. J. Modeling sucrose hydrolysis in dilute sulfuric acid solutions at pretreatment conditions for lignocellulosic biomass. *Bioresour. Technol.* **2008**, *99*, 7354.
- (47) Rhim, J. W.; Nunes, R. V.; Jones, A.; Swartzel, K. R. Determination of kinetic parameters using linearly increasing temperature. *J. Food Sci.* **1989**, *54*, 446.
- (48) Miles, J. J.; Swartzel, K. R. Development of sucrose inversion kinetics under continuous flow conditions. *J. Food Qual.* **1995**, *18*, 369.
- (49) Khajavi, S. H.; Kimura, Y.; Oomori, T.; Matsuno, R.; Adachi, S. Kinetics on sucrose decomposition in subcritical water. *LWT - Food Sci. Technol.* **2005**, *38*, 297.
- (50) Torres, A. P.; Oliveira, F. A. R.; Silva, C. L. M. The Influence of pH on the kinetics of acid hydrolysis of sucrose. *J. Food Process. Eng.* **1994**, *17*, 191.
- (51) Plazl, I.; Leskovsek, S.; Koloin, T. Hydrolysis of sucrose by conventional and microwave heating in stirred tank reactor. *Chem. Eng. J.* **1995**, *59*, 253.
- (52) Dickson, A. G.; Wesolowski, D. J.; Palmer, D. A.; Mesmer, R. E. Dissociation Constant of Bisulfate Ion in Aqueous Sodium Chloride Solution to 250 °C. *J. Phys. Chem.* **1990**, *94*, 7978.
- (53) Chang, C.; Ma, X.; Cen, P. Kinetic Studies on Wheat Straw Hydrolysis to Levulinic Acid. *Chinese J. Chem. Eng.* **2009**, *17*, 835.
- (54) Chang, C.; Ma, X.; Cen, P. Kinetics of Levulinic Acid Formation from Glucose Decomposition at High Temperature. *Chinese J. Chem. Eng.* **2006**, *14*, 708.
- (55) McKibbins, S. W.; Harris, J. F.; Saeman, J. F.; Neill, W. K. Kinetics of the Acid Catalyzed Conversion of Glucose to 5-Hydroxymethyl-2-Furaldehyde and Levulinic Acid. *Forest Prod. J* **1962**, *12*, 17.
- (56) Girisuta, B.; Janssen, L. P. B. M.; Heeres, H. J. A kinetic study on the decomposition of 5-hydroxymethylfurfural into levulinic acid. *Green Chem.* **2006**, *8*, 701.
- (57) Heimlich, K. R.; Martin, A. N. A Kinetic Study of Glucose Degradation in Acid Solution. *J. of Pharm. Sci.* **1960**, *49* (9), 592.
- (58) Asghari, F. S.; Yoshida, H. Kinetics of the decomposition of fructose catalyzed by hydrochloric acid in subcritical water: Formation of 5-hydroxymethylfurfural, levulinic, and formic acids. *Ind. Eng. Chem. Res.* **2007**, *46* (23), 7703.
- (59) Li, Y.; Lu, X.; Yuan, L.; Liu, X. Fructose Decomposition Kinetics in Organic Acids-Enriched High Temperature Liquid Water. *Biomass Bioenergy* **2009**, *33* (9), 1182.

- (60) Carniti, P.; Gervasini, A.; Biella, S.; Auroux, A. Niobic acid and niobium phosphate as highly acidic viable catalysts in aqueous medium: fructose dehydration reaction. *Catal. Today* **2006**, *118*, 373.
- (61) Baugh, K. D.; McCarty, P. L. Thermochemical Pretreatment of Lignocellulose to Enhance Methane Fermentation: I. Monosaccharide and Furfurals Hydrothermal Decomposition and Product Formation Rates. *Bio-technol. Bioeng.* **1988**, *31*, 50.
- (62) Kupiainen, L.; Ahola, J.; Tanskanen, J. Kinetics of glucose decomposition in formic acid. *Chem. Eng. Res. Des.* **2011**, *89*, 2706.
- (63) Shen, J.; Wyman, C. E. Hydrochloric Acid-Catalyzed Levulinic Acid Formation from Cellulose: Data and Kinetic Model to Maximize Yields. *AIChE J.* **2012**, *58*, 236.
- (64) Akaike, H. A New Look at The Statistical Model Identification. *IEEE Trans. Autom. Control.* **1974**, *AC-19*, 716.
- (65) Goldberg, R.; Tewari, Y.B. Thermodynamics of Enzyme Catalyzed Reactions: Part 5. Isomerases and Ligases. *J. Phys. Chem. Ref. Data* **1995**, *24*, 1775.

APPENDIX FOR CHAPTER 2:

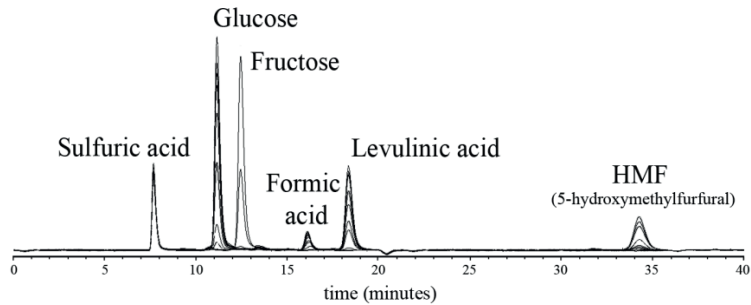


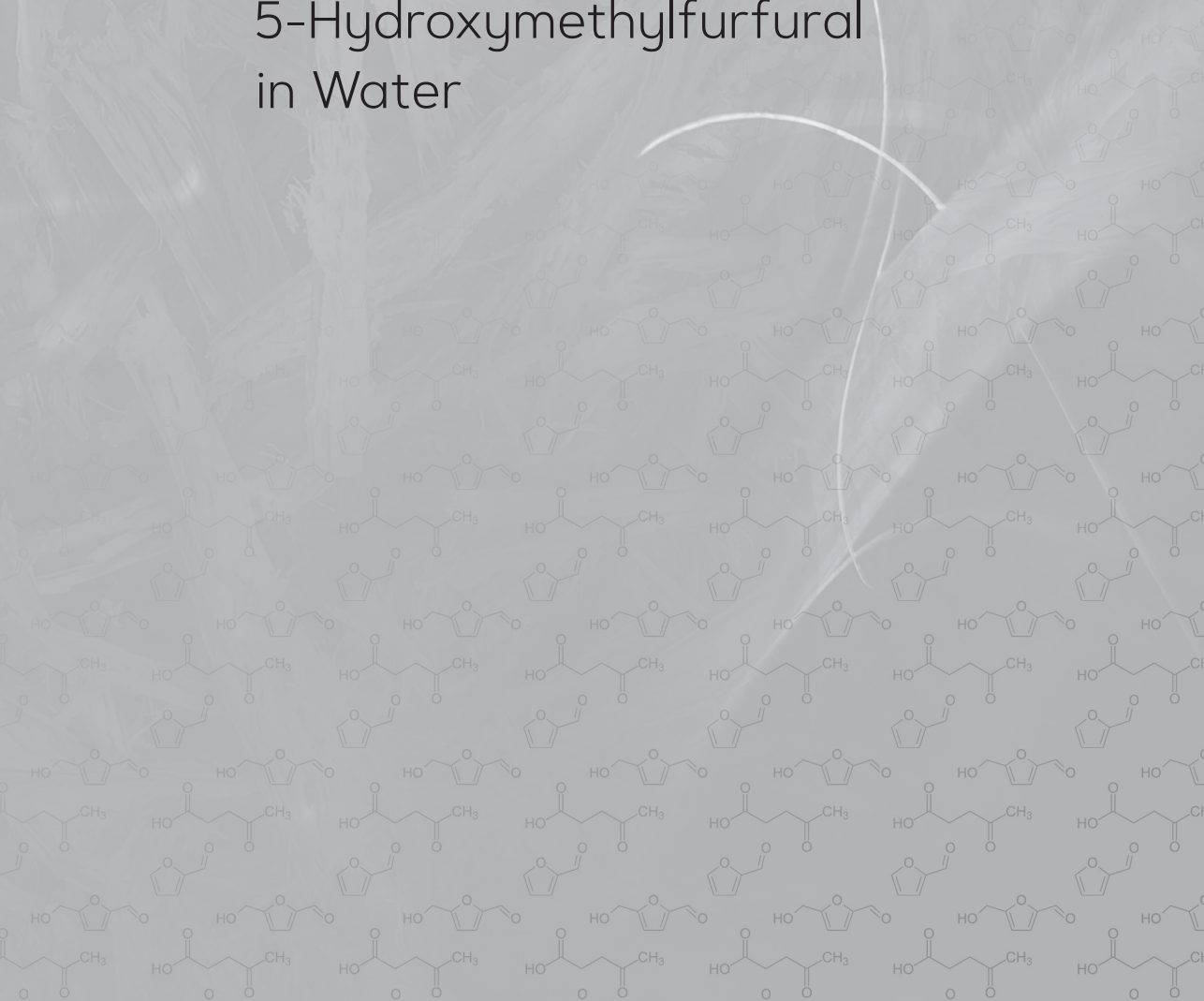
Figure S1. Typical HPLC chromatogram using a HPX-87H Biorad Aminex organic acid column

Table S1: Orders in substrates using a powerlaw model (Model 2)

	model value	\pm
α_G	1.50	1.00
α_F	1.58	0.20
α_H	0.94	0.08

CHAPTER 3.

Reactivity Studies on the
Acid-Catalysed Dehydration
of 2-Ketohexoses to
5-Hydroxymethylfurfural
in Water



ABSTRACT

We here report an experimental and kinetic study on the reactivity of the four possible ketohexoses (fructose, tagatose, sorbose and psicose) for HMF synthesis in water using sulphuric acid as the catalyst ($C_{\text{sugar}} = 65 \text{ g/L}$ (0.36 M), 137°C , acid concentrations between 33 and 300 mM). Significant differences in reactivity were observed and tagatose and psicose were by far more reactive than fructose and sorbose. The best results when considering HMF yield was found for psicose (50% at 90% ketohexose conversion), indicating that this ketohexose is a very suitable source for HMF synthesis. A more detailed study for psicose (9 experiments, $C_{\text{psicose}} = 65 \text{ g/L}$ (0.36 M), 100, 120 and 137°C , acid concentrations between 33 and 300 mM) reveals that the conversion versus time curves for the batch experiments are well described with a first order dependency in psicose and acid. The activation energy for the reaction was calculated to be $158 \pm 9 \text{ kJ/mol}$. The reactivity of the sugars in water was significantly lower than previously found for methanol.

The results described in this Chapter were obtained in a collaboration with Avantium, The Netherlands. Jenny N. M. Tan-Soetedjo and Robert Jan van Putten contributed to this Chapter and it is therefore (partly) included in both PhD theses.

Part of the research described in this Chapter is published in:
van Putten, R.J.; Soetedjo, J. N. M.; Pidko, E. A.; van der Waal, J. C.; Hensen, E. J. M.; de Jong, E.; Heeres, H. J., Dehydration of Different Ketoses and Aldoses to 5-Hydroxymethylfurfural, *ChemSusChem* **2013**, 6 (9), pp 1681–1687.

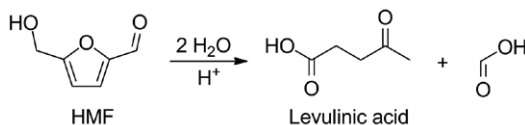
1. INTRODUCTION

The replacement of fossil feedstocks with sustainable resources for energy generation, transportation fuels, bulk and fine chemicals and materials is currently considered as a pivotal challenge, receiving increasing social and scientific interest. To achieve this, alternative sources of organic carbon need to be identified. Biomass is an attractive option as it is the most abundant non-fossil source of organic carbon. Biomass mainly comprises carbohydrates, lignin, fatty acids, lipids and proteins. Carbohydrates represent the largest fraction of biomass, predominantly present in polymeric form (cellulose, hemi-cellulose, starch, inulin) and are built up from hexoses (glucose, fructose, mannose, galactose) and pentoses (arabinose, xylose). The acid-catalysed dehydration of pentoses¹⁻³ and hexoses⁴ leads to the formation of furfural and 5-hydroxymethylfurfural (HMF), respectively, along with many by-products. Both molecules, and derivatives thereof, are in Bozell's 'Top 10 + 4' list of biobased chemicals and are considered to be key components in the greening up of the chemical industry⁵. This has led to an enormous increase in research published on acid-catalysed dehydration of sugars over the last decade^{3,4}.

Both furfural and HMF can be used in different application areas. Furfural has high potential in fuel and solvent applications. HMF is considered a promising platform chemical due to its high derivatisation potential. It can be converted to a wide range of interesting bulk and fine chemicals, for instance as a monomer for novel biobased polymers. Avantium is currently developing a process for the production of polyethylenefurandicarboxylate (PEF) from C6 sugars as a next generation replacement material for PET, having improved barrier properties⁶⁻⁹.

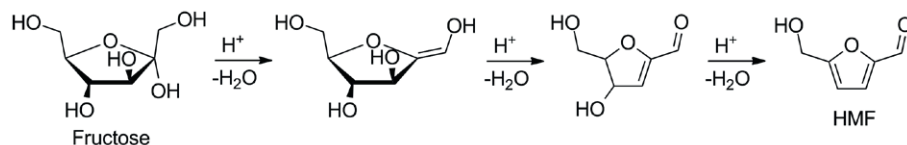
The attention for the development of highly efficient routes to HMF has strongly increased in recent years⁴. Glucose or glucose-based oligomers and polymers, especially those derived from lignocellulosic sources, are favoured feedstocks due to their availability and presence in agricultural side streams and other waste^{10,11}. The vast majority of experimental studies, however, shows that fructose, a ketose, is much more efficiently dehydrated to HMF than glucose, an aldose. Under aqueous acidic conditions fructose yields a maximum of around 50% HMF at best, due to the formation of polymeric material, known as humins, and hydration of HMF to levulinic and formic acids (Scheme 1)^{4,12,13}. For glucose the maximum HMF yield is only around 5%. Higher HMF yields from fructose (>80%) have been reported in other solvent systems, especially in ionic liquids and aprotic polar solvents such as DMSO⁴. Work on glucose dehydration with heterogeneous base/acid bi-catalytic

systems^{14–17}, chromium catalysed glucose dehydration in ionic liquids^{18,19} and organic solvents²⁰ and other catalysts^{21,22}, indicate that apart from an acid, an additional catalyst is required to efficiently dehydrate glucose to HMF. This additional catalyst is generally believed to facilitate the isomerisation of glucose to fructose prior to dehydration to HMF⁴.



Scheme 1. The hydration of HMF to levulinic acid and formic acid

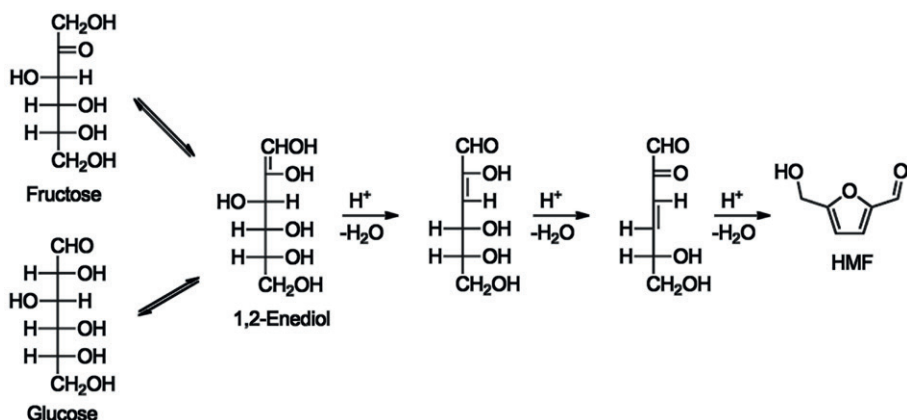
To improve the yields, significant steps must be made in the development of catalysts, preferably heterogeneous in nature. In order to do so detailed knowledge of the reaction mechanism of the main and side reactions is required. A number of reaction mechanisms have been proposed for the dehydration reaction in water, though no definitive evidence has yet been found to confirm these⁴. The postulated mechanisms can be divided in mechanisms with cyclic (Scheme 2) or acyclic intermediates (Scheme 3).



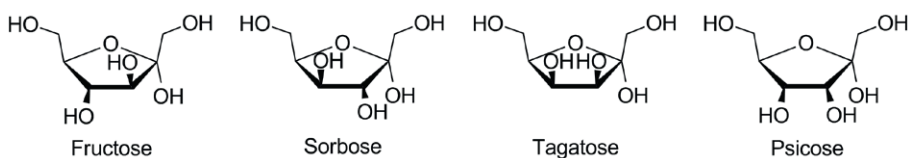
Scheme 2. Proposed dehydration mechanism with cyclic intermediates

Knowledge about the effect of the relative orientation of the hydroxyl groups of different ketoses on the dehydration rate and selectivity to HMF is scarcely available in the literature. Seri *et al.* reported a lower HMF yield from sorbose than from fructose in DMSO, though no conversion data were provided²³. Determination of the influence of the orientation of hydroxyl groups in ketohexoses could very well provide new insights in the mechanism of ketohexose dehydration. For this reason, the acid-catalysed dehydration of 4 possible ketohexoses, viz. fructose, sorbose, tagatose and psicose (Scheme 4) was investigated.

Qualitative studies in methanol using the four ketohexoses have been reported recently by our group and revealed that tagatose and psicose the most reactive in methanol, and that psicose gave the highest selectivity towards HMF and its methyl ether methoxymethylfurfural (MMF)²⁴.



Scheme 3. Proposed dehydration mechanism with acyclic intermediates



Scheme 4: The α -D-furanose structures of the four ketohexoses used in this study

The current study involves a kinetic modeling study on the acid-catalysed dehydration of fructose, tagatose, sorbose and psicose in water using sulphuric acid as the catalyst. We have recently reported a screening study in a high throughput screening device for these four ketohexoses in water using sulphuric acid as the catalyst (33 mM H_2SO_4) at a fixed temperature of 120 °C. Significant differences in reactivity were observed and tagatose (48% conversion after 75 min) and psicose (35% conversion after 75 min) were clearly more reactive than fructose and sorbose (around 20% conversion after 75 min). The selectivity to HMF was found to be higher for fructose and psicose than for tagatose and sorbose. However, the sugar conversion window was limited to max. 50% and this hampered analysis of the data and particularly to determine the conditions and ketohexose conversion level at which the HMF yield is highest for the various ketohexoses.

The objectives of the current study were i) to experimentally determine the reactivity of the 4 sugars in water at a much wider ketohexose conversion

range and to ii) to quantify the results in terms of kinetic data (kinetic constants and activation energies). Initial experiments were performed in batch at limited experimental conditions using all ketohexoses and relevant kinetic parameters were determined. In the second stage, more detailed studies were performed using psicose to obtain better kinetic insights for this particular ketohexose. Finally, the reactivity patterns in water will be compared with those previously obtained in methanol by our group.

2. EXPERIMENTAL SECTION

2.1 Kinetic Experiments

Initial Experiments with the 4 Ketohexoses

Fructose (99%), sorbose (98%), tagatose (98%) and sulphuric acid (96%) were purchased from Sigma-Aldrich while psicose (98%) was purchased from Carbosynth. Milli-Q quality water was used for all experiments and sample preparations. All experiments were performed at 0.5 mL scale in sealed glass ampoules. The ampoules were filled with 65 gL⁻¹ (0.36 M) of the sugar in water containing sulphuric acid (concentrations of 33, 100 and 300 mM). The ampoules were placed in an oven at a temperature of 137 °C. After the pre-determined reaction time, the ampoules were taken out and cooled in water (8 °C). The reaction mixture was then filtered over a 0.45 µm PTFE syringe filter and diluted 7–9 times in water before analysis by HPLC. These were carried out using an Agilent 1200 HPLC with a Bio-rad Aminex HPX-87H column. A 5 mM sulphuric acid solution in water was used as the eluent with a flow rate of 0.55 mL min⁻¹. Detection was performed using a refractive index and UV (210 nm) detector.

Detailed Kinetic Studies using Psicose

Psicose (98%) was purchased from Carbosynth. Milli-Q quality water was used for all experiments. The experiments were performed at 0.5 mL scale in sealed glass ampoules which were heated in an oven at three different temperatures (100 °C, 120 °C, 137 °C). A substrate concentration of 65 gL⁻¹ (0.36 M) in water was used and the sulphuric acid concentration was 33, 100 or 300 mM.

The ampoules were directly cooled in cold water after the appropriate reaction time. The reaction mixture was filtered over a 0.45 μm PTFE syringe filter and diluted 7–9 times in water for analysis on an Agilent 1200 HPLC with a Bio-rad Aminex HPX-87H column. A 5 mM sulphuric acid solution in water was used as the eluent with a flow rate of 0.55 mLmin^{-1} . Detection was performed using a refractive index and UV (210 nm) detector.

Determination of the Kinetic Parameters

The kinetic parameters were determined using a maximum likelihood approach, which is based on minimization of errors between the experimental data and the kinetic model. For each hexose, the datasets obtained at the three different acid concentrations were solved simultaneously. Error minimisation was performed using the MATLAB toolbox lsqnonlin.

For the more detailed study using psicose, 9 experimental datasets ($T = 100, 120, 137^\circ\text{C}$, $C_{\text{H}_2\text{SO}_4} = 33, 100, 300 \text{ mM}$) were modeled simultaneously.

3. RESULTS AND DISCUSSION

3.1 Screening Studies for The Four Ketohexoses

Experiments to quantify the differences in reactivity and the maximum attainable HMF yield for the 4 ketohexoses were performed at 137°C with 33, 100 and 300 mM sulphuric acid as the catalysts with batch times between 0 and 90 minutes. The concentration versus batch time curves for the ketohexoses at 33 mM sulphuric acid are given in Figure 1. Clear differences in reactivity are visible, and it is evident that psicose and tagatose are the most reactive of the 4 and show about equal reactivity. Fructose and sorbose are also equally reactive, though are by far less reactive than tagatose and psicose. When considering the stereochemistry of the four ketohexoses (Scheme 4) at the C3 and C4 position, it appears that the highest reactivity is found when the two alcohol groups are oriented in a *cis* position.

Figure 2 shows the HMF yield versus the ketohexose conversion for all experiments. At low conversions ($< 50\%$), the general trend is the same as for the experiments in the high-throughput screening reported earlier by our group, with approximately 30–40% HMF yield at 50% sugar conversion.

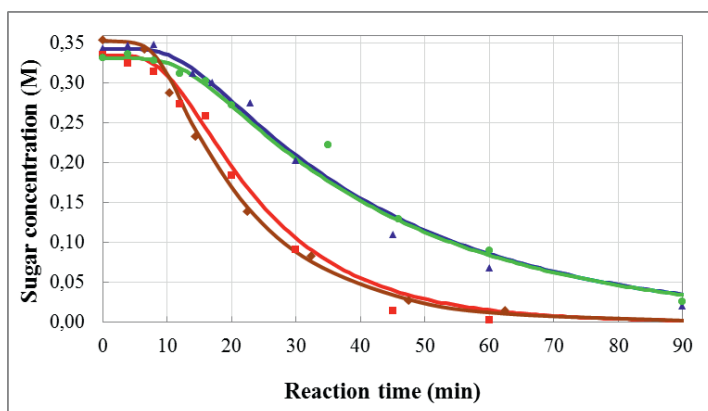


Figure 1. Ketohexose concentrations versus batch time at 137 °C with 33 mM sulphuric acid. Points: experimental data (fructose ▲, tagatose ■, sorbose ●, and psicose ◆). Lines: model prediction.

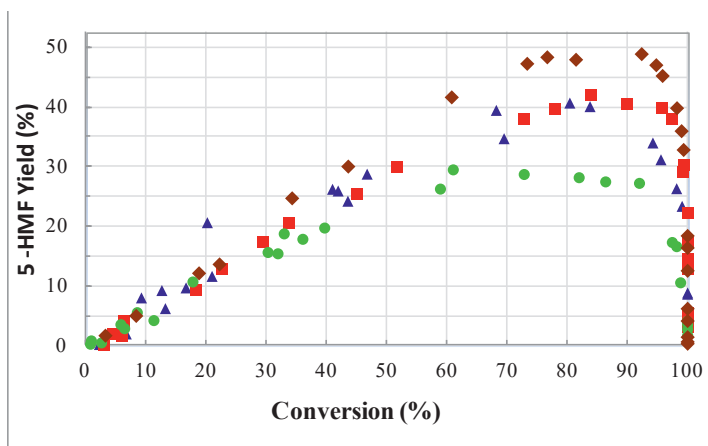


Figure 2. HMF yield versus conversion for the ketohexoses at 137 °C and three acid concentrations (33, 100 and 300 mM; fructose ▲, tagatose ■, sorbose ● and psicose ◆)

The differences in HMF yields versus conversion for the various ketohexoses become by far more pronounced at higher conversion levels (Figure 2). The highest HMF yields were obtained at about 80–90% ketohexose conversion. At higher conversion levels, the yield drops due to the formation of levulinic acid. Remarkable differences between the 4 ketohexoses when considering

the maximum attainable HMF yield were observed. Best results were obtained for psicose, with a maximum HMF yield of about 50%. Fructose and tagatose showed similar profiles with a maximum HMF yield of about 40%, whereas the maximum HMF yield for sorbose is only 30%. Thus, psicose not only is the most reactive ketohexoses (Figure 1), but also give the highest HMF yields, and as such are the preferred ketohexoses for HMF formation when performing the reactions using sulphuric acid as the catalyst in aqueous media.

3.2 Kinetic Studies for The Four Ketohexoses

3

The experimental data (Figure 1) were modeled using a simple kinetic expression assuming first order in sugar and acid (equations 1 and 2).

$$R_{sugar} = -k \cdot C_{sugar} \cdot C_{H^+} \quad (1)$$

$$k = k_{ref} e^{-\left(\frac{E_a}{R}\right) \times \left(\frac{1}{T} - \frac{1}{T_{ref}}\right)} \quad (2)$$

Here, k_{ref} is the reaction rate constant at 137 °C (T_{ref}) and T_i is the initial temperature (25 °C). At the initial stage of the reaction, the temperature is not constant as it takes typically 5–10 minutes to reach 137 °C. This effect was compensated for by extending the model with an energy balance. After integration, equation 7 is obtained, which, combined with the mass balances in batch, allows calculation of the concentration and the temperature as a function of the batch time. The values for the parameter h were determined experimentally.

$$T = T_{ref} - (T_{ref} - T_i) \cdot e^{(-ht)} \quad (3)$$

The experimental data (137 °C, 33 mM sulphuric acid) and the model lines for the four ketoses are provided in Figure 1. Agreement between model and experimental data is very satisfactory (c.f. R^2 values and the error in $k_{1,ref}$ as given in Table 1). The results from the kinetic study are in line with the screening experiments reported earlier by our group, with tagatose and psicose being the most reactive ketoses. This is clearly illustrated by the significantly higher $k_{1,ref}$ values for tagatose and psicose than for fructose and sorbose. The $k_{1,ref}$ values for the two most reactive sugars (tagatose and psicose) and the least reactive ones (sorbose and fructose) are equal within the experimental error, which is also in line with the experimental observations (Figure 1).

Table 1. Kinetic data for the acid-catalysed dehydration of different ketoses

Ketose	k _{ref} (L.mol ⁻¹ min ⁻¹)	E _a (kJ mol ⁻¹)	R ²
Fructose	0.90 ± 0.11	120 ± 22	0.99
Tagatose	1.9 ± 0.60	89 ± 15	0.99
Sorbose	0.90 ± 0.19	140 ± 42	0.98
Psicose ^a	2.0 ± 0.21	158 ± 9	0.99

^aData obtained with a more extended experimental program

3.3 Extended Kinetic Studies for Psicose

Given the fact that psicose is among the most reactive ketohexose in this study (Figure 1), and gives the highest HMF yield, extended kinetic studies were conducted using psicose. A total of 9 experiments were performed with an initial sugar concentration of 65 mg/L (0.36 M) at three temperatures (100 °C, 120 °C and 137 °C) and three sulphuric acid concentrations (33, 100 and 300 mM). All experiments were conducted in a batch mode using glass ampoules. The experimental data were modeled simultaneously using a simple kinetic expression assuming a first order dependency in psicose and acid (equations 1 and 2). Here, k_{ref} describes the reaction rate constant at 137 °C (T_{ref}) and T_i is the initial temperature (25 °C). The temperature dependence of the h value was determined experimentally and found to be linearly related with the temperature (eq 4), where T is the temperature in K.

$$h = 0.00128 \times T \quad (4)$$

The experimental data and the model lines for two representative experiments are given in Figure 3. The other data are presented in Figure S1 in Supplementary Data. Good agreement between the model and experimental datapoints was obtained. The k value at reference temperature was 2.0 ± 0.2 L.mol⁻¹min⁻¹, which is within the experimental error similar to the one obtained for tagatose (Table 1).

The good agreement between the model and the experimental data is also evident from the R^2 value of 99.04% and the parity plot as given in Figure 4.

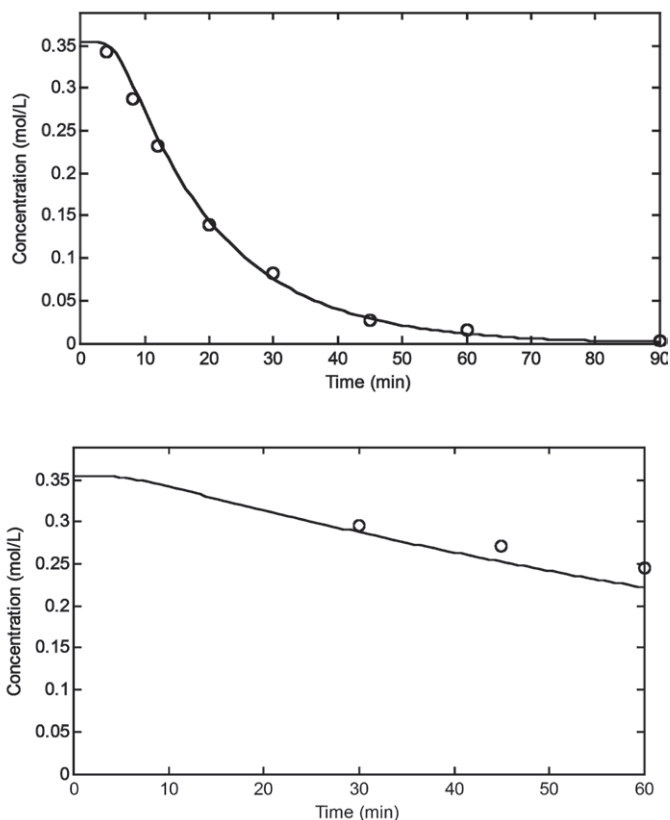


Figure 3. Experimental data points and model lines for two representative experiments using psicose (top: $T = 137\text{ }^{\circ}\text{C}$, $C_{\text{H}_2\text{SO}_4} = 0.033\text{ M}$; bottom: $T = 120\text{ }^{\circ}\text{C}$, $C_{\text{H}_2\text{SO}_4} = 0.033\text{ M}$).

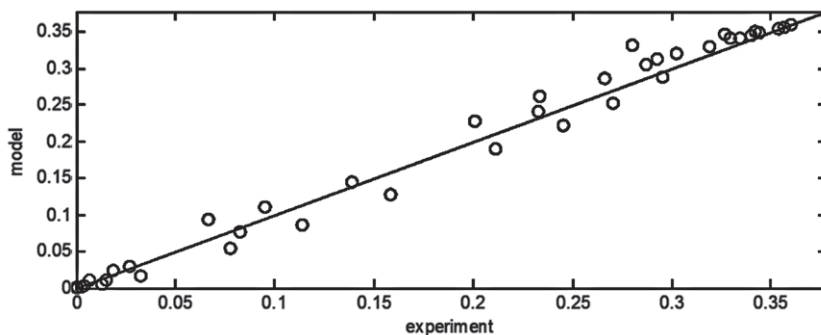


Figure 4. Experimental versus model psicose concentrations

3.4 Solvent Effects: Reactivity in Water versus Methanol

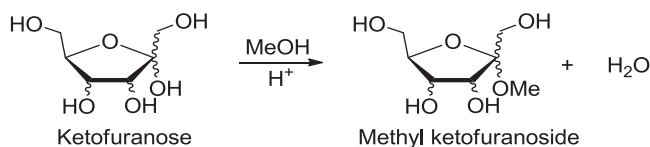
Solvent effects are well established in sugar conversions to platform chemicals and may be used to enhance reaction rates and product selectivities. As such it is of interest to compare the reactivity of the 4-ketohexoses in water (as reported here) with to those obtained in methanol (previous study by our group)²⁴. It appears that the reactivity of the hexoketoses is by far lower in water than in methanol, indicating that the ketohexoses are apparently more stable in water than in methanol. For instance, about 50% tagatose conversion was observed after 20 min batch time in water (137 °C, 33 mM sulphuric acid, Figure 1), whereas in methanol the same conversion was obtained after 15 min under much less severe conditions (100 °C, 17 mM sulphuric acid)²⁵. Thus solvent effects are pronounced when considering the conversion of ketohexoses to HMF. Possible explanations include i) differences in stabilisation of the 4-ketohexoses or reactive intermediates by hydrogen bonding in water and methanol, ii) differences in the tautomeric distribution in water and methanol and iii) the formation of methyl ketosides in the case of methanol.

When considering point ii), it is well known that the time scale of tautomeric rearrangements of sugars in water²⁶ is in general much faster than that of the dehydration reaction of hexoses to HMF²⁷. As such, the tautomeric distribution is not expected to be of major influence when considering solvent effects. However, the formation of methyl ketosides in methanol (point iii) likely plays an important role (Scheme 5). It is well known that methyl ketosides are formed in acidic methanol at relatively mild conditions and as such are expected to be formed rapidly in our window of operation and play a major role²⁴. It is well possible that the rates of the dehydration reactions to HMF are faster for methylketosides than for the parent ketohexose.

In the earlier studies performed in methanol in our group, a reaction mechanism was proposed involving cyclic intermediates (Scheme 2 for D-fructose). When considering that the reactivity pattern for the four ketohexoses in water follows the same order as in methanol, this mechanism is most likely also valid for reactions in water.

4. CONCLUSIONS

Significant differences in reactivity between the four ketohexoses for the acid-catalysed dehydration to HMF in water were observed. Psicose and tagatose



Scheme 5: The formation of methyl ketosides in methanol

were shown to be more reactive and were converted at a higher rate than fructose and sorbose. Furthermore, the selectivity for HMF formation was higher for psicose and fructose than for sorbose and tagatose. For psicose, the highest HMF yield at 137 °C was about 50% at a sugar conversion of 80–90%. Thus, psicose appears to be the best substrate for HMF production in water, as it has a higher selectivity for HMF formation than sorbose and tagatose, and a higher reactivity than fructose. Therefore, psicose is a very suitable ketohexose for the synthesis of HMF and its derivatives²⁸. However, psicose is a rare sugar, present in only small amounts in some biomass sources like wheat, *Itea* plants, processed sugar cane and beet molasses^{29–32}. As such either a psicose producing organism or an isomerisation process to obtain psicose from readily accessible sugars would be required to develop a techno-economically viable process for HMF production from psicose³³.

5. ACKNOWLEDGEMENT

J.N.M. Tan-Soetedjo acknowledges the Ministry of Education of the Indonesian Government, particularly the Directorate General of Higher Education (DIKTI) for providing a PhD scholarship. We also acknowledge support by Henk van de Bovenkamp from the Department of Chemical Engineering of the University of Groningen for kinetic modeling. R.J. van Putten, J.C. van der Waal and E. de Jong from Avantium, the Netherlands are thanked for various discussions and valuable input.

REFERENCES

1. Dias, A. S.; Lima, S.; Pilinger, M.; Valente, A. A. III. Chemical Reactions, Sustainable Processes, and Environment: 8. Furfural and Furfural-Based Industrial Chemicals. In *Ideas in Chemistry and Molecular Sciences: Advances in Synthetic Chemistry*; Pignataro, B., Ed.; Wiley-VCH Verlag GmbH & Co. KGaA: Weinheim, Germany, 2010; pp 167–186.
2. Lange, J.-P.; van der Heide, E.; van Buijtenen, J.; Price, R. Furfural—A Promising Platform for Lignocellulosic Biofuels. *ChemSusChem* **2012**, *5* (1), 150–166.
3. van Putten, R.-J.; Dias, A. S.; de Jong, E. 4. Furan-Based Building Blocks from Carbohydrates. In *Catalytic Process Development for Renewable Materials*, 1st ed.; Imhof, P., van der Waal, J.-K., van der Waal, J. C., Eds.; Wiley-VCH Verlag GmbH & Co.: Weinheim, Germany, 2013; pp 81–117.
4. van Putten, R.-J.; van der Waal, J. C.; de Jong, E.; Rasrendra, C. B.; Heeres, H. J.; de Vries, J. G. Hydroxymethylfurfural, A Versatile Platform Chemical Made from Renewable Resources. *Chemical Reviews* **2013**, *113* (3), 1499–1597.
5. Bozell, J. J.; Petersen, G. R. Technology development for the production of biobased products from biorefinery carbohydrates—the US Department of Energy’s “Top 10” revisited. *Green Chemistry* **2010**, *12* (4), 539–554.
6. Gruter, G. J. M.; Dautzenberg, F. Avantium International BV. WO 2007104514, 2007.
7. Munoz, d. D.; Schammel, W. P.; Dam, M. A.; Gruter, G. J. M. Furanix Technologies BV. WO2011043660, 2011.
8. Sipos, L. Furanix Technologies BV. WO2010077133, 2010.
9. de Jong, E.; Dam, M. A.; Sipos, L.; Gruter, G. J. M. Biobased Monomers, Polymers and Materials. *ACS Symp. Ser.*, Anaheim, CA, 2012; pp 1–11.
10. Bauen, A.; Berndes, G.; Junginger, M.; Londo, M.; Vuille, F.; Ball, R.; Bole, T.; Chudziak, C.; Faaij, A.; Mozaffarian, H. *Bioenergy: a Sustainable and Reliable Energy Source: A Review of Status and Prospects*; Main Report; IEA Bioenergy, 2009.
11. Serrano-Ruiz, J. C.; Dumesic, J. A. Catalytic Routes for The Conversion of Biomass Into Liquid Hydrocarbon Transportation Fuels. *Energy Environ. Sci.* **2011**, *4* (1), 83–99.
12. Girisuta, B.; Janssen, L. P. B. M.; Heeres, H. J. A kinetic study on the decomposition of 5-hydroxymethylfurfural into levulinic acid. *Green Chemistry* **2006**, *8*, 701–709.

13. Kuster, B. F. M. 5-Hydroxymethylfurfural (HMF). A Review Focusing on its Manufacture. *Starch/Starke* **1990**, *42*, 314–321.
14. Ohara, M.; Takagaki, A.; Nishimura, S.; Ebitani, K. Syntheses of 5-Hydroxymethylfurfural and Levoglucosan by Selective Dehydration of Glucose Using Solid Acid and Base Catalysts. *Appl. Catal., A* **2010**, *383* (1–2), 149–155.
15. Nikolla, E.; Román-Leshkov, Y.; Moliner, M.; Davis, M. E. “One-Pot” Synthesis of 5-(Hydroxymethyl)furfural from Carbohydrates using Tin-Beta Zeolite. *ACS Catal.* **2011**, *1* (4), 408–410.
16. Grande, P. M.; Bergs, C.; de Maria, P. D. Chemo-Enzymatic Conversion of Glucose into 5-Hydroxymethylfurfural in Seawater. *ChemSusChem* **2012**, *5* (7), 1203–1206.
17. Chareonlimkun, A.; Champreda, V.; Shotipruk, A.; Laosiripojana, N. Reactions Of C5 and C6-Sugars, Cellulose, and Lignocellulose under Hot Compressed Water (HCW) in The Presence of Heterogeneous Acid Catalysts. *Fuel* **2010**, *89* (10), 2973–2880.
18. Zhao, H.; Holladay, J. E.; Brown, H.; Zhang, Z. C. Metal Chlorides in Ionic Liquid Solvents Convert Sugars to 5-Hydroxymethylfurfural. *Science* **2007**, *316* (5831), 1597–1600.
19. Pidko, E. A.; Volkan, D.; van Santen, R. A. Glucose Activation by Transient Cr²⁺. *Angew. Chem. Int. Ed.* **2010**, *49*, 2530–2534.
20. Binder, J. B.; Raines, R. T. J. Simple Chemical Transformation of Lignocellulosic Biomass into Furans for Fuels and Chemicals. *J. Am. Chem. Soc.* **2009**, *131*, 1979–1985.
21. Ståhlberg, T.; Rodriguez-Rodriguez, S.; Fristrup, P.; Riisager, A. Metal-Free Dehydration of Glucose to 5-(Hydroxymethyl) furfural in Ionic Liquids with Boric Acid as a Promoter. *A. Chem. Eur. J.* **2011**, *17* (5), 1456–1464.
22. Hu, S.; Zhang, Z.; Song, J.; Zhou, Y. Efficient Conversion of Glucose into 5-Hydroxymethylfurfural Catalyzed by a Common Lewis Acid SnCl₄ in an Ionic Liquid. *Green Chem.* **2009**, *11*, 1746–1749.
23. Seri, K.-i.; Inoue, Y.; Ishida, H. Highly Efficient Catalytic Activity of Lanthanide (III) Ions for Conversion of Saccharides to 5-Hydroxymethyl-2-Furfural in Organic Solvents. *Chem. Lett.* **2000**, *29* (1), 22–23.
24. van Putten, R.-J.; van der Waal, J. C.; Harmse, M.; van de Bovenkamp, H. H.; de Jong, E.; Heeres, H. J. A Comparative Study on The Reactivity of Various Ketohexoses to Furanics in Methanol. *ChemSusChem* **2016**, *9* (14), 1827–1834.
25. van Putten, R.-J.; Winkelman, J. G. M.; Keihan, F.; van der Waal, J. C.; de Jong, E.; Heeres, H. J. Experimental and Modeling Studies on the Solubility

- of D-Arabinose, D-Fructose, D-Glucose, D-Mannose, Sucrose and D-Xylose in Methanol and Methanol-Water Mixtures. *Ind. Eng. Chem. Res.* **2014**, *53*, 8285–8290.
26. Wertz, P. W.; Garver, J. C.; Anderson, L. Anatomy of A Complex Mutarotation—Kinetics of Tautomerization of Alpha-D-Galactopyranose and Beta-D-Galactopyranose in Water. *Journal of The American Chemical Society* **1981**, *103* (13), 3916–3922.
27. van Putten, R.-J.; Soetedjo, J. N. M.; Pidko, E. A.; van der Waal, J. C.; Hensen, E. J. M.; de Jong, E.; Heeres, H. J. Dehydration of Different Ketoses and Aldoses to 5-Hydroxymethylfurfural. *Chemsuschem* **2013**, *6* (9), 1682–1687.
28. van Putten, R.-J.; van der Waal, J. C.; de Jong, E. A process for the catalysed conversion of psicose into 5-hydroxymethylfurfural or an alkyl ether thereof. WO2015133902 A1, September 11, 2015.
29. Miller, B. S.; Swain, T. *J. Sci. Food Agric.* **1960**, *11*, 344–348.
30. Binkley, W. W. *Int. Sugar J.* **1963**, *65*, 105–106.
31. Hossain, A.; Yamaguchi, F.; Matsunaga, T.; Hirata, Y.; Kamitori, K.; Dong, Y.; Sui, L.; Tsukamoto, I.; Ueno, M.; Tokuda, M. *Biophys. Res. Commun.* **2012**, *425*, 717–723.
32. Baek, S. H.; Park, S. J.; Lee, H. G. *J. Food Sci.* **2010**, *75*, 49–53.
33. Izumori, K.; Yamakita, M.; Tsumura, T.; Kobayashi, H. *J. Ferment. Bioeng.* **1990**, *70*, 26–29.

APPENDIX FOR CHAPTER 3:

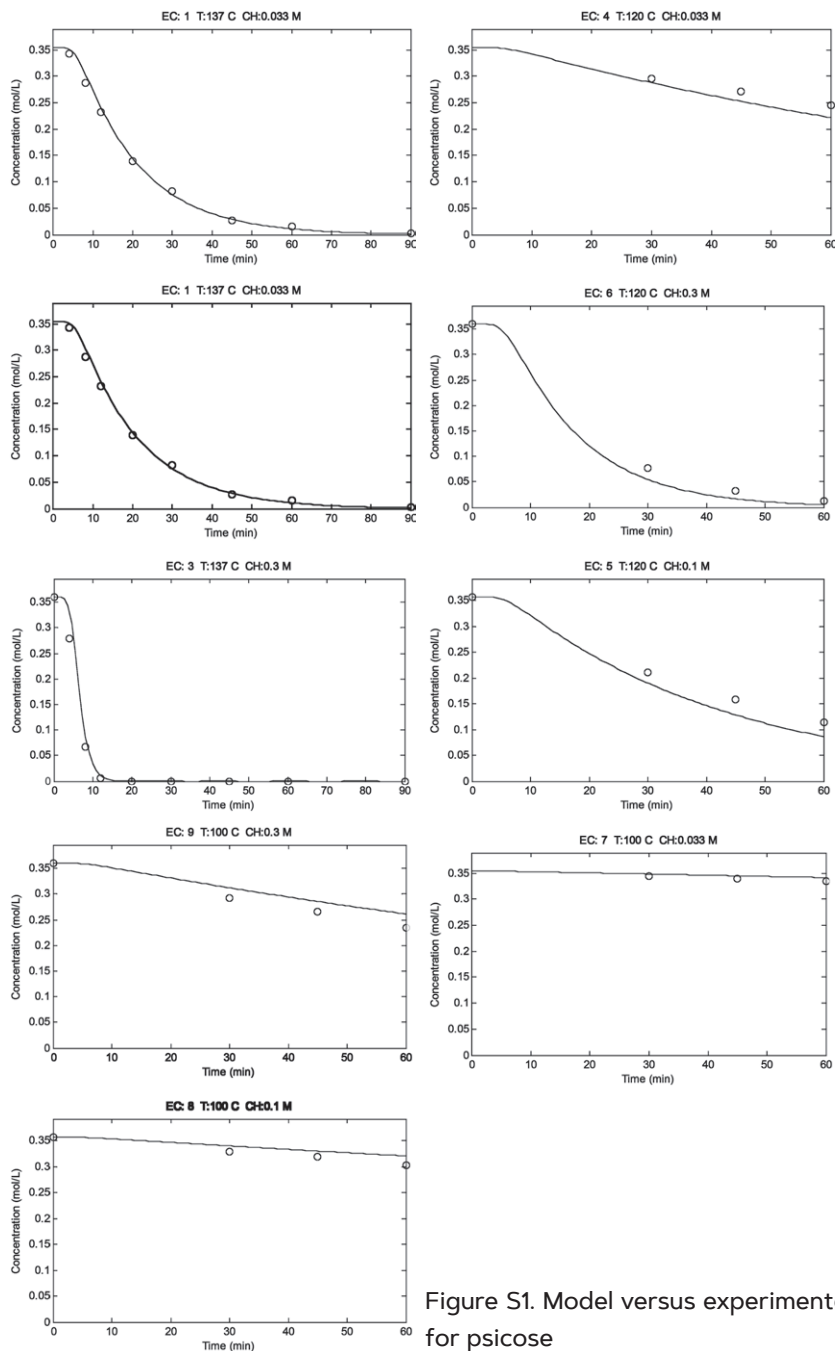
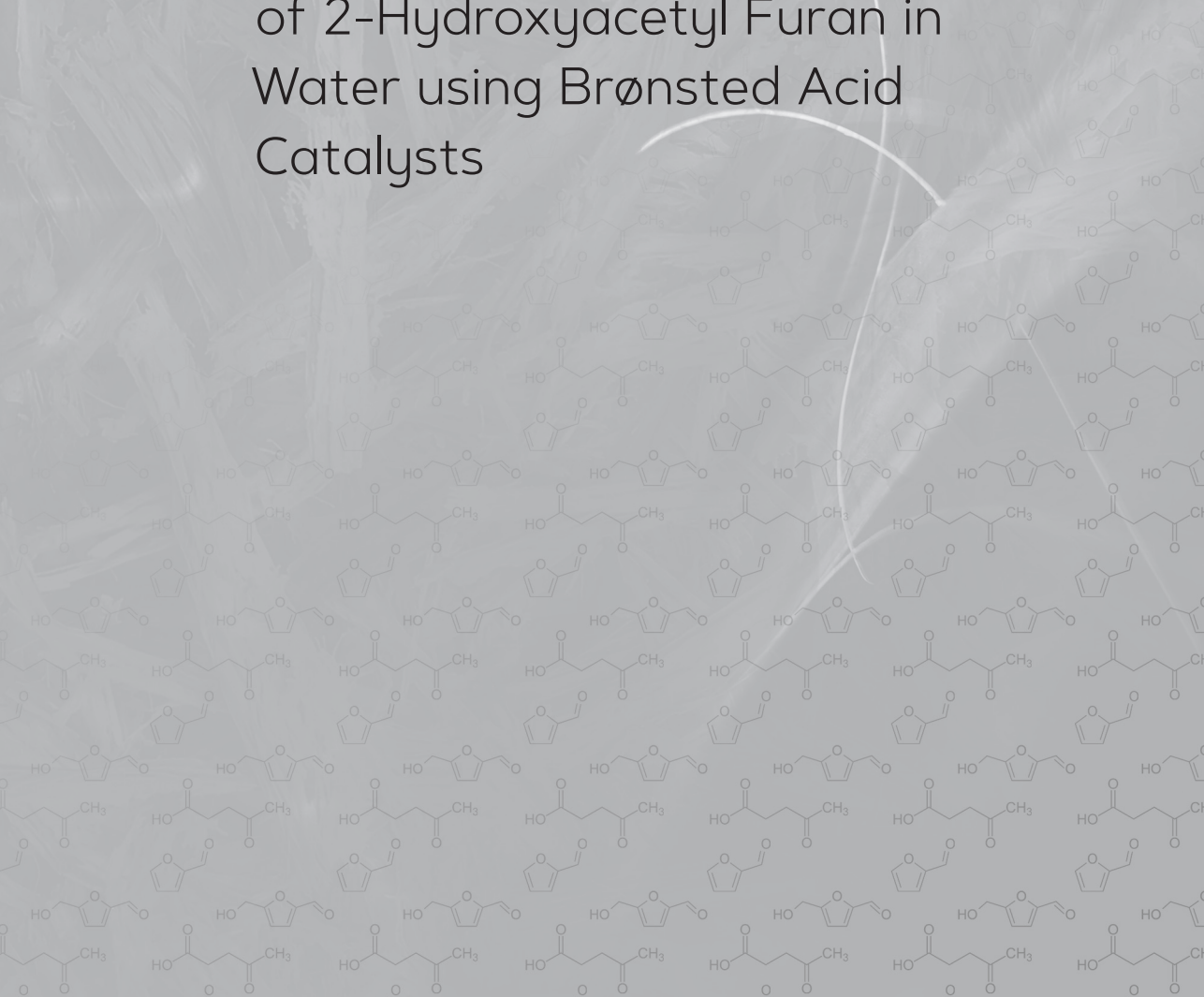


Figure S1. Model versus experimental data for psicose

CHAPTER 4.

Biobased Furanics: Kinetic
Studies on the Acid
Catalysed Decomposition
of 2-Hydroxyacetyl Furan in
Water using Brønsted Acid
Catalysts



ABSTRACT

Biobased furanics like 5-hydroxymethylfurfural (5-HMF) are interesting platform chemicals for the synthesis of biofuel additives and polymer precursors. 5-HMF is typically prepared from C6 ketoses like fructose, psicose, sorbose and tagatose. A known byproduct is 2-hydroxyacetylfuran (2-HAF), particularly when using sorbose and psicose as the reactants. We here report an experimental and kinetic modeling study on the rate of decomposition of 2-HAF in a typical reaction medium for HMF synthesis (water, Brønsted acid), with the incentive to gain insights in the stability of HAF. A total of 12 experiments were performed (batch set-up) in water with sulphuric acid as the catalyst (100–170 °C, $C_{H_2SO_4}$ ranging between 0.033 and 1.37 M and an initial HAF concentration between 0.04 and 0.26 M). Analysis of the reaction mixtures showed a multitude of products, of which levulinic acid (LA) and formic acid (FA) were the most prominent ($Y_{max,FA} = 24$ mol%, $Y_{max,LA} = 10$ mol%) when using HCl. In contrast, both LA and FA were formed in minor amounts when using H_2SO_4 as the catalyst. The decomposition reaction of HAF using sulphuric acid was successfully modeled ($R^2 = 99.67\%$) using a first order approach in 2-HAF and acid. The activation energy was found to be $98.7 (+ 2.2)$ kJ.mol⁻¹.

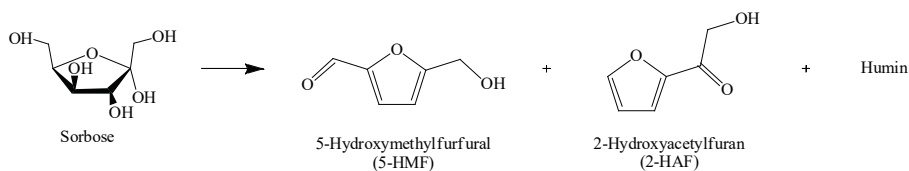
The research described in this Chapter is published in:

Soetedjo, J. N. M.; van de Bovenkamp, H. H.; Deuss, P. J.; Heeres, H. J., Biobased Furanics: Kinetic Studies on the Acid Catalyzed Decomposition of 2-Hydroxyacetyl Furan in Water Using Brønsted Acid Catalysts, *ACS Sustainable Chem. Eng.*, **2017**, 5(5), pp 3993–4001.

1. INTRODUCTION

Biobased furanics like 5-hydroxymethylfurfural (5-HMF) are interesting platform chemicals for the synthesis of biofuel additives and polymer precursors like 2,5-furandicarboxylic acid and derivatives¹. 5-HMF is typically prepared from C6-sugars, with a high preference for D-fructose. We have recently performed extensive experimental studies on the use of other C6-ketoses (fructose, psicose, sorbose and tagatose) for HMF formation^{2–5} in water using sulphuric acid as the catalyst and it was shown that particularly sorbose is also a good source for HMF synthesis (Scheme 1).

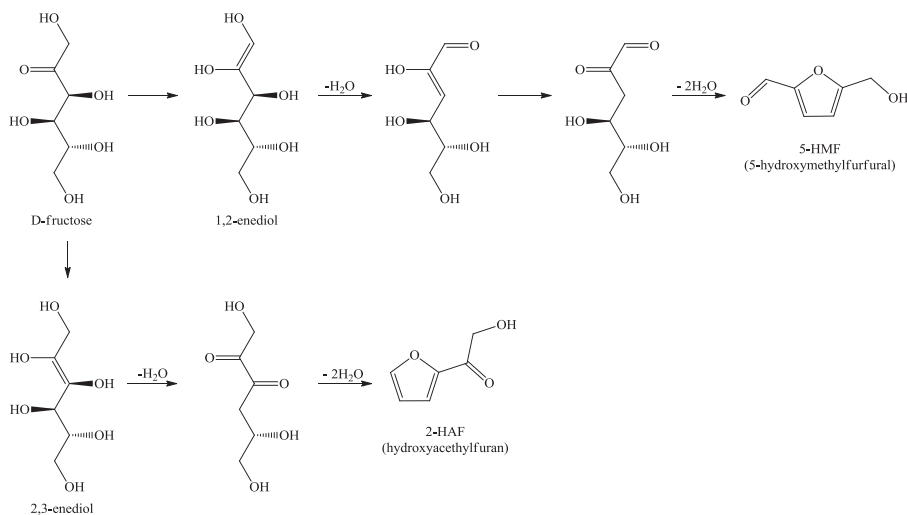
Besides the target component HMF, considerable amounts of 2-hydroxyacetylfuran (2-HAF) or 2-furoylcarbinol were formed, the exact amount being a function of the ketose used. When using D-sorbose, the amount of 2-HAF was up to 10 mol%³. 2-HAF is potentially an interesting biobased furanics with a high derivatization potential and activities to increase the HAF yields from ketoses are in progress.



Scheme 1. Reaction scheme for the acid catalysed hydrolysis of sorbose in aqueous solutions

2-HAF was already reported as the side product of sucrose dehydration in acidic condition in the 1950s^{6,7}. Later studies showed that it is also formed during the dehydration of the monomeric aldoses like glucose^{6,8–10} and mannose¹¹ and ketoses like fructose^{11,12}. A number of studies have been performed to elucidate the mechanism of 2-HAF formation from C6 sugars^{8,9,12–15}. It is postulated that 2-HAF is formed from D-fructose by an acyclic 2,3-enolization, which though, is less favourable than the direct dehydration after a 1,2-enolization to form 5-HMF (Scheme 2).

To optimize the synthesis of 2-HAF from C6 sugars, it is essential to gain insights in the stability of 2-HAF in the reaction medium and to obtain information about the reaction products, both qualitatively and quantitatively. We here describe an experimental study on the conversion of 2-HAF in water using



Scheme 2. Proposed, simplified mechanism for the acid catalysed reaction of D-fructose to 5-HMF and 2-HAF [8,9,12,14,15]

sulphuric acid as the catalyst at conditions of relevance (100–170 °C, $\text{C}_{\text{H}_2\text{SO}_4}$ ranging between 0.033 and 1.37 M, $\text{C}_{\text{HAF},0}$ between 0.04 and 0.26 M). The reaction mixtures were analysed with HPLC and GC/MS-FID for product identification. A kinetic model was developed and the kinetic parameters were determined. To investigate possible Brønsted catalyst effects, a number of experiments with HCl were performed as well. With this information, the rate of decomposition of HAF can be determined as a function of process conditions and provide input in the research aimed to optimize HAF yields from various sugars.

2. METHODS AND ANALYSIS

2.1 Experimental Procedures

All chemicals were used as received without further purification. Concentrated sulphuric acid (95–97 wt%), hydrochloric acid (37 wt%) and formic acid (98% purity) were purchased from Merck KGaA (Darmstadt, Germany). 2-(Hydroxyacetyl)furan (2-HAF) with a purity > 95% was acquired from Otava Chemicals Ltd (Ontario, Canada). Glucose (> 99.5% purity), 5-hydroxymethylfurfural (99% purity) and levulinic acid (98% purity) were obtained

from Sigma-Aldrich Chemie GmbH (Steinheim, Germany). Deionised water was applied to prepare all solutions.

The reactions were carried out in glass ampoules with an internal diameter of 3 mm, a wall thickness of 1.5 mm, and a length of 15 cm. The ampoules were filled at room temperature with a solution (0.5 cm³) of 2-HAF and sulphuric acid in the predetermined amounts and subsequently sealed with a torch. A series of ampoules was placed in a rack and subsequently positioned in a constant temperature oven (+ 0.1 °C) which was pre-set at the desired reaction temperature. At different reaction times, an ampoule was taken from the oven and directly cooled in an ice-water bath to quench the reaction. The liquid content was then filtered using a PTFE syringe filter (0.45 mm, VWR, the Netherlands). The particle free aliquot was diluted 7–8 times with water prior to analysis.

2.2 Method of Analysis

4

The composition of the liquid phase was determined using an Agilent 1200 HPLC, consisting of a Hewlett Packard 1200 pump, a Bio-Rad organic acid column (Aminex HPX-87H) and an RID detector. The mobile phase consists of an aqueous sulphuric acid solution in water (5 mM) at a flow rate of 0.55 cm³ per min. The column was operated at 60 °C. Sample analysis was complete within 60 min. A typical chromatogram is shown in Figure 1. The concentrations of HAF, LA and FA in the product mixture were determined using calibration curves obtained by analyzing a number of standard solutions of known concentrations.

GC-MS analysis was performed using a HP6890 GC equipped with an HP1 column (dimethylpolysiloxane, length: 25 m, inside diameter: 0.25 mm, film

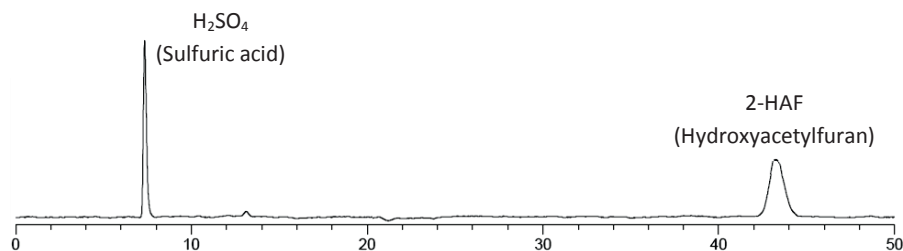


Figure 1. Typical chromatogram for a reaction mixture (HPX-87H Biorad Aminex organic acid column, RI detector)

thickness: 0.25 μm) in combination with a HP5973 mass selective detector. Peak identification was done using the NIST05a mass spectra library. The injection and detection temperature was set at 280 °C. The oven temperature was increased linearly over time from 30 to 280 °C with an increment of 5 °C/min.

2.3 Determination of The Heat Transfer Coefficient in The Oven

At the initial phase of the reaction, the reaction takes place non-isothermally due to heating of the contents of the ampoule from room temperature to the oven temperature. To gain insight in the time required to heat up the reaction mixture and to compensate for this effect in the kinetic modeling studies, the temperature inside the ampoules as a function of the time during the heat up process was determined experimentally. For this purpose, an ampoule equipped with a thermocouple was filled with glycerine. The ampoule was subsequently placed in the oven and the temperature versus time profile was recorded. A typical profile is given in Figure 2. This procedure was repeated for a number of oven temperatures. The experimental profiles at different temperatures were modeled using a heat balance for the contents in an ampoule:

$$\frac{d(MC_p T)}{dt} = U \cdot A_t \cdot (T_{oven} - T) \quad (1)$$

Here M is the mass of the solution, C_p is the heat capacity and A_t is the contact surface area.

When assuming that the heat capacity of the reaction mixture is constant and not a function of temperature, rearrangement of equation (1) gives:

$$\frac{d(T)}{dt} = \frac{U \cdot A_t}{M \cdot C_p} \cdot (T_{oven} - T) = h \cdot (T_{oven} - T) \quad (2)$$

Solving the ordinary differential equation (2) with the initial value $t = 0$, $T = T_i$ leads to

$$T = T_{oven} - (T_{oven} - T_i) \exp^{-ht} \quad (3)$$

Equation (3) was incorporated in the kinetic model to describe the non-isothermal behavior of the system at the start-up of the reaction. The value of h was determined by fitting the temperature-time profile for an experiment

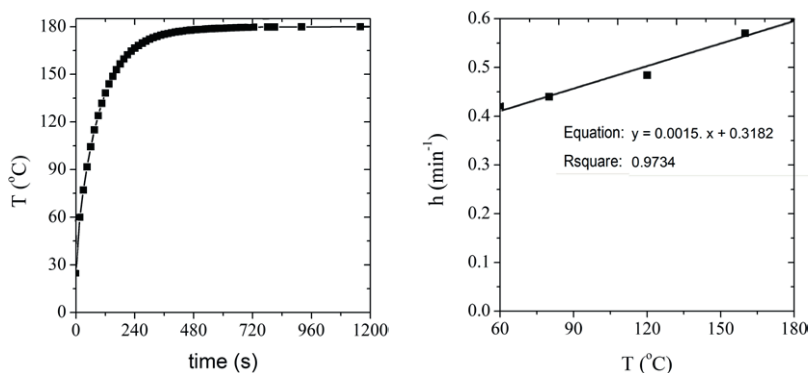


Figure 2. (a) The heating profile of the reaction mixture at $T_{\text{oven}} = 180\text{ °C}$ (■: experimental data, solid curve: modelled profile according to equation 3); (b) h value versus the oven temperature

using a non-linear regression method. A representative example with the experimental values and the model line is given in Figure 2. The h -value is a function of the temperature and varied from 0.4147 min^{-1} ($T_{\text{oven}} = 60\text{ °C}$) to 0.5985 min^{-1} ($T_{\text{oven}} = 180\text{ °C}$). The temperature dependence of the h value was found to be essentially linear, see Figure 2 right for details.

Definitions:

The conversion of HAF and the yield of LA are defined in equations 4 and 5 and are mol% based.

$$X_{\text{HAF}} = \frac{(C_{\text{HAF},0} - C_{\text{HAF}})}{C_{\text{HAF},0}} \quad (4)$$

$$Y_{\text{LA}} = \frac{(C_{\text{LA}} - C_{\text{LA},0})}{C_{\text{HAF},0}} \quad (5)$$

2.4 Determination of The Kinetic Parameters

The kinetic parameters were determined using a maximum likelihood approach, which is based on minimization of the errors between the experimental data and the kinetic model. Details about this procedure can be found in the literature^{16,17}. Error minimization to determine the best estimate of the kinetic

parameters was performed using the MATLAB toolbox *lsqnonlin*, a non-linear least squares method which is based on Trust-Region-Reflective algorithm.

3. RESULTS AND DISCUSSION

3.1 2-HAF Reactivity in Water using H_2SO_4 as the Catalyst

Screening Studies

In the first stage of experimentation, the effect of process conditions on the conversion of HAF in water using sulphuric acid as the catalyst was investigated in a batch set-up. A total of 12 experiments was performed in a temperature window of 100–170 °C, $C_{\text{H}_2\text{SO}_4}$ ranging between 0.033 and 1.37 M, and an initial HAF concentration ($C_{\text{HAF},0}$) between 0.04 and 0.26 M. A typical concentration-time profile for an experiment is shown in Figure 3.

After reaction, the solution was slightly yellowish, and in case of the experiments at more severe conditions, also contained some brown solids (humins). The main detectable soluble component was LA, though the amount was always less than 4 mol%. HPLC revealed the presence of numerous other peaks with small intensities, of which none could be assigned unequivocally (See Supplementary material, Figure S1)

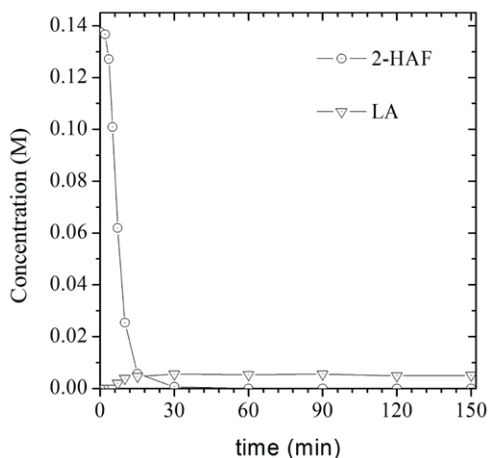


Figure 3. Typical reaction profile for the acid-catalysed decomposition of 2-HAF at $T=170$ °C, $C_{\text{H}_2\text{SO}_4} = 1.37$ M, $C_{\text{HAF},0} = 0.14$ M

When analysing the reaction mixture with GC-MS, a peak at a retention time of about 11 min was assigned by the GC-MS library as butyrolactone (73% confidence level). However spiking of a representative HPLC sample with butyrolactone, showed that the latter was detected at a retention time of 26.1 min. The initial HPLC sample did not show this peak, a clear indication that butyrolactone is not formed during reaction.

In conclusion, the results indicate that HAF is not stable under the conditions employed during its synthesis from C6-ketoses. As such, HAF is an intermediate product and optimum reaction conditions need to be employed to maximize its yield. In this respect, there are strong resemblances with the synthesis of furfural from C5-sugars in water using Brønsted acids as the catalyst. Here furfural is also prone to decomposition to complex mixture of products and selection of proper reaction conditions to reduce the rate of furfural decomposition is of prime importance to obtain high furfural yields. In addition, it is clear that 2-HAF is not easily converted to LA and as such, is not a major source of LA when converting C6 sugars like for instance sorbose to HMF.

The effect of temperature, sulphuric acid concentration and initial 2-HAF concentration on the decomposition rate of 2-HAF were determined and the results are given in Figure 4, 5 and 6. It is evident that higher temperatures and sulphuric acid concentrations result in higher decomposition rates of 2-HAF. In contrast, the conversion of 2-HAF is almost independent of the initial 2-HAF concentration (Figure 6), an indication that the reaction order in 2-HAF is close to 1 (*vide infra*).

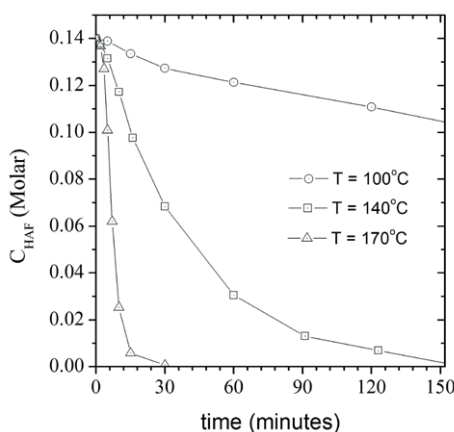


Figure 4. Concentration of 2-HAF versus time at different temperatures ($C_{\text{HAF},0} = 0.14 \text{ M}$, $C_{\text{H}_2\text{SO}_4} = 1.37 \text{ M}$)

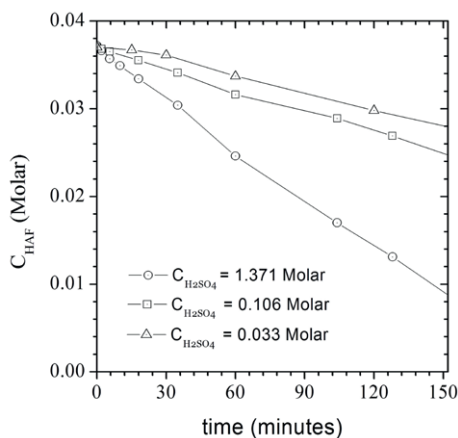


Figure 5. Concentration of 2-HAF versus time at different sulphuric acid concentration ($C_{\text{HAF},0} = 0.04$ M, $T = 120$ °C)

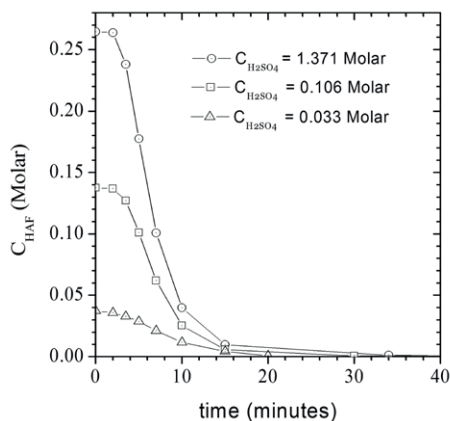
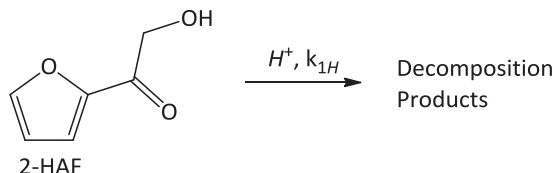


Figure 6. Concentration of 2-HAF versus time at different initial 2-HAF concentration ($C_{\text{H}_2\text{SO}_4} = 1.37$ M, $T = 170$ °C)

LA was formed in detectable amounts only for the experiments performed at relatively severe conditions, i.e. the highest sulphuric acid concentration (1.37 M) and temperatures of 140 °C and above. However, the yields of LA were always below 4 mol%, a clear confirmation that HAF is not a major precursor for LA formation.

Development of A Kinetic Model

The conversion of HAF was modeled based on the simplified reaction scheme given in Scheme 3.



Scheme 3. Simplified reaction scheme for the acid catalysed decomposition of HAF

The reaction rate was initially modeled using a power-law approach, see equation 6 for details.

$$R_{1HAF} = k_{1H}(C_{HAF})^{\alpha_1}(C_{H^+})^{\alpha_1} \quad (6)$$

The temperature dependency of the kinetic constant is defined in terms of a modified Arrhenius equation:

$$k_{1H} = k_{1RH} \exp\left[\frac{E_{1H}}{R} \left(\frac{T - T_R}{T_R T}\right)\right] \quad (7)$$

In this equation T is the reaction temperature and T_R is the reference temperature which was set at 140 °C for this study. The acid concentration is included in the reaction rates and calculated as follows:

$$C_{H^+} = C_{H_2SO_4} + \frac{1}{2} \left(-K_{a,HSO_4^-} - C_{H_2SO_4} + \sqrt{(K_{a,HSO_4^-} + C_{H_2SO_4})^2 + 4C_{H_2SO_4}K_{a,HSO_4^-}} \right) \quad (8)$$

Where K_{a,HSO_4^-} is the dissociation constant of HSO_4^- which was calculated using equation (9).

$$K_{a,HSO_4^-} = 10^{-pK_a} \quad (9)$$

Here the pK_a is calculated with equation (10) using a correction for the temperature of the mixture (T):

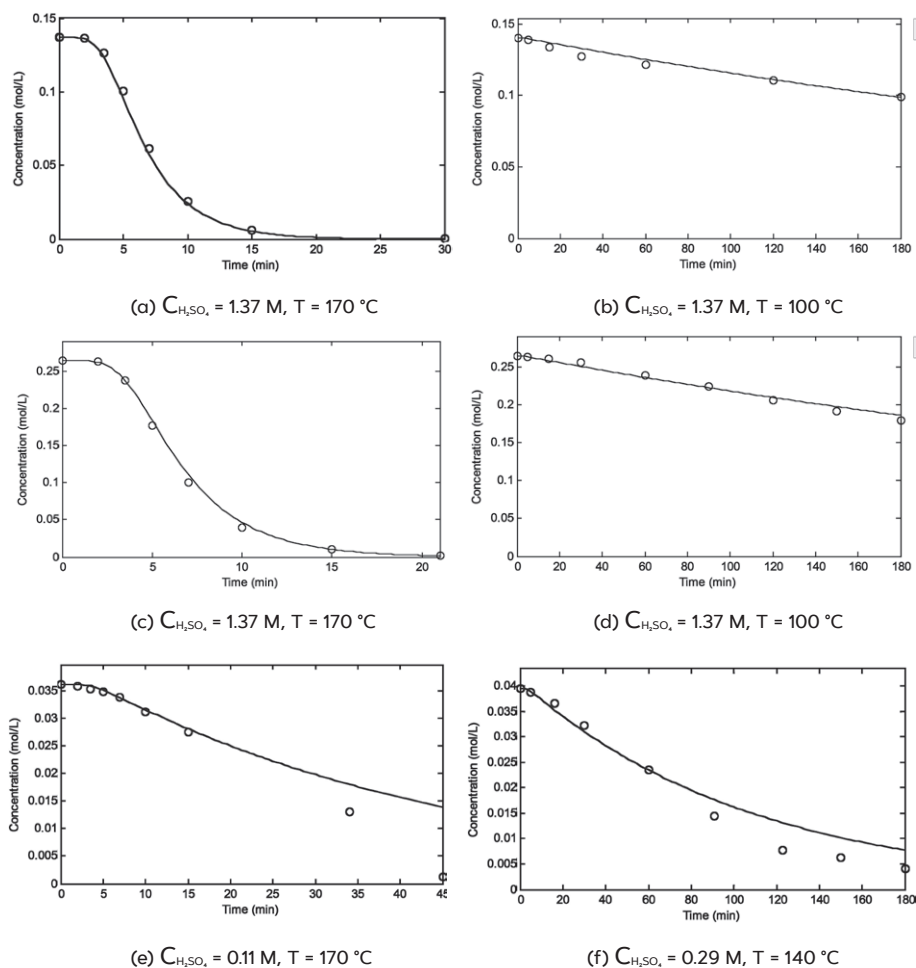


Figure 7. Comparison of experimental data (o) and kinetic model (solid lines) for different initial HAF concentrations, temperature and acid catalyst concentrations

$$p_{K_a} = 0.0152 T - 2.636 \quad (10)$$

For a batch reactor set-up, the concentration of the HAF as a function of time is represented by the following differential equation:

$$\frac{dC_{HAF}}{dt} = -R_{1HAF} \quad (11)$$

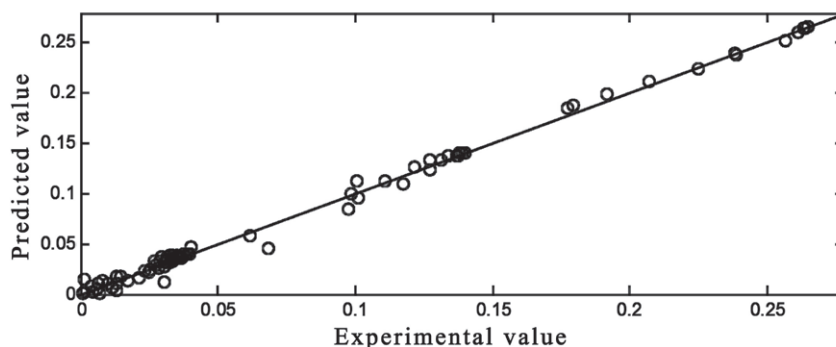


Figure 8. Parity plot with the experimental and corresponding model values (C_{HAF} , M)

Table 1. Kinetic parameter estimation for decomposition of 2-HAF using H_2SO_4 as the acid catalyst

Parameter	Value
R^2	99.57%
E_{ix} (kJ mol ⁻¹)	98.7 ± 2.2
k_{rx} (M ⁻¹ min ⁻¹) ^a	0.032 ± 0.001

^a The values were determined at a reference temperature (T_R) of 140 °C

Modelling Results

A total of 12 experiments gave 122 experimental data points which consist of the concentrations of 2-HAF at different batch times. The best estimation of the kinetic parameters and their standard deviations were determined using a MATLAB optimization routine. The results when using the power law model are given in the supplementary information (Table S1). However, the values of the powers in the reactants (HAF and H^+) were close to 1 for the power law model and as such the number of model parameters was reduced by taking orders of 1 for both HAF and H^+ ($a_H = a_{\text{HAF}} = 1$) in the model.

Good agreement between model and experimental values was observed. This is evident from the R^2 of 0.9957 (Table 1), the experimental and model graphs (Figure 7) and a parity plot in Figure 8.

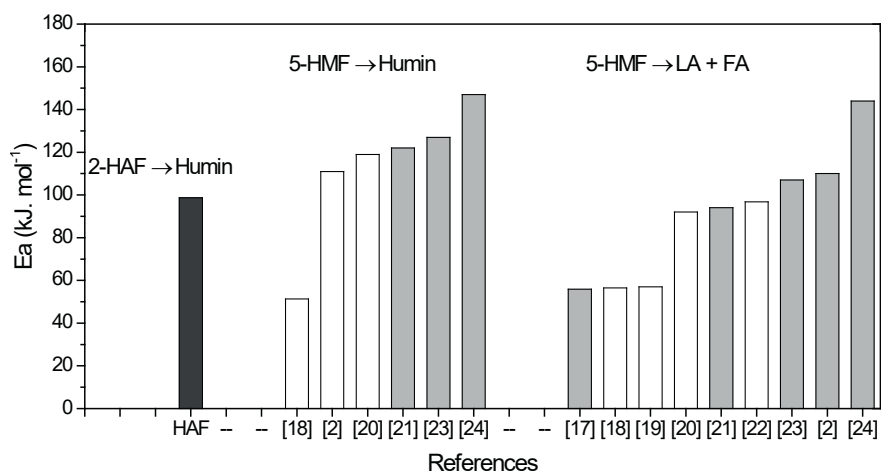


Figure 9. Activation energies for the conversion of 2-HAF (black bar) and 5-HMF (white bars: using H_2SO_4) and other homogeneous acid catalysts (grey bars)

The activation energy for the reaction is 98.7 kJ/mol. A comparison with literature data is difficult as no studies have been reported for the decomposition reaction of HAF. However, it is informative to compare the activation energy with those reported for the reaction of HMF to either LA and/or humins. An overview is given in Figure 9 and detailed information is shown in Table 2.

The data reveal that the activation energy for the decomposition of HAF is in the range as reported for that of 5-HMF to humins and slightly lower than for 5-HMF to LA. However, a good comparison is difficult as the activation energies from HMF cover a large range due to the use of various catalysts. When only considering the reactions with sulphuric acid (white bars in the Figure 9), it can be concluded that the activation energy for the decomposition of 2-HAF to humins is comparable with that for 5-HMF to humins.

For the optimization of the conversion of C6 sugars to either HAF or HMF, it is of interest to compare the relative stability of both compounds under reaction conditions. In Figure 10, the relative ratio of the reaction rates for the decomposition of HAF (R_{HAF}), as presented in this study, and those for HMF ($R_{\text{HMF,tot}}$) are provided. The data for HMF were taken from an earlier publication of our group using sulphuric acid as the catalyst². For HMF, the reaction rate was the sum of the rate of reactions ($R_{\text{HMF,tot}}$) to both LA ($R_{\text{HMF,LA}}$) and humins ($R_{\text{HMF,humin}}$).

Table 2. Overview of the activation energies for the conversion of 2-HAF and 5-HMF using several homogeneous acid catalysts in water

No	Feed		Acid		T (°C)	Ea (kJ. mol ⁻¹)		Ref
	Name	C _{feed}	Name	Concentration		to LA	to humins	
1	Glucose	0.0057–0.333M	Buffer: butyric acid/ H ₃ PO ₄ and NaOH	pH 1–4	170–230	56	n.d.	18
2	Wheat	16:1 w/w water:wheat	H ₂ SO ₄	1–5 w/w-%	190–230	56	51	19
3	5-HMF	5%-w/v	H ₂ SO ₄	1–5 w/w-%	170–210	57	n.d.	20
4	5-HMF	0.1–1 M	H ₂ SO ₄	0.005–1	140–180	92	119	21
5	5-HMF	n.d.	HCl,subcriti- cal water	1.8	210–270	94	122	22
6	5-HMF	0.06–0.14 M	H ₂ SO ₄	0.025–0.4 N	160–220	97	n.d.	23
7	Glucose	56–112 mM	CH ₃ COOH	5–20 w/w-%	180–220	107	127	24
8	5-HMF	0.1–1 M	H ₂ SO ₄	0.05–1 M	98–181	110	111	22
9	Cellulose	49.8–149 mM	HCl	0.309–0.927M	160–200	144	147	25
10	2-HAF	0.04–0.26 M	H ₂ SO ₄	0.033–1.37 M	100–170	n.d.	99	This study

4

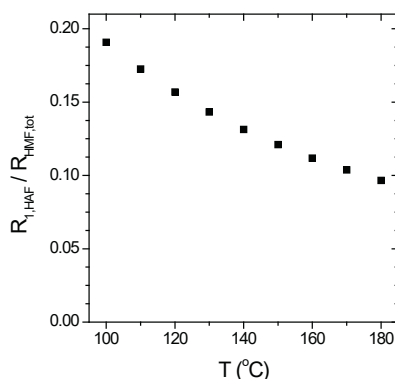


Figure 10. Ratio of reaction rates for HMF and HAF decomposition versus the temperature ($C_{H^+} = 0.1$ M, $C_{HMF} = C_{HAF} = 0.25$ M)

On the basis of these data, we can conclude that HAF is more stable under the given reaction conditions than HMF. Moreover, this effect is more pronounced at higher temperatures, in line with the lower experimental activation energy found for the reaction of HAF (99 kJ.mol⁻¹) compared to HMF (110 kJ.mol⁻¹) when using sulphuric acid as the catalyst.

3.2 2-HAF Reactivity in Water Using HCl as The Catalyst

To gain insights in the role of the Brønsted acid catalyst, a number of exploratory experiments were carried out with HCl instead of sulphuric acid ($C_{\text{HAF},0} = 0.14 \text{ M}$, $C_{\text{H}^+} = 1.37 \text{ M}$, $T = 170 \text{ }^{\circ}\text{C}$). The concentration time profiles for HAF and LA for both inorganic acids are provided in Figure 11.

The conversion rate of HAF was slightly higher when using HCl. The kinetic constant at $170 \text{ }^{\circ}\text{C}$ for HCl was calculated from the concentration time profile in Figure 11 using a first order approach in HAF and H^+ and found to be 0.32 min^{-1} , which is 1.5 higher than for sulphuric acid (0.21 min^{-1}) at similar conditions. Of interest is the significantly higher concentration of LA and FA in the product mixture when using HCl as the catalyst. For this particular experiment, the yield of LA was 10 mol%, and the FA yield was up to 24 mol%, the remainder being unidentified soluble products and insoluble resinous compounds known as humins.

On the basis of the product composition, a tentative reaction network is proposed, see Figure 12 for details. It involves the formation of humins by acid-catalysed (aldol) condensation reactions of the starting materials and subsequent reactions with intermediates. LA and FA may be formed from an intermediate α -hydroxy-keto-aldehyde, obtained by the ring opening of HAF followed by an acid catalysed rearrangement. However, detailed mechanistic studies, beyond the scope of this paper, will be required to strengthen this proposal.

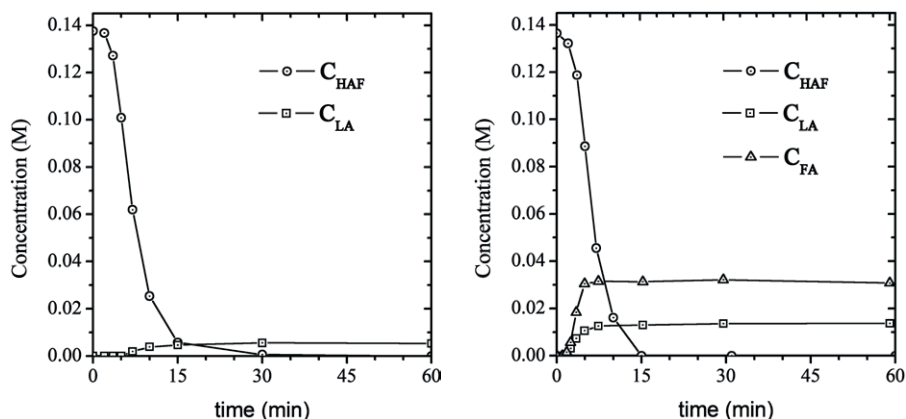


Figure 11. Comparison of the concentration-time profiles for the acid-catalysed decomposition of 2-HAF in water at $170 \text{ }^{\circ}\text{C}$, $C_{\text{HAF},0} = 0.14 \text{ M}$ using $\text{C}_{\text{H}_2\text{SO}_4}$ (left) and C_{HCl} (right) at a concentration of 1.37 M

The differences in reaction rate and product composition between HCl and sulphuric acid indicate that the outcome of the reaction is depending on the inorganic acid used as the catalyst for the reaction. Based on the fact that both acids are strong and as such the H^+ concentrations are about equal, the anion must play an important role. Such anion effects also have been reported for Brønsted acid catalysed furfural decomposition reactions in water. The activation energy for HCl ($E_a = 48.1 \text{ kJ/mol}^{26}$) was reported to be about half of that when using H_2SO_4 ($E_a = 83.6 \text{ kJ/mol}^{27}$). The authors explained these results by assuming a difference in reaction mechanism for both acids due to anion effects, involving a ring opening mechanism when using Cl^- versus a direct dehydration mechanism when using sulphuric acid^{28–31}. Anion effects have also been reported for the conversion of HMF, another example of a biobased furanic, to LA and formic acid. For instance, Yoshida *et al.*³² reported on the acid-catalysed production of HMF from D-fructose and the subsequent rehydration to LA in subcritical water using both sulphuric acid and HCl as the catalysts. Remarkable differences in the rate of reaction were observed

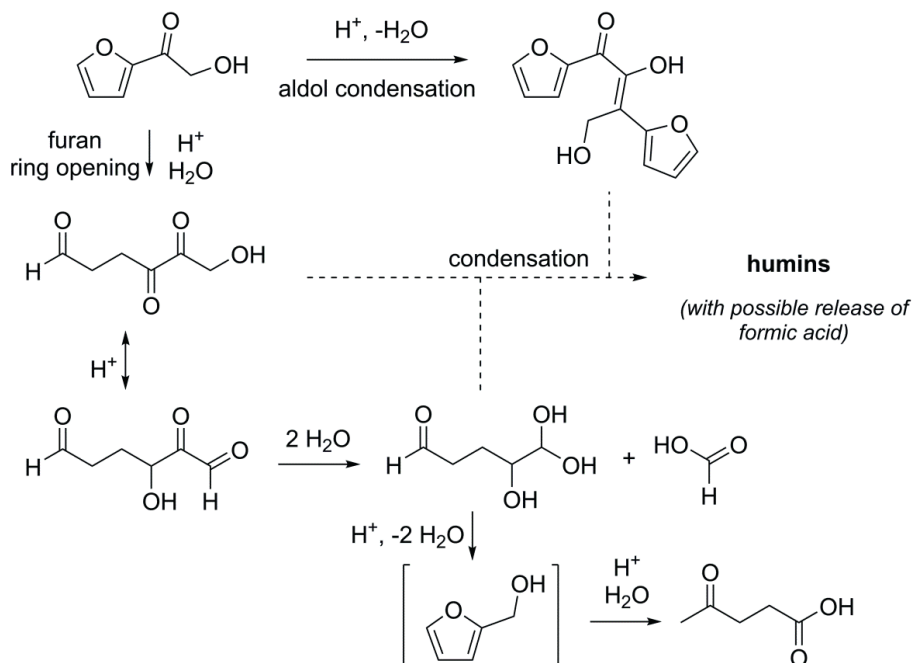


Figure 12. Proposed reaction network for HAF decomposition in aqueous media using Brønsted acids

between both acids at similar pH values, with HCl giving higher HMF yields. In addition, the addition of salts like NaCl and Na₂SO₄ showed that Cl⁻ ions accelerate the conversion of fructose to HMF and the subsequent reaction of HMF to LA whereas sulphate ions have an inhibiting effect on the rehydration reaction to LA. However, to the best of our knowledge, detailed mechanistic studies to explain and rationalize these anion effects on the stability of biobased furanics like furfural and HMF have not been reported to date.

4. CONCLUSIONS

2-HAF is a known side product from the acid catalysed dehydration of C6 sugars to 5-HMF in water using Brønsted acid catalysts. For optimization of the HAF yields from C6-sugars, information about the stability of HAF in the reaction medium at relevant conditions is required. In this paper, the kinetics of 2-HAF decomposition using sulphuric acid as the catalyst in water have been determined. Good agreement between model and experimental data ($R^2 = 99.57\%$) was obtained when using a first order approach in both HAF and H⁺. The activation energy was 98.7 ± 2.2 kJ/mol. At 170 °C, the kinetic constant for HCl was found to be 0.32 min^{-1} which is 1.5 higher than H₂SO₄ (0.21 min^{-1}), implying an anion effect on the rate of decomposition. The reaction does not lead to the formation of a single reaction product; instead a multitude of soluble non-identified products was observed (HPLC) and solids formation was also inevitable. The only exceptions are LA and FA, which were present in significant amounts when using HCl as the catalyst ($Y_{\text{LA}} = 10 \text{ mol}\%$ and $Y_{\text{FA}} = 24 \text{ mol}\%$). The findings described in this paper will be of relevance for the development of an efficient route for HAF from C6 sugars and allow selection of optimum conditions to reduce the rate of HAF decomposition.

REFERENCES

1. Bozell, J. J.; Petersen, G. R. Technology development for the production of biobased products from biorefinery carbohydrates — the US Department of Energy's "Top 10" revisited. *Green Chemistry* **2010**, *12* (4), 539–554.
2. Girisuta, B.; Janssen, L. P. B. M.; Heeres, H. J. A kinetic study on the decomposition of 5-hydroxymethylfurfural into levulinic acid. *Green Chemistry* **2006**, *8*, 701–709.
3. van Putten, R.-J.; Soetedjo, J. N. M.; Pidko, E. A.; van der Waal, J. C.; Hensen, E. J. M.; de Jong, E.; Heeres, H. J. Dehydration of Different Ketoses and Aldoses to 5-Hydroxymethylfurfural. *Chemsuschem* **2013**, *6* (9), 1682–1687.
4. Rasrendra, C. B.; Soetedjo, J. N. M.; Makertihartha, I. G. B. N.; Adisasmito, S.; Heeres, H. J. The Catalytic Conversion of D-Glucose to 5-Hydroxymethylfurfural in DMSO Using Metal Salts. *Topics in Catalysis* **2012**, *55* (7–10), 543–549.
5. van Putten, R.-J.; van der Waal, J. C.; de Jong, E. A process for the catalysed conversion of psicose into 5-hydroxymethylfurfural or an alkyl ether thereof. WO2015133902 A1, September 11, 2015.
6. Miller, R. E.; Cantor, S. M. 2-Hydroxyacetyl furan from sugars. *Journal of American Chemical Society* **1952**, *74* (20), 5236–5237.
7. Aso, K.; Sugisawa, H. 2-Hydroxyacetyl-furan from sucrose. *Tohoku Journal of Agricultural Research* **1954**, *2*, 143–146.
8. Harris, D. W.; Feather, M. S. An intramolecular hydrogen transfer during the conversion of D-glucose to 2-(hydroacetyl)-furan. *Tetrahedron Letters* **1972**, *47*, 4813–4816.
9. Harris, D. W.; Feather, M. S. Evidence for A C-2-->C-1 Intermolecular Hydrogen Transfer During Acid-Catalyzed Isomerization of D-Glucose to D-Fructose. *Carbohydrate Researches* **1973**, *30*, 359–365.
10. Harris, D. W.; Feather, M. S. Intramolecular C-2-->C-1 Hydrogen Transfer-Reactions During Conversion of Aldoses to 2-Furaldehydes. *Journal of Organic Chemistry* **1974**, *39*, 724–725.
11. Harris, D. W.; Feather, M. S. Studies on Mechanism of Interconversion of D-Glucose, D-Mannose, and D-Fructose in Acid Solution. *Journal of the American Chemical Society* **1975**, *97*, 178–182.
12. Shaw, P. E.; Tatum, J. H.; Berry, R. E. Acid-catalyzed degradation of D-fructose. *Carbohydrate Research* **1967**, *5* (3), 266–273.

13. Anet, E. F. L. J. Degradation of carbohydrates. V. Isolation of intermediates in the formation of 5-(Hydroxymethyl)-2-furaldehyde. *Australian Journal of Chemistry* **1965**, *18* (2), 240–248.
14. Feather, M. S.; Harris, J. F. Dehydration Reactions of Carbohydrates. *Advances in Carbohydrate Chemistry and Biochemistry* **1973**, *28*, 161–224.
15. Moreau, C.; Durand, R.; Razigade, S.; Duhamet, J.; Faugeras, P.; Rivalier, P.; Ros, P.; Avignon, G. Dehydration of fructose to 5-hydroxymethylfurfural over H-mordenites. *Applied Catalysis A: General* **1996**, *145*, 211–224.
16. Bard, Y. *Nonlinear parameter estimation*; Academic Press: New York, 1974; pp 61–71.
17. Knights, C. D.; Peters, C. A. Statistical Analysis of Nonlinear Parameter Estimation for Monod Biodegradation Kinetics Using Bivariate Data. *Biotechnology and bioengineering* **2000**, *69*, 160–170.
18. Baugh, K. D.; McCarty, P. L. Thermochemical Pretreatment of Lignocellulose to Enhance Methane Fermentation: I. Monosaccharide and Furfurals Hydrothermal Decomposition and Product Formation Rates. *Biotechnology and Bioengineering* **1988**, *31*, 50–61.
19. Chang, C.; Ma, X.; Cen, P. Kinetic Studies on Wheat Straw Hydrolysis to Levulinic Acid. *Chinese Journal of Chemical Engineering* **2009**, *17* (5), 835–839.
20. Chang, C.; Ma, X.; Cen, P. Kinetics of Levulinic Acid Formation from Glucose Decomposition at High Temperature. *Chinese J. Chem. Eng.* **2006**, *14* (5), 708–712.
21. Fachri, B. A.; Abdilla, R. M.; van de Bovenkamp, H. H.; Rasrendra, C. B.; Heeres, H. J. Experimental and Kinetic Modeling Studies on the Sulfuric Acid Catalyzed Conversion of DFructose to 5Hydroxymethylfurfural and Levulinic Acid in Water. *ACS Sustainable Chem. Eng.* **2015**, *3*, 3024–3034.
22. Asghari, F. S.; Yoshida, H. Kinetics of the decomposition of fructose catalyzed by hydrochloric acid in subcritical water: Formation of 5-hydroxymethylfurfural, levulinic, and formic acids. *Industrial and Engineering Chemistry Research* **2007**, *46* (23), 7703–7710.
23. McKibbins, S. W.; Harris, J. F.; Saeman, J. F.; Neill, W. K. Kinetics of the Acid Catalyzed Conversion of Glucose to 5-Hydroxymethyl-2-Furaldehyde and Levulinic Acid. *Forest Products* **1962**, *12* (1), 17–23.
24. Kupiainen, L.; Ahola, J.; Tanskanen, J. Kinetics of glucose decomposition in formic acid. *Chemical Engineering Research and Design* **2011**, *89*, 2706–2713.
25. Shen, J.; Wyman, C. E. Hydrochloric Acid-Catalyzed Levulinic Acid Formation from Cellulose: Data and Kinetic Model to Maximize Yields. *AIChE Journal* **2012**, *58* (1), 236–246.

26. Rose, I. C.; Epstein, N.; Watkinson, A. P. Acid-Catalyzed 2-Furaldehyde (Furfural) Decomposition Kinetics. *Industrial Engineering Chemistry Research* **2000**, 39 (3), 843–845.
27. Williams, D. L.; Dunlop, A. P. Kinetics of furfural destruction in acidic aqueous media. *Industrial Engineering Chemistry* **1948**, 40, 239–241.
28. Binder, J. B.; Blank, J. J.; Cefali, A. V.; Raines, R. T. Synthesis of Furfural from Xylose and Xylan. *ChemSusChem* **2010**, 3 (11), 1268–1272.
29. Marcotullio, G.; de Jong, W. Chloride ions enhance furfural formation from D-xylose in dilute aqueous acidic solution. *Green Chemistry* **2010**, 12, 1739–1746.
30. Antal, M. J. J.; Leesomboon, T.; Mok, W. S. Mechanism of Formation of 2-Furfural From D-Xylose. *Carbohydrate Research* **1991**, 217 (1), 71–85.
31. Vinueza, N. R. Tandem mass spectrometric characterization of the conversion of xylose to furfural. *Biomass and Bioenergy* **2015**, 74, 1–5.
32. Asghari, F. S.; Yoshida, H. Acid-catalyzed production of 5-hydroxymethylfurfural from D-fructose in subcritical water. *Industrial Engineering Chemistry Research* **2006**, 45, 2163–2173.

APPENDIX FOR CHAPTER 4

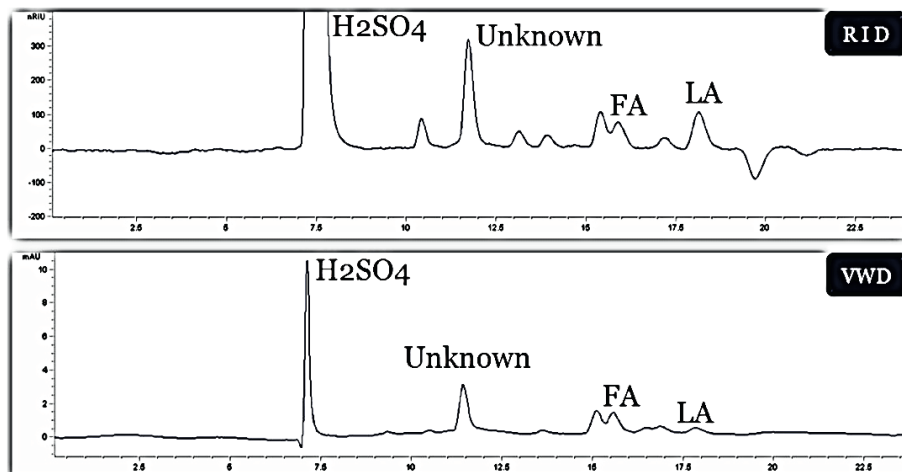


Figure S1: HPLC chromatograms for a typical reaction product using sulphuric acid as the catalyst

Kinetic Modeling: Model Discrimination

Equations (1–4) below describe the four different models used to model the decomposition of HAF. The first (1) assumes that the reaction is first order in both the HAF and the H^+ . Models 2 and 3 in eq. (2) and (3) represent a power law model in respectively the HAF concentration and the acid concentration. In model 4, both the acid and HAF concentration are described by a power law model.

1st order.

$$\frac{dC_{HAF}}{dt} = k_{ref} * e^{\left[\frac{E_a}{R} \left(\frac{T - T_{ref}}{T_{ref} T} \right) \right]} * C_{HAF} * C_H^+ \quad (1)$$

Power in HAF concentration.

$$\frac{dC_{HAF}}{dt} = k_{ref} * e^{\left[\frac{E_a}{R} \left(\frac{T - T_{ref}}{T_{ref} T} \right) \right]} * C_{HAF}^a * C_H^+ \quad (2)$$

Power in H^+ concentration.

$$\frac{dC_{HAF}}{dt} = k_{ref} * e^{\left[\frac{E_a}{R} \left(\frac{T - T_{ref}}{T_{ref} T} \right) \right]} * C_{HAF} * C_H^{+b} \quad (3)$$

Power in both substrate and catalyst.

$$\frac{dC_{HAF}}{dt} = k_{ref} * e^{\left[\frac{Ea}{R} \left(\frac{T - T_{ref}}{T_{ref} T} \right) \right]} * C_{HAF}^a * C_H^{+b} \quad (4)$$

The values for the parameters in the model were obtained using the MATLAB lsqnonlin error minimization routine and the results are given in Table S1.

Table S1. Modeled kinetic parameters for models 1–4.

Model	k_{ref}	Ea	a	b	r^2
1	0.0315 ± 0.0014	98.7 ± 2.2	-	-	0.9957
2	0.0418 ± 0.0063	100.4 ± 2.3	1.14 ± 0.07	-	0.9965
3	0.0333 ± 0.0018	98.3 ± 2.1	-	0.80 ± 0.12	0.9962
4	0.0566 ± 0.0091	101.1 ± 1.9	1.23 ± 0.07	0.60 ± 0.12	0.9975

4

The R^2 values for all models are high and within a very narrow range, indicating that all four models represent the experimental data well (see parity plots in Figures S2–S5). The values for the activation energy are also similar when considering the confidence intervals of the different models. The first order model has the smallest confidence interval for the reaction rate constant of all models tested. Based on these observations, coupled with the fact that the first order model has the lowest number of parameters, this model was selected as the model of choice.

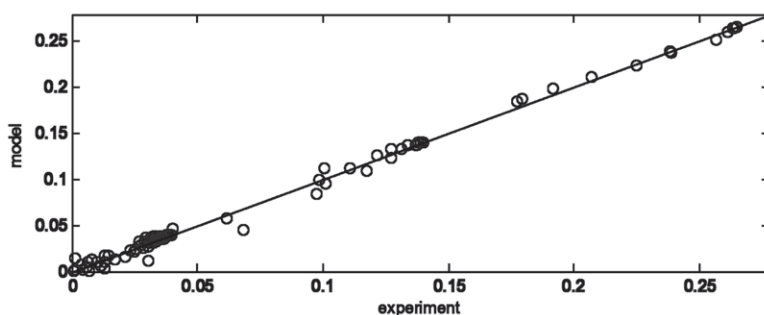


Figure S2. Parity plot for model 1

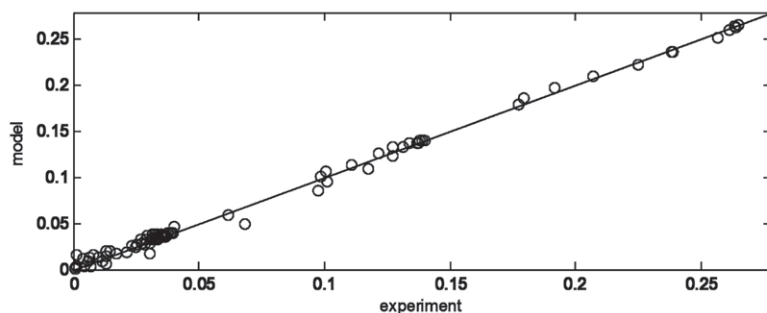


Figure S3. Parity plot For model 2

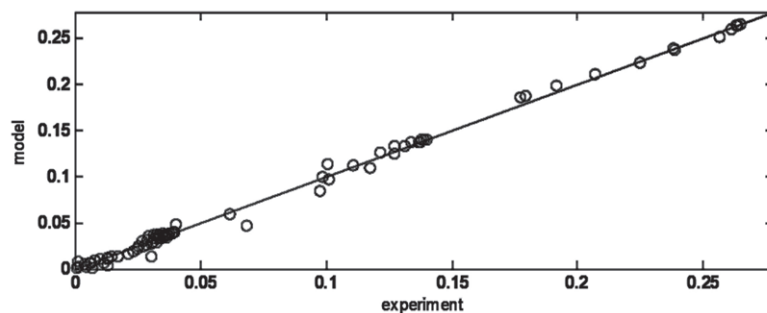


Figure S4. Parity plot for model 3

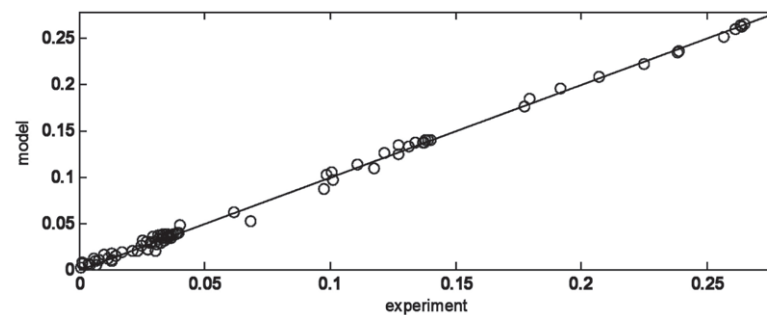


Figure S5. Parity plot For model 4



CHAPTER 5.

Remarkable Solvent Effects
on The Dehydration
of Xylose to Furfural in
Ethanol/Water Mixtures
Using Homogeneous and
Heterogeneous Brønsted
Acid Catalysts.

ABSTRACT

Furfural is an interesting renewable, platform chemical. We here report an experimental study in a batch set-up on the conversion of xylose to furfural in water and ethanol/water mixtures using homogeneous Brønsted acids (150 °C, H₂SO₄ (0.1 M and 0.5 M) and HCl (0.2 M)). The best results when using sulphuric acid as the catalyst were obtained in solvent mixtures with 70–90% ethanol, giving furfural yields up to 73 mol%. This is a considerable improvement compared to experiments in water only at similar reaction conditions giving a maximum furfural yield of 59 mol%. Individual reactions with furfural showed that the rate of furfural decomposition is a function of the ethanol content and shows the lowest degradation rate at ethanol concentrations between 40 and 60%. Comparable maximum furfural (FF) yield (71 mol%) was obtained using HCl. The use of solid Brønsted acid catalysts (Amberlyst® 15, Nafion® SAC-13, Dowex® 50WX8) was also explored. Dowex® 50WX8 showed comparable performance as found for the homogeneous Brønsted acids and a maximum FF yield of 68 mol% was obtained in 90/10-ethanol/water ratio. The elemental composition and morphology (TEM) of the isolated humins products obtained from reactions with furfural in water, ethanol and ethanol/water mixtures using sulphuric acid and HCl showed considerable differences. The humins samples obtained using sulphuric acid as the catalyst showed the presence of significant amounts of sulphur, likely from sulphonate groups.

1. INTRODUCTION

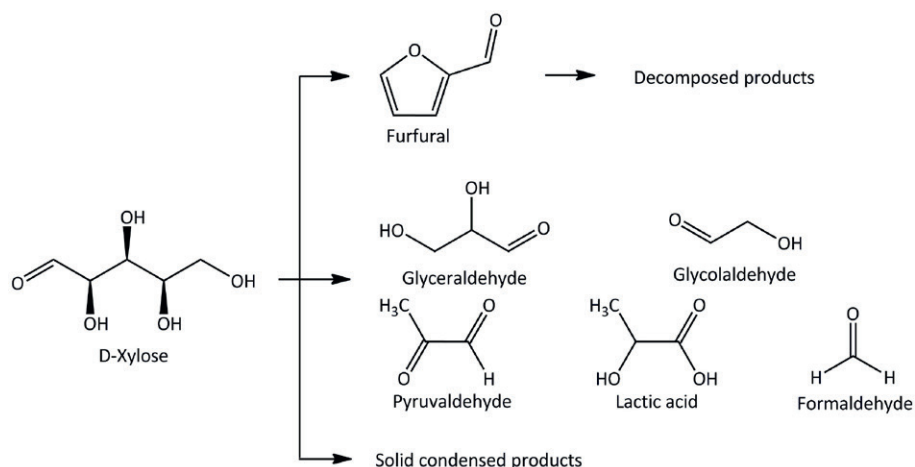
Furfural or furan-2-carbaldehyde (FF), for the first time isolated by Doebernier in 1821¹, is an important commercially available renewable, non-petroleum based chemical building block and used for the productions of amongst others furfuryl alcohol, furoic acid and furans^{1–6}. Recent studies have shown that the application range of FF can be extended considerably and new derivatives and outlets have been identified⁷. As such, FF has been classified as a top 12 chemicals from biomass⁸.

FF has been produced commercially since the 1920s^{5,6}. It is formed by the conversion of the C5 sugars (mainly xylose) present in the biomass feed. Sugarcane bagasse and corncobs are typically used as the biomass feed in combination with sulphuric acid as the catalyst in water at elevated temperatures (150–210 °C). The global production capacity was about 800,000 tons in 2012, mainly in South Africa and the Dominican Republic⁹. A number of process concepts have been commercialised (Quacker, Agrifurane, Rosenlew, Escher Wyss), though all suffer from relatively low FF yields (50% range)⁶.

A large number of kinetic studies have been conducted to i) determine the mechanism of the conversion of xylose to FF and ii) to design optimum reactor configurations^{10–23}. Based on this study, a simplified reaction network for xylose has been proposed (Scheme 1). Xylose not only reacts to the desired product FF but is also converted to a number of low molecular weight products with two or three carbon atoms, mainly by reverse aldol condensations (e.g. glyceraldehyde, pyruvaldehyde, formic acid) and solid condensation products, also known as humins. In addition, FF is typically not stable under the prevailing reaction conditions and may be converted to amongst others humins and formic acid.

Humins formation not only lowers the FF yield but also poses operational issues due to adherence to (reactor) walls leading to blockage and reduced heat transfer rates. Furthermore, humins formation reduces the potential to use solid acid catalyst as these may irreversibly deposit on the solid catalyst and lead to catalyst deactivation. FF yield improvements have been made possible by the addition of salts to the reaction mixture^{18,21,23}, the use of biphasic liquid-liquid systems^{19,22,24,25}, ionic liquids^{26–30} and organic solvents^{17,31–35} instead of water.

The addition of inorganic salts such as NaCl, KI and CrCl₃ in aqueous systems has a positive effect of FF yields^{21,23}, see Table 1 for details. The addition of 5 wt% of NaCl in combination with HCl was shown to increase the FF yield



Scheme 1. Global reaction network for the acid catalysed reactions of D-xylose in aqueous solutions

Table 1. Representative examples of xylose conversion to FFI in single solvent systems using homogeneous catalyst.

Entry	C _{Xylose}	T (°C), t	Acid	C _{acid}	Salt	Solvent	Y _{FF,max} (mol%)	Ref
1.	35 mM	200, 485 s	H ₂ SO ₄	0.05 M	KI-KCl 250–500mM	H ₂ O	88	23
2.	35 mM	200, 250 s	HCl	0.05 M	NaCl 5 wt%	H ₂ O	81	20
3.	42 mM	240, 215 s	H ₂ SO ₄	0.025 N	-	H ₂ O	71	11
4.	68 mM	200, 15 min	HCOOH	0.12 M	-	H ₂ O	66	36
	200 mM	200, 20 min					65	
5.	196 mM	220, 37 min	-	-	-	H ₂ O	65	37
6.	10 wt%	100, 4 h	-	-	LiBr 10 wt% CrCl ₃ 6 mol%	DMA	56	27
7.	196 mM	220, 1 min	H ₂ SO ₄	0.10 M	-	H ₂ O	50	37
	72 mM	220, 50 min	-	-	-	H ₂ O	50	38
8.	33 mM	180, 20 min	HCl	0.10 M	-	H ₂ O	38	39
			H ₂ SO ₄				32	
			H ₃ PO ₄				28	
			HCOOH				24	
			CH ₃ COOH				16	
			HNO ₃				4	
9.	56 mM	145, 300 min	HCl	0.10 M	CrCl ₃ 6 mM	H ₂ O	39	40
			HCl	0.10 M	-	H ₂ O	29	

to 81 mol%. The best results obtained so far were achieved by Marcotullio *et al.* and a FF yield of 88 mol% was reported using a mixture of KI and KCl and sulphuric acid as the catalyst²³.

Besides water, organic solvents have also been explored, though mainly in combination with heterogeneous catalysts (Table 2). A well-known example is dimethylsulphoxide (DMSO) which gave 77–83 mol% FF yield with MCM-41 and Amberlyst® 70 as the catalysts (Table 2). However, its high boiling point (189 °C) is an issue and seriously complicates down-stream processing.

The use of relatively low boiling point solvents like short-chain alcohols (C1 until C4) has also been explored, again mainly in combination with heterogeneous catalysts. For instance, Hu *et al.* performed experimental studies on the conversion of xylose to FF in a number of alcohols using 5 wt% of Amberlyst® 70 as the catalyst at 160 °C⁴¹. Secondary alcohol gave better results than primary alcohols. The best yield, up to about 56 mol% after 100 minutes, was obtained when using 2-butanol, see Table 2 for details. Recently, Chun-Li *et al.* reported studies on the use of a large number of solvents for the conversion of xylose to FF using a solid acid catalyst (Amberlyst® 70; 5 wt% catalyst intake⁴¹). Major

Table 2. Representative examples of xylose conversion to FF in single solvent systems using heterogeneous catalyst

Entry	C _{Xylose}	T (°C), t	Acid	C _{acid}	Salt	Solvent	Y _{FF,max} (mol%)	Ref
1.	0.13 g/mL	160, 100 min	Amberlyst® 70	0.1 g/mL	-	DMSO	83	41
						Toluene	70	
						Methylformate	66	
						THF	61	
						Guaiacol	56	
						2-Butanol	56	
						Methylacetate	52	
						Iso-propanol	50	
						Acetone	47	
						1-Butanol	46	
						1-Propanol	44	
						Diethyl ether	41	
						Methanol	38	
						Cyclopentanone	28	
						Hexadecane	25	
						Furan	20	
						Water	18	
						Ethylene glycol	13	
						Hydroxyl acetone	5	
						DTF	2	
2.	5.58 wt%	170, 40 min	Amberlyst® 70	5 wt%	-	H ₂ O:methanol 1:4.5	52	42
3.	20.0 mM	140, 4 h	MCM-41-SO ₃ Hc	xylose:catalyst 3:2-w/w	-	DMSO	77	17
4.	200 mM	140, 4 hs	H-mordenite	xylose:catalyst 3:1-w/w	-	DMSO	39	43
5.	27.5 mM	150, 5 h	H-β zeolite (Si/Al=19)	xylose:catalyst 4:1-w/w	-	xylose:2-propanol 1:50-mol/mol	50	35
6.	27.5 mM	150, 8 h	H-β zeolite (Si/Al=19)	xylose:catalyst 4:1-w/w	-	xylose:methanol 1:50-mol/mol	15	35
7.	27.5 mM	150, 2 h	H-β zeolite (Si/Al=19)	xylose:catalyst 4:1-w/w	-	xylose:ethanol 1:50-mol/mol	15	35

differences in FF yields were obtained, ranging from 2 to 83 mol% (Table 2). The effect of combinations of solvents on FF yield was also studied for methanol-water mixtures with different compositions (xylose loading: 5.58 wt%, methanol/water ratio: 10, 4.5, 1, 0.22) in a broad temperature range (90 to 170 °C)⁴². The highest FF yield (up to 50 %) was obtained using a 4.5 methanol/water weight ratio at 170 °C and 40 min reaction time. A reaction network was proposed including methyl-xylosides and FF acetal (2-(dimethoxymethyl)furan) as intermediates. Iglesias *et al.* performed studies on the use of solid acid catalyst for the dehydration of xylose to FF in alcohols (methanol, ethanol, 2-propanol)³⁵. Alkyl xylosides were observed as intermediates. 2-Propanol, gave the highest FF yield (around 50 mol%) after 6 h batchtime (150 °C, substrate/alcohol molar ratio = 1:50, substrate/catalyst mass ratio = 4:1).

Considerable FF yield improvements have also been realised by using biphasic liquid-liquid systems (see Table 3). For instance, the application of an MIBK-water mixture gave a maximum FF yield of 70 mol%²². Furthermore, the combination of a biphasic system (toluene-water) and salt addition (NaCl) resulted in FF yield up to 83 mol%⁴⁴. Performance in biphasic systems using heterogeneous catalysts is worse and FF yields of at maximum 50% have been reported using H-beta in 2-propanol (Table 3)³⁵.

To the best of our knowledge, (systematic) studies on the acid catalysed hydrolysis of xylose to FF using alcohols in general and ethanol and ethanol-water mixtures in particular in single phase systems using homogeneous catalysts have not been reported so far. In this manuscript, the effect of ethanol to water ratios on the acid-catalysed hydrolysis of xylose to FF using sulphuric acid and HCl is reported. The yields of FF versus time were determined and relevant properties of the solid byproducts (humins) were determined. A reaction network is proposed to explain the effects of solvent composition on FF yields. In addition, three solid catalysts were tested in ethanol/water mixtures and performance was compared with reactions in water only.

2. EXPERIMENTAL SECTION

2.1 Chemicals

Xylose (99.5%), absolute ethanol and Nafion® SAC-13 were obtained from Sigma-Aldrich, FF (99%) was from Fluka-Aldrich. H₂SO₄ (95–97 wt-%) and HCl (37 wt-%) were purchased from Merck GmbH (Darmstadt, Germany).

Table 3. Representative examples of xylose conversion to FF in biphasic solvent systems

Entry	Xylose Concentration	T (°C), t	Acid	Acid concentration or ratio	Salt	Solvent	Yield (mol%)	Ref
Homogeneous catalysts								
1.	1 mM	140, 45 min	-	-	AlCl ₃ ·6H ₂ O – NaCl 0.4 – 24mmol	H ₂ O:THF 1:3-v/v	75	45
2.	10%-wt	100–110, 300 min	H ₂ SO ₄	10%-w/w	NaCl 2.4g	H ₂ O:toluene 1:15-v/v	83	44
3.	10%-wt	170, 65min	HCl	0.10 M	-	H ₂ O:MIBK 1:1-w/w	70 (85) ^a	22
Heterogeneous catalysts								
4.	27.5 mM	150, 8 h	H-β zeolite (Si/Al=19)	substrate: catalyst 4:1-w/w	-	substrate: methanol 1:50-mol/mol	15	35
5.	27.5 mM	150, 2 h	H-β zeolite (Si/Al=19)	substrate: catalyst 4:1-w/w	-	substrate: ethanol 1:50-mol/mol	15	35
6.	27.5 mM	150, 5 h	H-β zeolite (Si/Al=19)	substrate: catalyst 4:1-w/w	-	substrate: 2-propanol 1:50-mol/mol	50	35

^a Value in bracket is the yield based on a kinetic model

Amberlyst® 15 was obtained from Rohm and Haas Company and Dowex® 50WX8 from Dow Water and Process. All chemicals were used as received. Milli-Q water was used for all reactions and analysis procedures.

5

2.2 Experimental Procedures

All reactions were carried out in a microwave device (Discover from CEM) in reactor vials of 10 mL. Micro-magnetic teflon bars (10 x 3 mm) were used for stirring. PTFE (polytetrafluoroethylene) filters (0.45 μm) used to filter reaction mixtures prior to HPLC analysis were obtained from VWR, the Netherlands.

Representative Experimental Procedure for A Homogeneous Catalyst

A solution of xylose (0.1 M, 2 mL) and a mineral acid (H₂SO₄ or HCl) in an ethanol/water mixture was added to a microwave vial (10 mL) and closed with a plastic cap. The tube was placed in the microwave device and heated under stirring (800 rpm) to 150 °C and kept at this temperature for the pre-determined

reaction time. After reaction, the vial was rapidly cooled to 40 °C. The liquid content was then filtered using a 0.45 µm PTFE syringe filter and diluted 6–7 times with water prior to analysis by HPLC.

Representative Experimental Procedure for A Heterogeneous Catalyst

A similar procedure as for the homogeneous catalysts was used, with the exception that a solid acid catalyst was applied. The amount of solid acid catalyst was different for each catalyst as a similar acid concentration (meq H⁺/ml liquid) was used for experiments with the different catalysts to allow for a proper comparison of catalyst activity (94.2 mg of DOWEX® 50WX8, 42.6 mg of Amberlyst® 15, 250 mg of Nafion® SAC-13). The acid capacity (meq H⁺/g cat) of the solid catalysts is given in Table S1, supplementary information.

Isolation of Humins Samples from Reactions with FF

Reactions were carried out using FF as the feed and either HCl or sulphuric acid as the catalyst at 150 °C using three solvent compositions (pure water and pure ethanol and an ethanol-water mixture with 70 wt-% ethanol). After reaction in the microwave reactor (150 min), the solids were separated from the liquid by decantation and the humins were washed several times with water and filtered using a 2.5 µm cellulose filter (Sigma-Adrich) until the pH of the washing water was neutral and HPLC analyses showed the absence of peaks from dissolved organics. The humins sample were isolated and dried overnight in an oven at 50 °C.

Product Analysis

The composition of the liquid phase after reaction was determined by HPLC using an Agilent 1200 HPLC equipped with a HP 1200 pump, a Bio-Rad organic acid column (Aminex HPX-87H), and an RID or an UV detector. The mobile phase consists of aqueous sulphuric acid (5 mM) at a flow rate of 0.55 cm³/min. The column was operated at 60 °C. The analysis for a sample was complete in 60 minutes. A typical chromatogram is shown in Figure S1 (Supplementary information). The concentrations of each compound in the

product mixture were determined using calibration curves obtained by analyzing standard solutions of known concentrations.

GC-MS analyses were performed using an HP6890 GC equipped with a HP1 column (dimethylpolysiloxane, length: 25 m, inside diameter: 0.25 mm, film thickness: 0.25 μm) in combination with a HP5973 mass selective detector. Peak identification was done using the NIST05a mass spectra library. Injection and detection were performed at 280 °C and an oven temperature heating profile from 30 to 280 °C with an increment of 5 °C/min was used.

The APT ^{13}C -NMR spectra were performed in CDCl_3 at room temperature using a Varian AS200 NMR Spectrometer (8192 scans and a relaxation delay of 1 s).

High-Resolution Transmission Electron Microscopic (HRTEM) images were recorded on a JEOL JEM 2010F TEM (JEOL Ltd., Tokyo, Japan) operated at 200 kV, 1.9 A in vacuum.

Scanning Electron Microscope (SEM) images were measured on a Philips XL30 Environmental SEM FEG device operated at 5 or 10 kV.

The elemental composition (C, H, N and S) of humins were determined using an Euro Vector 3400 CHN-S analyzer. The oxygen content was determined by difference. All experiments were carried out in duplicate and the average value is provided. The Cl analyses were carried out by Mikro-lab (Germany) using a modified Schöniger Aufschluss method.

Definitions

The xylose conversion (X_{XYL}), FF yield (Y_{FF}) and FF selectivity (S_{FF}) are mol% based and calculated using equations 1–3:

$$X_{\text{XYL}} = \frac{(C_{\text{XYL},i} - C_{\text{XYL},t})}{C_{\text{XYL},i}} \quad (1)$$

$$Y_{\text{FF}} = \frac{C_{\text{FF},t}}{C_{\text{XYL},i}} \quad (2)$$

$$S_{\text{FF}} = \frac{Y_{\text{FF}}}{X_{\text{XYL}}} \quad (3)$$

Here, $C_{\text{XYL},i}$ is the initial xylose concentration (mol/l), $C_{\text{FF},i}$ the initial FF concentration and $C_{\text{XYL},t}$ and $C_{\text{FF},t}$ the xylose and FF concentration at a certain batch-time. For experiments using FF as the feed, the FF conversion (X_{FF}) is defined as:

$$X_{\text{FF}} = \frac{(C_{\text{FF},i} - C_{\text{FF},t})}{C_{\text{FF},i}} \quad (4)$$

3. RESULTS AND DISCUSSION

3.1 Dehydration of Xylose to FF In Water-Alcohol Mixtures using Sulphuric Acid

The conversion of xylose to FF was investigated with sulphuric acid in ethanol-water mixtures (40, 50, 70, 90 wt% ethanol) and water as the reference. Experiments above 90% ethanol were not performed as the solubility of xylose in such mixtures at room temperature is insufficient and a solid-liquid system is obtained. All reactions were performed in a microwave reactor at a temperature of 150 °C with reaction times between 0 and 270 min. A fixed xylose concentration of 0.1 M was applied. Initial investigations were carried out using H₂SO₄ (0.1 M), as this acid is commonly used for commercial FF production in water^{5,6}. All reactions were carried out at least in duplicate and showed good reproducibility.

For reactions in water only, an orange-brown suspension was formed after reaction with a considerable amount of dark brown solids known as humins (Figure S2, supplementary information). In contrast, reactions in ethanol and ethanol-water mixtures led to the formation of an orange-brown solution with minor/no solids present. Apparently, solids formation is suppressed in ethanol-water mixtures and/or the humins formed during these reactions are more soluble in the reaction medium than for reactions in water only. The main reaction products detected by HPLC are FF, diethyl ether and 2 peaks which were tentatively identified as ethylxylosides (*vide infra*) (Figure S1, Supplementary information). Quantification of the diethyl ether produced proved very difficult due to its high volatility in combination with the use of a microwave reactor.

The xylose conversion and FF yield versus time curves for an experiment with an ethanol content of 90% (150 °C, C_{XYL,0} = 0.1 M, C_{H₂SO₄} = 0.1 M) is provided in Figure 1, together with profiles for a reaction in water only at the same conditions.

The xylose conversion and FF yield versus time curves differ considerably for the two cases. In water, the xylose conversion versus time profile shows a typical first order dependency and the conversion is about 90% after 180 min. The FF selectivity is high at the start but slowly levels off, likely due to the occurrence of side reactions (Scheme 1).

A different picture is obtained in ethanol/water mixtures. The most important feature is the observation that the FF yield after prolonged reaction times

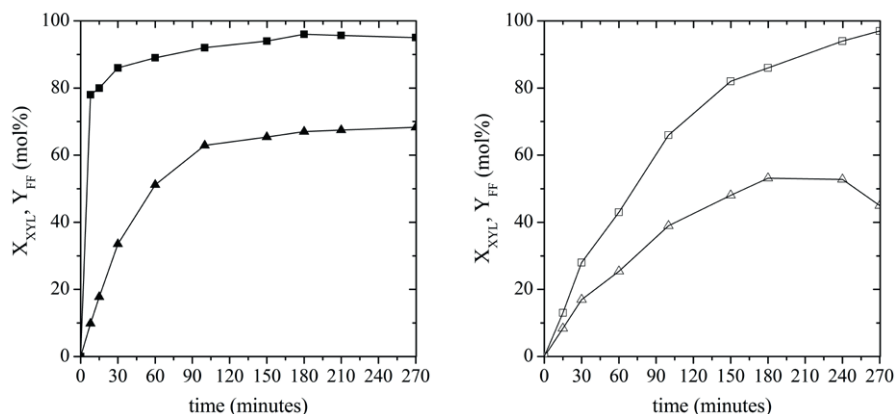


Figure 1. Xylose conversion (X_{XYL} , \square or \blacksquare) and FF yields (Y_{FF} , Δ or \blacktriangle) versus time for a reaction in 90/10 w/w ethanol-water (left) and water alone (right) at 150 °C ($C_{\text{XYL},0} = 0.1\text{M}$, $C_{\text{H}_2\text{SO}_4} = 0.1\text{M}$)

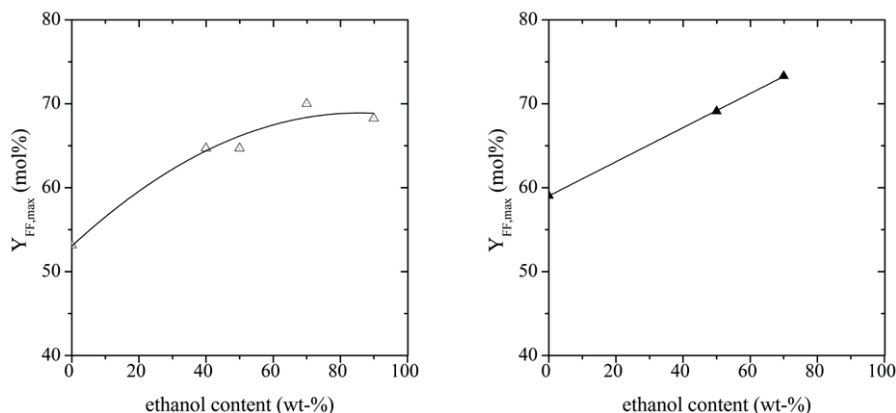
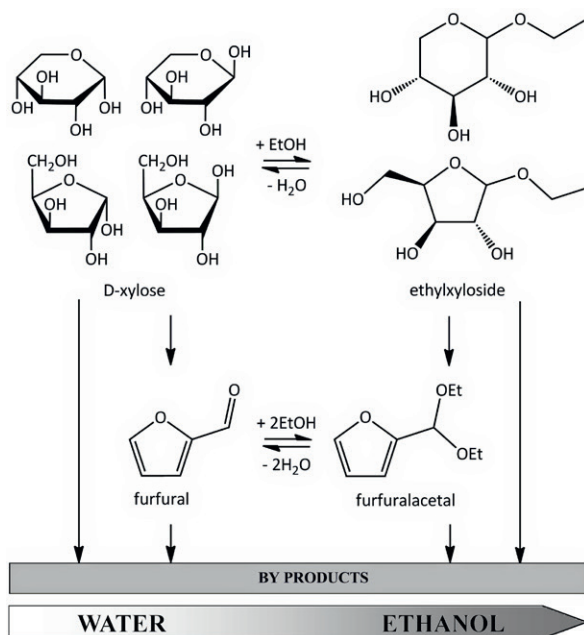


Figure 2. Maximum FF yield ($Y_{\text{FF,max}}$) versus ethanol content (wt%) for 0.1 M sulphuric acid (left) and 0.5 M sulphuric acid (right). Lines are for illustrative purposes only.

is higher than in water only, showing a positive effect on the addition of ethanol on FF yield (Figure 1, left). This is further illustrated in Figure 2, where the maximum FF yield for an experiment is given as a function of the ethanol content in the reaction mixture. It shows that the maximum FF yield increases with the ethanol content, though levels off at ethanol contents above 50–60 wt%. For experiments at the low acid concentration, the best results

were obtained at 70–90 wt% ethanol, giving a maximum FF yield of 72 mol% (70 wt% ethanol). This is about 20% higher than found for reactions in water.

Another important feature is the observation of high xylose conversions already at short reaction times when ethanol is present, see Figure 1 for details. This is indicative for the initial rapid conversion of xylose to an intermediate in the reaction sequence. In analogy with reactions of xylose in acidic methanol using solid acid catalysts, the intermediate is likely an ethyl-xyloside, obtained by the etherification of xylose (Scheme 2)^{35,42}.



Scheme 2. Proposed reaction network for xylose conversion to FF and byproducts

In theory, four ethylxylosides can be formed, *viz.* the furanose and pyranose forms and their anomers (α - and β -form). All species are rapidly interconverting though the pyranose forms appear to be thermodynamically favoured⁴⁶. The formation of alkylxylosides was also observed by Iglesia *et al.* when performing the conversion of xylose in various alcohols using solid acid catalysts³⁵. On the basis of the conversion-time profiles in the presence of ethanol, we can conclude that the reaction rate for the ethylxyloside formation is by far faster than for the reactions leading to FF.

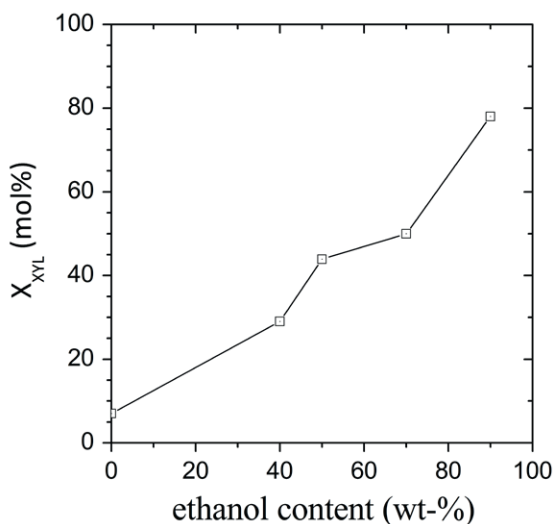


Figure 3. Xylose conversion (X_{XYL}) versus ethanol content (wt%) after 8 min reaction time (150 °C, $C_{XYL,0} = 0.1$ M, $C_{H_2SO_4} = 0.1$ M)

Alkylxyloside formation is known to be an equilibrium reaction and the position of the equilibrium is expected to be a function of the ratio of water to ethanol in the mixture. This is also clear when considering the xylose conversion at short batch times for the experiments conducted at different ethanol to water ratios (Figure 3). When assuming that in the initial stage of the reaction only ethylxyloside formation occurs, which is in line with a very low FF yield at the start of the reaction, this plot confirms that the reaction is indeed an equilibrium limited reaction and that higher ethanol contents lead to higher concentrations of ethylxylosides.

Clear maxima for the FF yield versus time curves when using 0.1 M sulphuric acid were not observed (Figure 2). As such, experiments with a higher acid concentration ($C_{H_2SO_4} = 0.5$ M) were performed and the results for an experiment with 70 wt% ethanol is given as an example in Figure 4. At the higher acid concentration, the reaction rates are, as expected, much higher than for the lower sulphuric acid concentration. In addition, the FF yield is a function of the batch time and clear optima were observed, both in the presence of ethanol and in water only. The maximum FF yield was 73 mol% for 70 wt% ethanol, compared to 59 mol% in water only (Figure 2, right). As such, the addition of ethanol has, like with low acid concentrations, a positive effect on the FF yield. The observation of clear maxima for the FF yield also indicates

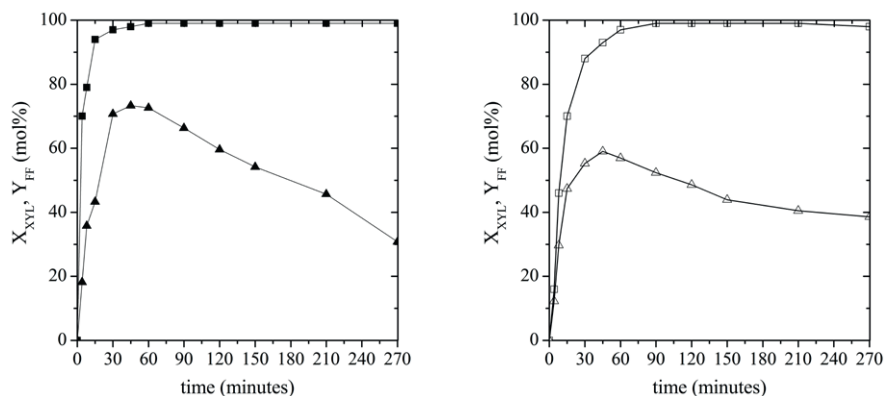


Figure 4. Xylose conversion (X_{XYL} , \square or \blacksquare) and FF yields (Y_{FF} , Δ or \blacktriangle) versus time for a reaction in 70/30 w/w ethanol-water (left) and water alone (right) at 150 °C, $C_{\text{XYL},0} = 0.1 \text{ M}$, $C_{\text{H}_2\text{SO}_4} = 0.5 \text{ M}$

that FF is prone to decomposition under the prevailing conditions. This is a well-known observation and a main issue when aiming for high FF yields.

3.2 Determination of The Rate of FF Decomposition in Water-Ethanol Mixtures

To gain insights in the rate of FF decomposition as a function of the solvent composition, a number of experiments with FF was performed for a wide range of ethanol to water ratios (0–95 wt-%) in a microwave reactor using sulphuric acid as the catalyst (150 °C, batch times between 0 and 4.5 h, initial FF concentration of 0.05 M and 0.1 M H_2SO_4). All reactions were carried out at least in duplicate and showed good reproducibility. The FF concentration versus time profiles are given in Figure 5. Products were not identified in detail, though analyses of the reaction mixture showed the presence of formic acid (FA) and other soluble, unidentified compounds (HPLC). In addition, considerable amounts of solids (humins) were formed by condensation/polymerization reactions^{3,10}.

The extent of FF decomposition is a clear function of the solvent composition (Figure 5, left). In water alone, FF decomposes with a significant rate and the concentration drops to 2/3 of the initial value within 1 h. In the presence of ethanol, the decomposition rate is retarded, provided that the ethanol content is below 90 wt%. At higher ethanol contents, the rate of FF decomposition increases again. As such, there is an optimum ethanol-water ratio when aiming

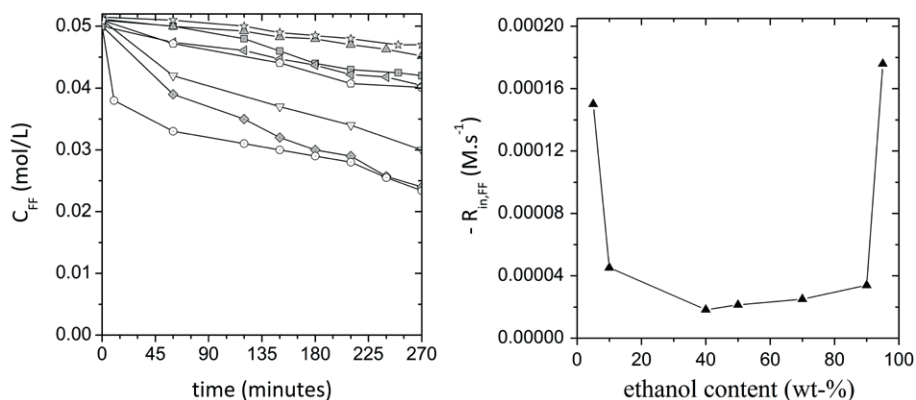
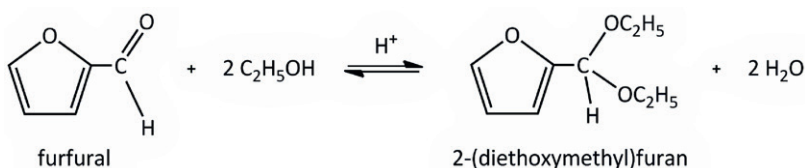


Figure 5. FF concentration versus time for several ethanol/water mixtures (wt-%): 95 (◇), 90 (◁), 70 (□), 50 (△), 40 (☆), 10 (◊), 5 (▽) and 100 wt% water (O) (left graph) and the initial rate of FF decomposition ($R_{in,FF}$) versus the ethanol content (wt-%, right graph). Conditions: 150 °C, microwave reactor, initial FF concentration of 0.05 M, $C_{H_2SO_4}$ = 0.1 M.

for a low rate of FF decomposition, see Figure 5 (right). Here, the initial rate of FF decomposition, obtained from the plots of the concentrations of FF versus time, for various solvent compositions is given. It is clear that an intermediate ethanol content is the best and leads to lowest rates of FF decomposition. A possible explanation for this trend is the involvement of FF acetals (Scheme 3).



Scheme 3. Acetal formation from FF

FF acetal formation was investigated by performing reactions of FF with absolute ethanol in the presence of H_2SO_4 (0.05 M). GC-MS analysis of reaction mixtures (Figure S3, Supplementary information) shows the presence of both FF and FF-acetal. This was confirmed by APT ^{13}C -NMR studies on a mixture of FF and ethanol in $CDCl_3$ in the presence of H_2SO_4 (Figure S4, Supplementary material). Acetal formation is known to be an equilibrium reaction

and it is expected that the equilibrium position is shifting towards FF-acetals at higher ethanol content⁴⁷.

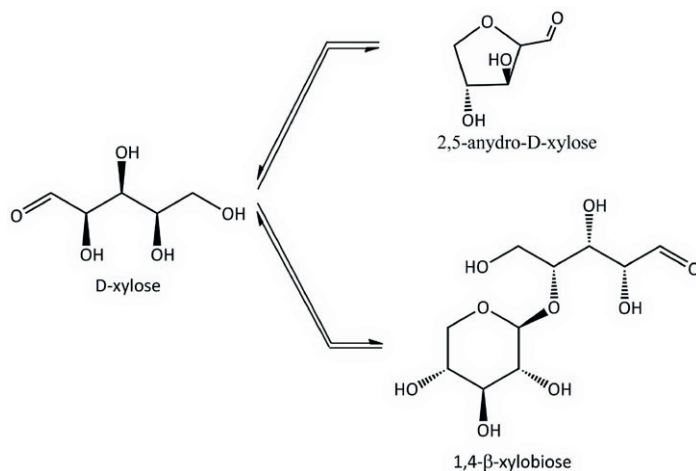
The observed experimental trends (Figure 5) i.e. the highest stability of FF at intermediate ethanol content suggests the occurrence of two opposing effects. The experimentally observed positive effect of the addition of ethanol to water may be due to a solvent effect, i.e. a lower reactivity of FF when increasing the amount of ethanol in the reaction mixture. At higher alcohol contents, the stability is reduced and this may be explained by assuming that FF-acetals, formed in significant amounts at alcohol content above 70%, react faster to byproducts than FF itself.

3.3 Mechanistic Considerations

The experimental observations may be rationalised using the reaction network given in Scheme 2. In water alone, xylose is converted to FF and by-product, and subsequently FF is prone to degradation to a number of soluble and insoluble components. Intermediates in the sequence (e.g. xylose isomers like xylulose and lyxose) are not given for brevity. This network predicts a maximum FF yield as a function of the batch time, the exact yield being a function of the rate of FF formation and decomposition reactions, in line with experimental findings (see e.g. Figure 1 and 4).

For the conversion of xylose in the presence of ethanol, a number of additional (equilibrium) reactions have to be considered, *viz.* i) the formation of ethylfructosides, ii) the formation of FF-acetals from FF and iii) the formation of xylose reversion products (Scheme 3). The latter reactions were not considered as these are only of importance at high xylose concentrations⁴⁸.

Alkylxyloside formation is known to be an equilibrium reaction with quantitative alkyl-xyloside formation in pure alcohols. In water-ethanol mixtures, the equilibrium ratio of xylose and ethylxylosides is expected to be a function of the solvent composition, see also Figure 3. Xylose and ethyl-xylosides are expected to react with different rates to FF and byproducts (Scheme 2). The latter was recently confirmed by Iglesia *et al.*³⁵ when studying the dehydration of xylose in alcohols (methanol, ethanol, isopropanol) using heterogeneous catalysts. When methyl- β -D-xylopyranoside was used as the starting material for reactions in methanol (in the presence of equivalent amounts of water), xylose was formed in moderate amounts, confirming the reversible nature of the etherification reaction. In addition, FF was also observed,



Scheme 4. Simplified reaction scheme for the formation of xylose reversion product: one of the possible xylose dimers and 2,5-anhydro-D-xylose

however in a lower yield than when starting from xylose. These findings suggest the existence of a separate reaction pathway from methyl-xylosides to FF, next to the direct reaction from xylose.

Our experimental data reveal that higher ethanol concentrations (till about 90%) have a positive effect on the yields of FF. In addition, the experiments with FF indicate that ethanol has a positive effect on the stability at ethanol concentrations up to about 90% and that higher ethanol contents result in a considerable reduction of the stability. These findings may be rationalised using Scheme 2 and the following assumptions:

- i) xyloses and ethylxylosides are in rapid equilibrium and with higher ethanol contents in the mixture leads to higher amounts of ethylxylosides, in line with our (Figure 3) and literature findings.
- ii) the reaction rate for the reaction of ethylxylosides to FF is much lower than the direct reaction of xylose to FF. In addition, it is assumed that ethylxylosides are more stable under the reaction conditions than xylose and that the rate of by- and decomposition product formation is lower than for xylose. This effectively means that ethylxylosides can be considered as a resting state for the more reactive xylose.
- iii) the rate of decomposition of furfuralacetals to byproducts is larger than the rate of decomposition of FF. This is rationalised by our experimental data (*vide supra*).

With these assumptions, the positive effect of intermediate amounts of alcohols in the reaction mixture on FF yields compared to reactions in water may be explained by i) the formation of relatively stable ethylxylosides, which effectively reduce the amounts of xylose in the reaction mixtures, and, when assuming that xylose is more reactive for byproduct formation than the xylosides, this will lead to lower amounts of byproduct and ii) a lower rate of decomposition of FF. However, at alcohol concentrations above about 70%, the maximum FF yields level off, which is likely due to the formation of higher amounts of FF acetals, which are less stable and lead to higher amounts of byproducts (*vide supra*). As such, the maximum FF yield is a function of the relative amount of ethylxylosides and FF-acetal in the reaction mixture. High amounts of the former have a positive effect on the FF yield whereas high amounts of acetals should be avoided. As such, intermediate ethanol content is required for high FF yields.

In addition, another side reaction that may have implication on the amounts of FF formed is the undesired acid catalysed etherification of ethanol to diethyl ether. The latter was observed in the reaction mixture, particularly for reactions with a high ethanol content. This reaction reduces the amount of ethanol and increases the amount of water, effectively reducing the ethanol content in the reaction mixture. Unfortunately, we were not able to quantify the amounts of diethyl ether, making it difficult to assess the exact effect of this side reaction on maximum FF yields.

As such, detailed kinetic studies, beyond the scope of this paper, will be required to get information on the rate of the individual reactions in Scheme 2 as a function of the solvent composition. These studies will provide information on the preferred reaction pathways at various solvent compositions, allowing to rationalise the experimental findings and particularly the maximum FF yields as a function of the solvent composition in a quantitative manner.

3.4 Conversion of Xylose to FF in Water-Alcohol Mixtures using HCl

For comparison, a number of reactions were carried out with HCl (0.2 M) instead of sulphuric acid (150 °C, 0.1 M xylose, 0, 50 and 70 wt%-ethanol). As with sulphuric acid, FF was the main product, byproducts were some solids (particularly in water only), diethyl ether and ethyl chloride (Figure S5, Supplementary information). Both are well known products from reactions of ethanol with HCl.

Diethyl ether is formed by the acid catalysed etherification⁴⁹, and ethyl chloride by a nucleophilic substitution reaction⁵⁰. The amounts of diethyl ether and ethyl chloride in the reaction mixtures were not quantified.

The yield of FF and the conversion of xylose as a function of the batchtime are provided in Figure 6. The highest FF yield was 71 mol% (150 °C, initial $C_{\text{XYL}} = 0.1 \text{ M}$, $C_{\text{HCl}} = 0.2 \text{ M}$), which is about similar to the best result found for sulphuric acid. All experiments show similar profiles, viz. a rapid increase in the conversion of xylose (complete conversion within about 60 min) and a maximum in the yield of FF after about 30 min. The latter is, as for the experiments with a high sulphuric acid concentration, indicative for a consecutive reaction network with FF as the intermediate.

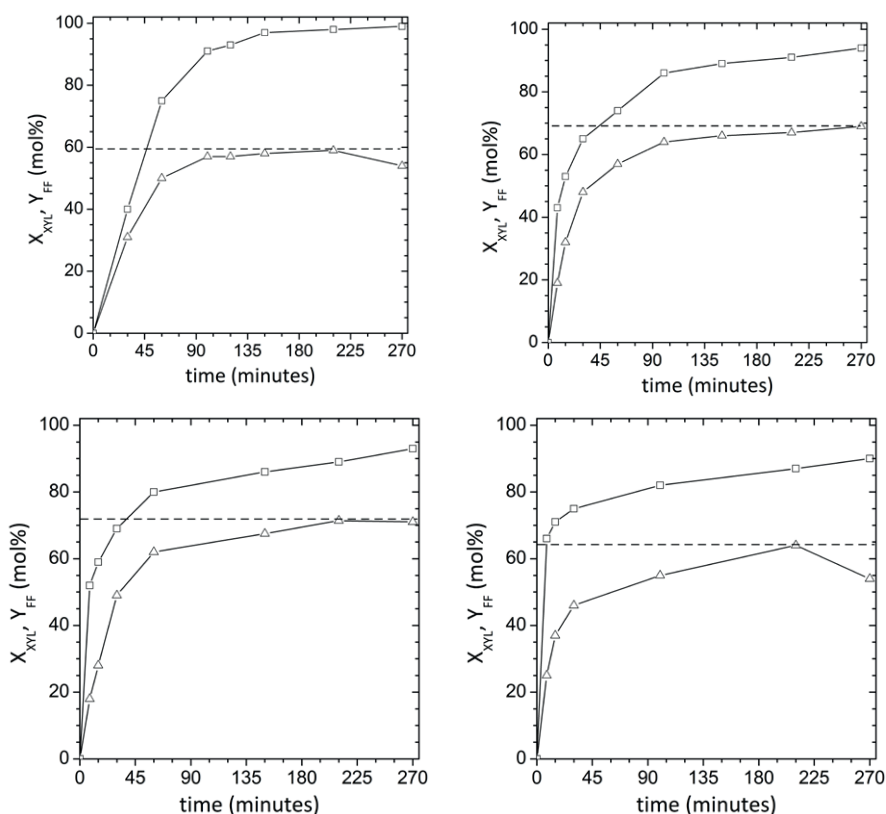


Figure 6. Xylose conversion (X_{XYL} , \square) and FF yields (Y_{FF} , \triangle) versus time for different ethanol-water ratio's using HCl: top left: 100 wt-% water; top right: 40 wt-% ethanol; bottom left: 50 wt-% ethanol and bottom right: 70 wt-% ethanol (microwave reactor, $T=150 \text{ }^{\circ}\text{C}$, initial xylose concentration of 0.1 M using 0.2 M HCl)

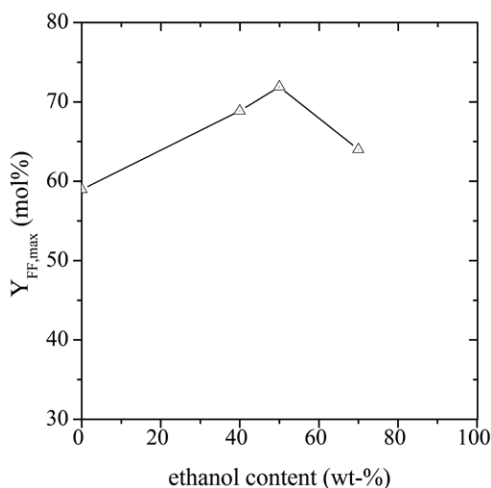


Figure 7. Maximum FF yield ($Y_{FF,max}$) versus ethanol content (wt%) for 0.2 M HCl. Lines are for illustrative purposes only

The maximum FF yield is a clear function of the solvent composition, see Figure 7 for details. The best results were obtained in a mixture with 50 wt% of ethanol. For sulphuric acid, a somewhat different trend was observed (Figure 2). At low ethanol contents, the trends are the same, i.e. a linear increase of maximum FF yield was observed at higher ethanol content. However, at ethanol content above 50%, the trends differ and a drop in FF yield is observed for HCl, which is by far less pronounced for sulphuric acid.

Table 4. Elemental composition of the isolated humins samples from reactions with FF

Sample	Catalyst	Solvent composition (wt-% ethanol)	Elemental composition (wt-%)			
			C	H	S	O ^a
A	HCl	0	66.22	4.02	--	29.76
B	H ₂ SO ₄	0	65.21	4.04	0.06	30.69
C	HCl	70	66.18	4.11	--	29.71
D	H ₂ SO ₄	70	62.03	3.02	1.02	21.87
E	HCl	100	68.31	3.17	--	28.52
F	H ₂ SO ₄	100	67.23	4.23	0.50	28.04

^aBy difference

3.5 Investigation in Humins Composition and Properties

All acid catalysed reactions of xylose and FF and particularly those in water resulted in the formation of solid byproducts, also known as humins. The humins formed after reactions with FF as the feed with different solvent compositions were isolated and characterised using elemental analysis and SEM. In addition, liquid samples were taken from the reaction mixtures and these were analysed by TEM after evaporation of the liquid. The latter approach gives information on the size and properties of the small humins particles ($< 1 \mu\text{m}$ level) in solution which are not visible when using the isolation protocol for humins samples.

Properties of Isolated Humins Samples

A total of 6 humins samples were isolated and characterised using elemental analyses and SEM. All of these were obtained from reactions using FF as the feed and either HCl (0.2 M) or sulphuric acid (0.1 M) as the catalyst and prepared at 150 °C for a batch time of 150 min. Three solvent compositions were used, viz pure water and pure ethanol and an ethanol-water mixture with 70% ethanol. The elemental composition of the isolated humins samples as determined by elemental analysis is given in Table 4. The C and H contents for all samples show a considerable variation and range from 62.03–68.31 wt% for C and 3.02–4.11 wt% for H.

The data are summarised in a van Krevelen plot given in Figure 8. All samples fall within the elemental composition range as reported for humins. However, there is considerable spread in the data and particularly the sample obtained in a solvent mixture with 70 wt%-ethanol using sulphuric acid shows a by far higher O/C ratio. A possible explanation is the relatively high amount of sulphur in this sample (1.02 wt%), most likely in the form of sulphonate groups (*vide infra*). This will lead to a relative increase in the oxygen content of the sample, in line with the experimental data.

The S content of the samples was also determined using elemental analyses and the results are given in Table 4. When using sulphuric acid as the catalyst, S was detected in 2 of the 3 samples in significant amounts ($> 0.5 \text{ wt}\%$). These samples were obtained from reactions in the presence of ethanol. These findings indicate that S may be incorporated in the humins structure during formation, an observation to the best of our knowledge not reported

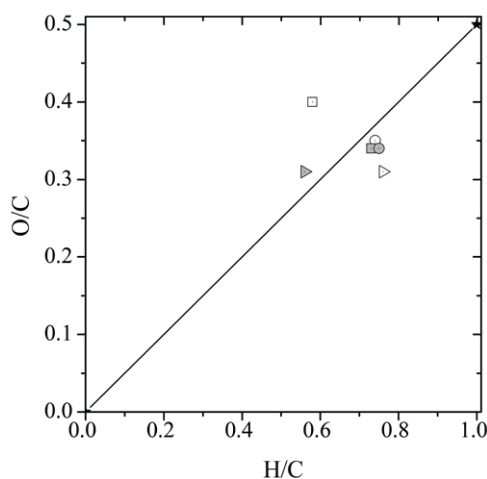


Figure 8. van Krevelen plot for the isolated humins samples from FF for water (O), 70 wt% ethanol (□) and 100 wt% ethanol (▷); white: H₂SO₄, grey: HCl. FF (★) is given as the reference. Conditions: 150 °C, microwave reactor, $C_{FF,initial} = 0.05$ M, $C_{H_2SO_4} = 0.1$ M, $C_{HCl} = 0.2$ M.

to date. The amount of S in the samples is a function of the solvent composition, and the highest S content was obtained at 70 wt% ethanol. Cl analysis were also performed and showed that the Cl content in the samples is below the detection limit of the elemental analysis technique used.

A possible reaction pathway involves sulphonation of the condensed humins structure by sulphuric acid, a well known reaction for instance the introduction of sulphonic acid groups to activated carbons⁵¹. For instance, the treatment of activated charcoal with concentrated sulphuric acid at 100 °C in water resulted in the introduction of sulphonic groups in the range of 90–170 µmol/g (as determined by elemental analysis). In our case, the maximum sulphur content was 1.02 wt% (Table 4), which corresponds to a sulphonic group concentration of 320 µmol/g. The dataset shows that the S content is the highest for the reaction in a mixture of ethanol and water (70% ethanol). As such, the rate of the sulphonation reaction seems to be a function of the solvent composition. So far, we do not have a sound explanation to explain this finding.

The morphology of the humins samples was determined using SEM and the results are given in Figure 9. All samples show the presence of agglomerated spherical humins particles, in line with literature data^{52,53}. The extent of agglomeration differs for the samples. For sample B, the individual particles

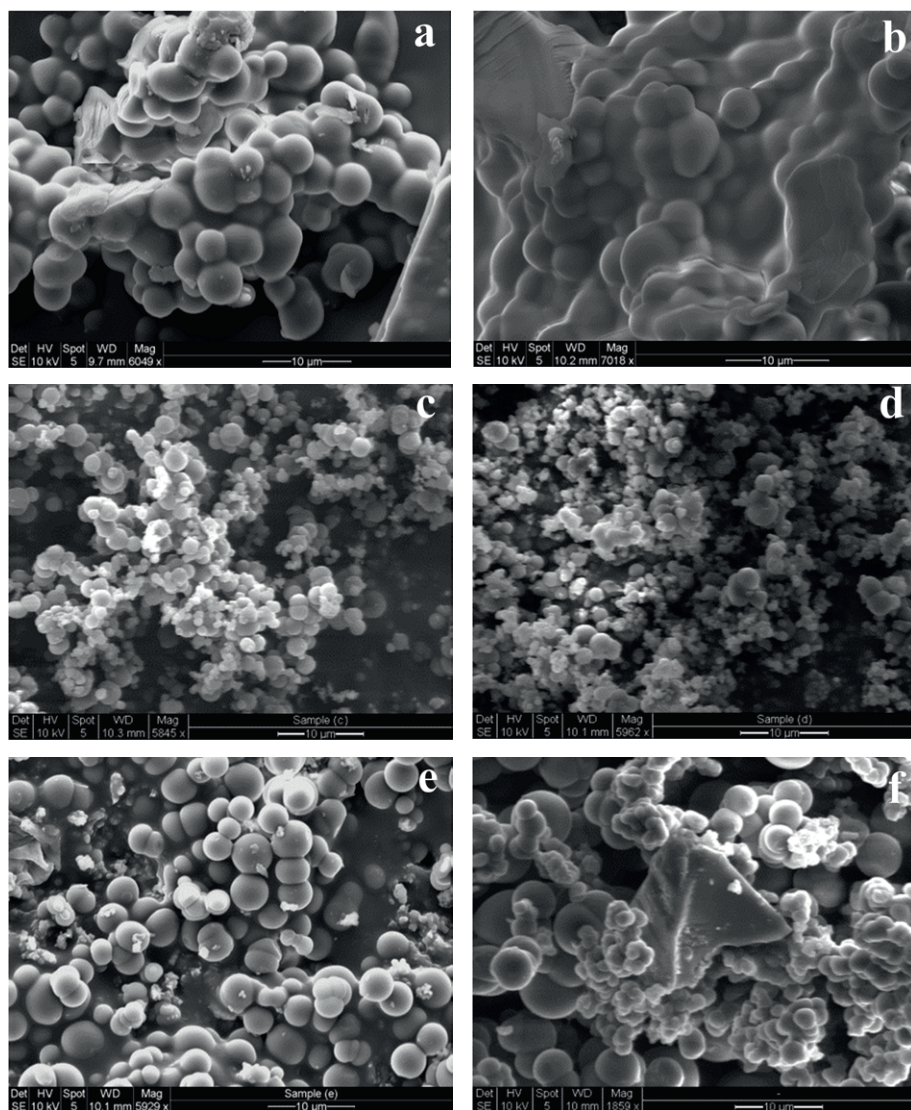


Figure 9. SEM analysis of isolated humins obtained from FF (a) HCl in water, (b) H_2SO_4 in water, (c) HCl in 70 wt-%-ethanol, (d) H_2SO_4 in 70 wt-%-ethanol, (e) HCl in 100 wt-%-ethanol and (f) H_2SO_4 in 100 wt-%-ethanol.

are highly agglomerated and actually fused. The average sizes of the individual particles are between 1 and 8 µm. The smallest particles were observed for sample C and D, both obtained from reactions in 70 wt% ethanol. Thus, the

solvent composition seems to play an important role in the sizes of individual humins particle both when using HCl and H₂SO₄ as the catalyst.

Analysis of Small Humins Particles

The previous paragraph involved analyses of the isolated humins samples. However, by using the isolation procedure provided, only larger humins particles are isolated, whereas the smaller ones will remain in the washing liquids. To gain insights in the morphology and size of the smaller humins particles, liquid samples were taken from the reaction mixture and transferred to a HRTEM and analysed. In this case, four samples were taken, obtained from reaction mixtures using FF (0.05 M) as the feed and HCl and sulphuric acid as the catalysts obtained at 150 °C and a batch time of 150 min using a microwave reactor. Two solvent compositions were used, viz. 100% water and an ethanol-water mixture with 70% ethanol. Representative TEM images are given in Figure 10.

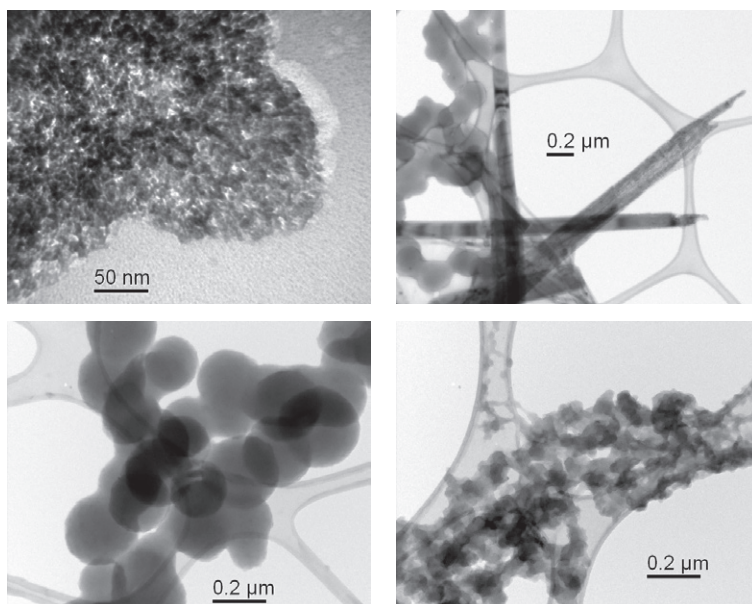


Figure 10. TEM image of humins from FF using H₂SO₄ in 100% water (top left), H₂SO₄ in ethanol/water with 70% ethanol (top right), HCl in 100% water (bottom left) and HCl in ethanol/water with 70% ethanol (bottom right)

Distinct differences in particle morphology and particle sizes were observed for the 4 samples. For water, the reactions catalysed by sulphuric acid resulted in the formation of aggregates consisting of small individual humins particles (< 10 nm), whereas larger individual particles were found for the reactions catalysed by HCl (up to 200 nm). For reactions in the presence of ethanol, the morphology of the humins differs considerably. Both (agglomerated) spherical particles, as well as needles were observed for reactions catalysed by sulphuric acid, whereas small agglomerated particles were visible for HCl. For HCl, the particles obtained in the presence of ethanol were by far smaller than for reactions in water only. As such, it appears that remarkable differences in humins morphology were present between HCl and sulphuric acid on the one hand and water and ethanol/water mixtures on the other. As such, the formation and growth mechanism of humins particles is a strong function of the catalyst and the solvent composition.

HRTEM was not only used to study the morphology of the humins particles, but also provided information on the crystallinity of the individual samples. The results are shown in Figure 11. The humins samples obtained using

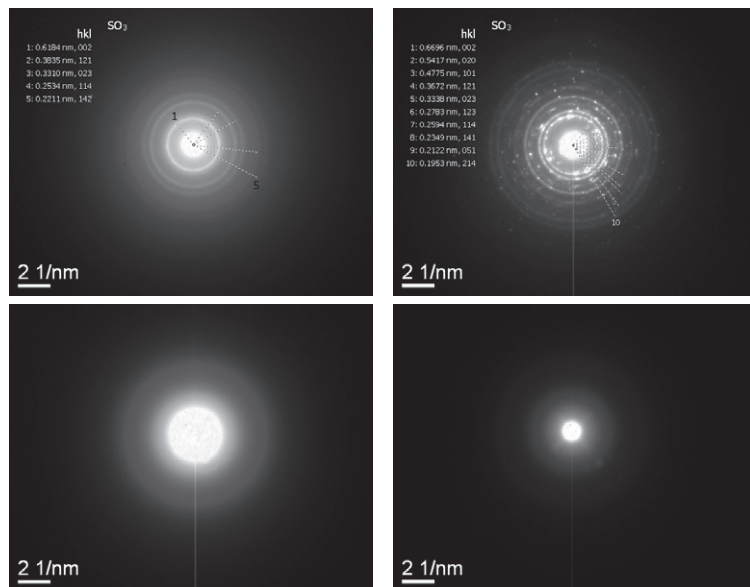


Figure 11. HRTEM electron diffraction pattern of humins from FF using H₂SO₄ in 100% water (top left), H₂SO₄ in ethanol/water with 70% ethanol (top right), HCl in 100% water (bottom left), HCl in ethanol/water with 70% ethanol (bottom right)

H₂SO₄ both in water and ethanol/water are partly crystalline, as evident from clear diffraction patterns. The extent of crystallinity appears to be larger for the samples obtained in water as evidenced by the absence of individual dots in the diffraction pattern from amorphous domains. The latter are clearly present in Sample C, obtained using an ethanol-water mixture. In contrast, the samples prepared using HCl as the catalyst do not show a clear diffraction pattern and are indicative for an amorphous structure.

The diffraction patterns for the samples obtained with sulphuric acid are associated with SO₃ groups, in line with the presence of S in the isolated humins samples. This finding supports our hypothesis that sulphuric acid reacts with the humins and introduces sulphonic groups by a sulphonation reaction.

3.6 Xylose Conversion to FF in Ethanol-Water Mixtures using Solid Brønsted Acid Catalysts

Heterogeneous catalysts have been used successfully for the conversion of xylose to FF, see introduction section for details. Their use has certain advantages compared to homogeneous catalysts like hydrochloric acid and sulphuric acid which require i) an expensive catalyst recycling step or ii) a catalyst neutralization step which will produce large amounts of salts^{54,55}. We have explored the use of 3 heterogeneous catalysts i.e. Amberlyst® 15, Nafion® SAC-13 and Dowex® 50WX8 as alternatives for H₂SO₄ and HCl for the conversion of xylose to FF in water and in water-ethanol mixtures (50, 70 and 90 wt-% ethanol). In all cases, the initial xylose concentration was 0.1 M, the temperature was 150 °C, and a batch time of 150 min was applied. The experiments were performed at constant acidity (meq H⁺). Each catalyst has a different acidity (meq H⁺/g), and as such the catalyst intake (in g) was a function of the catalyst. An overview of experimental conditions is given in Table 5.

When comparing the performance of the three catalyst, the best resulting regarding FF yield were obtained using Dowex® 50WX8. The highest FF yield in the range was 68 mol%, at a 96% xylose conversion in a mixture of ethanol-water with 90% ethanol. This value is close to the best results in sulphuric acid (73 mol%) and HCl (71 mol%) and comparable to the result reported for MCM-41-SO₃Hc in DMSO (77 mol%). It is by far higher than obtained with H-β zeolite both in ethanol (15 mol%) and in 2-propanol (50 mol%), see Table 2 for details^{35,42}. The other two catalysts performed worse. It is difficult with this limited dataset to identify catalyst property-performance relations.

Table 5 Experimental overview for the reaction of xylose to FF using solid acid catalysts at different ethanol-water ratios^a

Entry	Solid catalyst	Catalyst intake (mg)	Ethanol/water ratio (w/w)	X _{XYL,max}	Y _{FF,max}
1.	Amberlyst®-15	42.6	0	33	20
			50	66	20
			70	81	39
			90	91	48
2.	Dowex® 50WX8	94.2	0	68	32
			50	79	36
			70	87	57
			90	96	68
3.	Nafion® SAC-13	250	0	19	8
			50	59	12
			70	67	13
			90	81	19

^a C_{XYL} = 0.1 M, T = 150 °C, for each experiment, equal acidity was aimed for, leading to different solid acid catalyst intakes (see experimental section)

However, differences in results may be due to differences in accessibility of the substrate to the active Brønsted acid site e.g. swellability of the catalysts and polarity of the catalyst pores⁵⁶.

The yield of FF and the conversion of xylose versus runtime for a representative run using the best catalyst (Dowex® 50WX8) in 90% ethanol, the best solvent composition according to the data in Table 5, are given in Figure 12. Quantitative xylose conversion was not observed with 150 min batchtime. In addition, the FF yield does not show a maximum yet, as with low sulphuric acid concentrations, meaning that the rates of the FF decomposition reactions are still slower than the formation reactions. The maximum experimentally observed FF yield is a function of the ethanol content in the reaction mixture, see Figure 12 right for details. It shows that performance of the catalyst is better in ethanol-water mixtures than in water alone. With the current dataset, however, it is not possible to determine the optimum solvent composition. This is due to the fact that the conversion at the end the reaction (150 min) was not quantitative and actually was different for each solvent composition (see also Table 5). Additional experiments at longer batch times will be required to draw conclusions regarding the optimum solvent composition for the Dowex® catalyst.

To make a proper comparison between performance of the best solid catalyst (Dowex®-50) and sulphuric acid, a plot with the FF yield versus the xylose conversion was prepared (Figure 13).

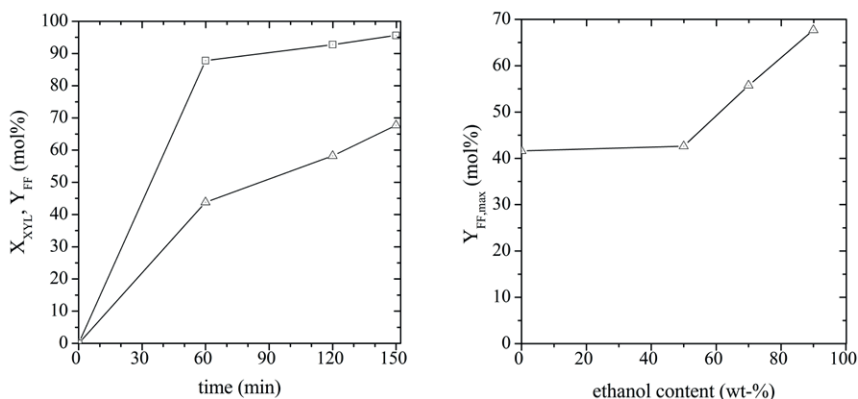


Figure 12. Conversion of xylose (X_{XYL} , □) and FF yields (Y_{FF} , Δ) versus time using Dowex[®] 50WX8 in 90 wt%-ethanol (left); Maximum FF yield ($Y_{FF,max}$, Δ) versus ethanol content (right). Conditions: 150 °C, microwave reactor, initial xylose concentration of 0.1 M.

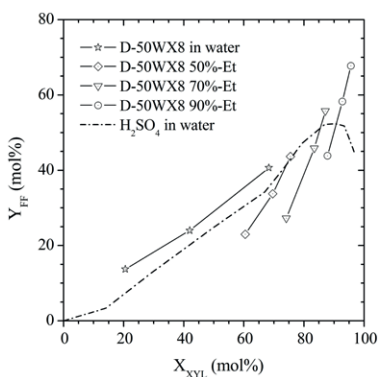


Figure 13. FF yield (Y_{FF} , mol%) versus xylose conversion (X_{XYL} , mol%) for Dowex[®] 50WX8 at different solvent composition and sulphuric acid (150 °C, $C_{XYL,0}$ = 0.1 M, $C_{H_2SO_4}$ = 0.1 M).

It shows that performance of the Dowex[®] catalyst in water is better than in for sulphuric acid when the conversion of xylose is below 70%. A comparison above 70% is not possible as experimental data at higher conversions are not (yet) available for the Dowex[®] catalyst. However, it does indicate that Dowex[®] is an attractive catalyst in water. The figure also clearly indicates that Dowex[®] performs well in ethanol-water mixtures and that such mixtures are preferred

above water. The most striking feature is that FF decomposition (as with sulphuric acid in water) does not occur to a significant extent with Dowex® in the experimental window of operation. Further experimental studies at high xylose conversion (> 96%) will be required to identify the full potential of the Dowex® catalyst.

4. CONCLUSIONS

An experimental study in a batch set-up on the conversion of xylose to FF in ethanol/water mixtures and water as the benchmark using homogeneous Brønsted acids (H_2SO_4 and HCl) is reported. The best results were obtained in ethanol-water mixtures with ethanol contents between 50–70 wt%, giving FF yields up to 73 mol%. This is a considerable improvement compared to experiments in water only at similar reaction conditions giving a maximum FF yield of about 60%. The results were rationalised by considering a reaction network involving ethylxylosides (from xylose) and furfuracetal (from FF) as intermediates. It is postulated that the rate of byproduct formation for ethylxylosides is lower than for xylose whereas the decomposition rate for FF acetal is higher than for FF. Ethylxyloside and acetal formation are both favoured in media with high ethanol contents due to equilibrium considerations. To maximise FF yields, it is thus best to operate the reaction using an intermediate ethanol to water ratio. Further kinetic studies will be required to quantify the rate of the individual reactions and to proof the reaction network. Humins, the oligomeric/polymeric byproducts formed during most of the reactions, were isolated and characterised using various techniques. It was found that the morphology of the soluble and insoluble humins is a function of reaction conditions and the acid catalyst used. One of the possible causes for these differences is the incorporation of S in the structure, likely in the form of sulphonate groups, when using sulphuric acid as the catalyst. The research was extended using heterogeneous catalysts in water-ethanol mixtures and Dowex® 50WX8 was found to be the best catalyst with FF yields up to 68% at 96% xylose conversion in a mixture with 90 wt% ethanol, demonstrating the potential of heterogeneous Brønsted acid catalysts for FF formation from xylose.

REFERENCES

1. Döbereiner, Ueber Die Medicinische und Chemische Anwendung und Die Vortheilhafte Darstellung der Ameisensäure. *Ann. Pharm.* **1832**, 3 (2), 141–146.
2. Corma, A.; Iborra, S.; Velty, A. Chemical Routes for the Transformation of Biomass into Chemicals. *Chem. Rev.* **2007**, 107 (6), 2411–2502.
3. Zeitsch, K. J. *The Chemistry And Technology Of Furfural And Its Many By-products*; Elsevier, 2000; Vol. 13.
4. Sain, B.; Chauduri, A.; Borgohain, J. N.; Baruah, B. P.; Ghose, J. L. Furfural and Furfural-based Industrial Chemicals. *J. Sci. Ind. Res.* **1982**, 41, 431–438.
5. Brownlee, H. J.; Miner, C. S. Industrial Development of Furfural. *Ind. Eng. Chem.* **1948**, 40 (2), 201–204.
6. Hoydonckx, H. E.; Rhijn, W. M. v.; Rhijn, W. v.; De Vos, D. E.; Jacobs, P. A. Furfural and Derivatives. In *Ullmann's Encyclopedia of Industrial Chemistry*; Wiley VCH Verlag GmbH & Co. KGaA: Weinheim Belgium, 2012; pp 285–313.
7. Xing, Q.; Subrahmanyam, V.; Olcay, ; Qi, W.; van Walsum, G. ; Pendse, H.; Huber, G. W. Production of jet and diesel fuel range alkanes from waste. *Green Chem.* **2010**, 12 (11), 1933–1946.
8. Bozell, J. J.; Petersen, G. R. Technology development for the production of biobased products from biorefinery carbohydrates — the US Department of Energy's "Top 10" revisited. *Green Chem.* **2010**, 12 (4), 539–554.
9. Ebert, J. Furfural: Future Feedstock for Fuels and Chemicals. *Biomass Magazine*, Sep, 2008, p 31–34.
10. Dunlop, A. P. Furfural Formation and Behavior. *Ind. Eng. Chem.* **1948**, 40 (2), 204–209.
11. Root, D. F.; Saeman, J. F.; Harris, J. F. Chemical Conversion of Wood Residues Part II: Kinetics of The Acid-Catalysed Conversion of Xylose to Furfural. *For. Prod. J.* **1959**, 9 (5), 158–165.
12. Feather, M. S.; Harris, J. F. Dehydration Reactions of Carbohydrates. *Adv. Carbohydr. Chem. Biochem.* **1973**, 28, 161–224.
13. Tanaka, Y.; Nakamura, T. Kinetic Study on The Thermal Decomposition of D-Xylose. *Thermochim. Acta* **1983**, 62 (2-3), 307–314.
14. Antal, M. J. J.; Leesomboon, T.; Mok, W. S. Mechanism of Formation of 2-Furfural From D-Xylose. *Carbohydr. Res.* **1991**, 217 (1), 71–85.
15. Ahmad, T.; Kenne, L.; Olsson, K.; Theander, O. The Formation of 2-Furaldehyde and Formic Acid From Pentoses In Slightly Acidic Deuterium Oxide Studied By ¹H NMR Spectroscopy. *Carbohydr. Res.* **1995**, 276 (2), 309–320.

16. Rose, I. C.; Epstein, N.; Watkinson, A. P. Acid-Catalyzed 2-Furaldehyde (Furfural) Decomposition Kinetics. *Ind. Eng. Chem. Res.* **2000**, 39 (3), 843–845.
17. Dias, A. S.; Pillinger, M.; Valente, A. A. Dehydration of Xylose Into Furfural over Micro-Mesoporous Sulfonic Acid Catalysts. *J. Catal.* **2005**, 229 (2), 414–423.
18. Liu, C.; Wyman, C. E. The Enhancement of Xylose Monomer and Xylotriose Degradation by Inorganic Salts in Aqueous Solution at 180 °C. *Carbohydr. Res.* **2006**, 341 (15), 2550–2556.
19. Chheda, J. N.; Roman-Leshkov, Y.; Dumesic, J. A. Production of 5-Hydroxymethylfurfural and Furfural by Dehydration of Biomass-derived Mono- and Poly-Saccharides. *Green Chem.* **2007**, 9, 342–350.
20. Marcotullio, G.; Cardoso, M. A. T.; Jong, W. D.; Verkooyen, H. M. Bioenergy II: Furfural Destruction Kinetics During Sulphuric Acid-Catalyzed Production From Biomass. *Int. J. Chem. React. Eng.* **2009**, 7 (A67).
21. Marcotullio, G.; de Jong, W. Chloride ions enhance furfural formation from D-xylose in dilute aqueous acidic solution. *Green Chem.* **2010**, 12, 1739–1746.
22. Weingarten, R.; Cho, J.; Conner, W. C. J.; Huber, G. W. Kinetics of Furfural Production By Dehydration of Xylose in A Biphasic Reactor With Microwave Heating. *Green Chem.* **2010**, 12, 1423–1429.
23. Marcotullio, G.; de Jong, W. Furfural formation from D-xylose: the use of different halides in dilute aqueous acidic solutions allows for exceptionally high yields. *Carbohydr. Res.* **2011**, 346, 1291–1293.
24. Zhang, J.; Zhuang, J.; Lin, L.; Liu, S.; Zhang, Z. Conversion of D-xylose into furfural with mesoporous molecular sieve MCM-41 as catalyst and butanol as the extraction phase. *Biomass Bioenergy* **2012**, 39, 73–77.
25. Ordonsky, V. V.; Schouten, J. C.; Schaaf, J. v. d.; Nijhuis, T. A. Biphasic single-reactor process for dehydration of xylose and hydrogenation of produced furfural. *Appl. Catal., A* **2013**, 451, 6–13.
26. Lima, S.; Neves, P.; Antunes, M. M. Conversion of mono/di/polysaccharides into furan compounds using 1-alkyl-3-methylimidazolium ionic liquids. *Appl. Catal., A* **2009**, 363 (1–2), 93–99.
27. Binder, J. B.; Blank, J. J.; Cefali, A. V.; Raines, R. T. Synthesis of Furfural from Xylose and Xylan. *ChemSusChem* **2010**, 3 (11), 1268–1272.
28. Sievers, C.; Musin, I.; Marzietti, T.; Olarte, M. V.; Agrawal, P.; Jones, C. Acid-Catalyzed Conversion of Sugars and Furfurals in an Ionic-Liquid Phase. *ChemSusChem* **2009**, 2 (7), 665–671.
29. Carlos Serrano-Ruiz, J.; Campelo, J. M.; Romero, A. A.; Luque, R.; Menéndez-Vázquez, C.; García, A. B.; García-Suárez, E. J. Efficient microwave-assisted

- production of furfural from C5 sugars in aqueous media catalysed by Brønsted acidic ionic liquids. *Catal. Sci. Technol.* **2012**, 2 (9), 1828–1832.
30. Zhang, L.; Yua, H.; Wang, P.; Do, H.; Peng, X. Conversion of xylan, d-xylose and lignocellulosic biomass into furfural using $AlCl_3$ as catalyst in ionic liquid. *Bioresour. Technol.* **2013**, 130, 110–116.
 31. Moreau, C.; Durand, R.; Peyron, D.; Duhamet, J.; Rivalier, P. Selective Preparation of Furfural from Xylose over Microporous Solid Acid Catalysts. *Ind. Crops and Prod.* **1998**, 7, 95–99.
 32. Hu, X.; Lievens, ; Larcher, A.; Li, C.-Z. Reaction pathways of glucose during esterification: Effects of reaction parameters on the formation of humins type polymers. *Bioresour. Technol.* **2011**, 102 (21), 10104–10113.
 33. Jia, X.; Ma, J.; Che, P.; Lu, F.; Miao, ; Gao, J.; Xu, J. Direct conversion of fructose-based carbohydrates to 5-ethoxymethylfurfural catalyzed by $AlCl_3 \cdot 6H_2O/BF_3 \cdot (Et)_2O$ in ethanol. *J. Energy Chem.* **2013**, 22 (1), 93–97.
 34. Mellmer, M. A.; Sener, D. C.; Gallo, D. J. M. R.; Luterbacher, D. J. S.; Alonso, D. D. M.; Dumesic, P. J. A. Solvent Effects in Acid-Catalyzed Biomass Conversion Reactions. *Angew. Chem.* **2014**, 126 (44), 12066–12069.
 35. Iglesias, J.; Melero, J. A.; Morales, G.; Paniagua, M.; Hernandez, B. Dehydration of Xylose to Furfural in Alcohol Media in the Presence of Solid Acid Catalysts. *ChemCatChem* **2016**, 8 (12), 2089–2099.
 36. Lamminpää, K.; Ahola, J.; Tanskanen, J. Kinetics of Xylose Dehydration into Furfural in Formic Acid. *Ind. Eng. Chem. Res.* **2012**, 51(18), 6297–6303.
 37. Ershova, O.; Kanervo, J.; Hellsten, S.; Sixta, H. The role of xylulose as an intermediate in xylose conversion to furfural: insights via experiments and kinetic modelling. *RSC Adv.* **2015**, 2, 66727–66737.
 38. Jing, Q.; Lu, X. Y. Kinetics of non-catalyzed decomposition of D-xylose in high temperature liquid water. *Chin. J. Chem. Eng.* **2007**, 15 (5), 666–669.
 39. Yemiş, O.; Mazza, G. Acid-catalyzed Conversion of Xylose, Xylan and Straw into Furfural by Microwave-assisted Reaction. *Bioresour. Technol.* **2011**, 102 (15), 7371–7378.
 40. Choudhary, V.; Sandler, S. I.; Vlachos, D. G. Conversion of Xylose to Furfural Using Lewis and Brønsted Acid Catalysts in Aqueous Media. *ACS Catal.* **2012**, 2 (9), 2022–2028.
 41. Hu, X.; Westerhof, R. J. M.; Dong, D.; Wu, L.; Li, C.-Z. Acid-Catalyzed Conversion of Xylose in 20 Solvents: Insight into Interactions of the Solvents with Xylose, Furfural, and the Acid Catalyst. *ACS Sustainable Chem. Eng.* **2014**, 2 (11), 2562–2575.

42. Hu, X.; Lievens, C.; Li, C.-Z. Acid-Catalyzed Conversion of Xylose in Methanol-Rich Medium as Part of Biorefinery. *ChemSusChem* **2012**, 5 (8), 1427–1434.
43. Kim, S. B.; You, S. J.; Kim, Y. T.; Lee, S.; Lee, H.; Park, K.; Park, E. D. Dehydration of D-xylose into furfural over H-zeolites. *Korean J. Chem. Eng.* **2011**, 28 (3), 710–716.
44. Rong, C.; Ding, X.; Zhu, Y.; Li, Y.; Wang, L.; Qu, Y.; Ma, X.; Wang, Z. Production of furfural from xylose at atmospheric pressure by dilute sulfuric acid and inorganic salts. *Carbohydr. Res.* **2012**, 350, 77–80.
45. Yang, Y.; Hu, C.-W.; Abu-Omar, M. M. Synthesis of Furfural from Xylose, Xylan, and Biomass Using $\text{AlCl}_3 \cdot 6\text{H}_2\text{O}$ in Biphasic Media via Xylose Isomerization to Xylulose. *ChemSusChem* **2012**, 5, 405–410.
46. Bishop, C. T.; Cooper, F. T. Glycosidation of Sugars. *Can. J. Chem.* **1963**, 41 (11), 2743–2758.
47. Vollhardt, P.; Schore, N. Acetals as Protecting Groups. In *Organic Chemistry: Structure and Function*, 6th ed.; W.H. Freeman and Company: New York, 2007; Chapter 17–8, pp 793–795.
48. Fusaro, M. B.; Chagnault, V.; Postel, D. Reactivity of D-Fructose and D-Xylose in Acidic Media in Homogeneous Phase. *Carbohydr. Res.* **2015**, 409, 9–19.
49. Carey, F. *On-Line Learning Center for "Organic Chemistry": Chapter 15. Alcohols, Diols, Thiols*, 5th ed.; McGraw-Hill Higher Education, 2000.
50. Carey, F. *On-Line Learning Center for "Organic Chemistry": Chapter 4. Alcohols and Alkyl Halides*, 5th ed.; McGraw-Hill Higher Education, 2000.
51. Foo, G. S.; Van Pelt, A. H. M.; Krötschel, D.; Sauk, B. F.; Rogers, A. K.; Jolly, C. R.; Yung, M. M.; Sievers, C.. Hydrolysis of Cellobiose over Selective and Stable Sulfonated Activated Carbon Catalysts. *ACS Sustainable Chem. Eng.* **2015**, 3 (9th), 1934–1942.
52. Girisuta, B.; Janssen, L. P. B. M.; Heeres, H. J. A kinetic study on the decomposition of 5-hydroxymethylfurfural into levulinic acid. *Green Chem.* **2006**, 8, 701–709.
53. Girisuta, B.; Janssen, L. P. B. M.; Heeres, H. J. Kinetic study on the acid-catalyzed hydrolysis of cellulose to levulinic acid. *Ind. Eng. Chem. Res.* **2007**, 46, 1969–1708.
54. Blaser, H.-U.; Müller, M. Heterogeneous Catalysis and Fine Chemicals II. *Studies in Surface Science and Catalysis*, Poitiers, France, 1991; pp 90–91.
55. Copéret, ; Chabanas, ; Saint-Arroman, R. P.; Basset, J.-M. A Review: Homogeneous and Heterogeneous Catalysis: Bridging the Gap through Surface Organometallic Chemistry. *Angew. Chem.* **2003**, 42 (2), 156–181.
56. Toteja, R. S. D.; Jangida, B. L.; Sundaresan, M.; Venkataramani, B. Water Sorption Isotherms and Cation Hydration in Dowex® 50W and Amberlyst®-15 Ion Exchange Resins. *Langmuir* **1997**, 13, 2980–2982.

APPENDIX FOR CHAPTER 5:

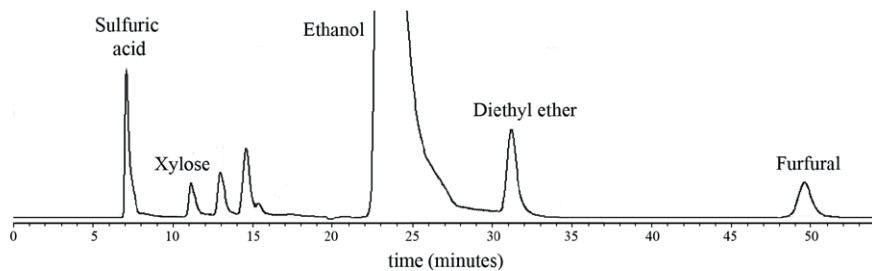


Figure S1. Typical HPLC chromatogram (RID detector) for a reaction product of xylose dehydration in ethanol-water mixtures using H_2SO_4 as the catalyst

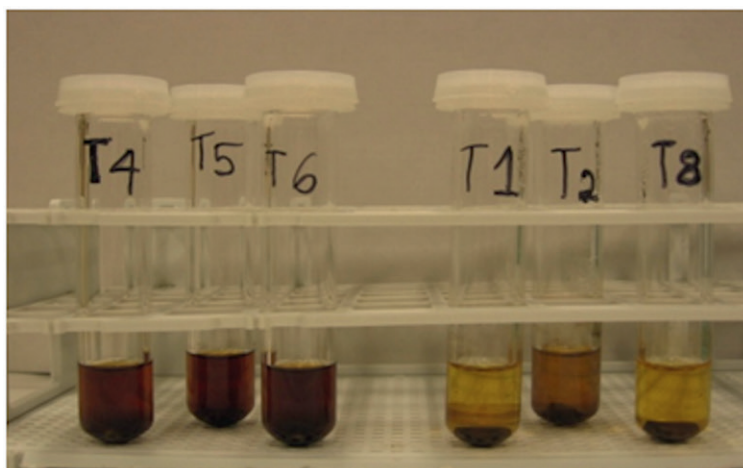


Figure S2. Visual observation of the reaction mixtures for 0.1 M xylose performed in ethanol-water (50 wt% ethanol, T_4 – T_6) and in water (T_1 , T_2 , T_8)

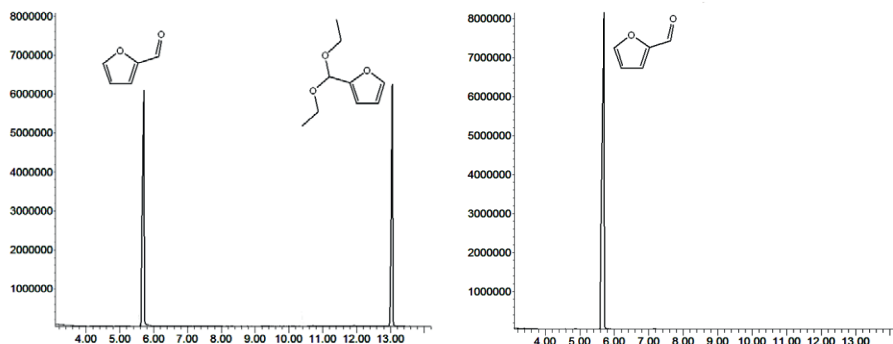


Figure S3. Comparison of the GC-MS analysis between (left) 0.06 M FF in 100% ethanol using 0.05 M H_2SO_4 and (right) 0.06 M FF in 100% ethanol without sulfuric acid

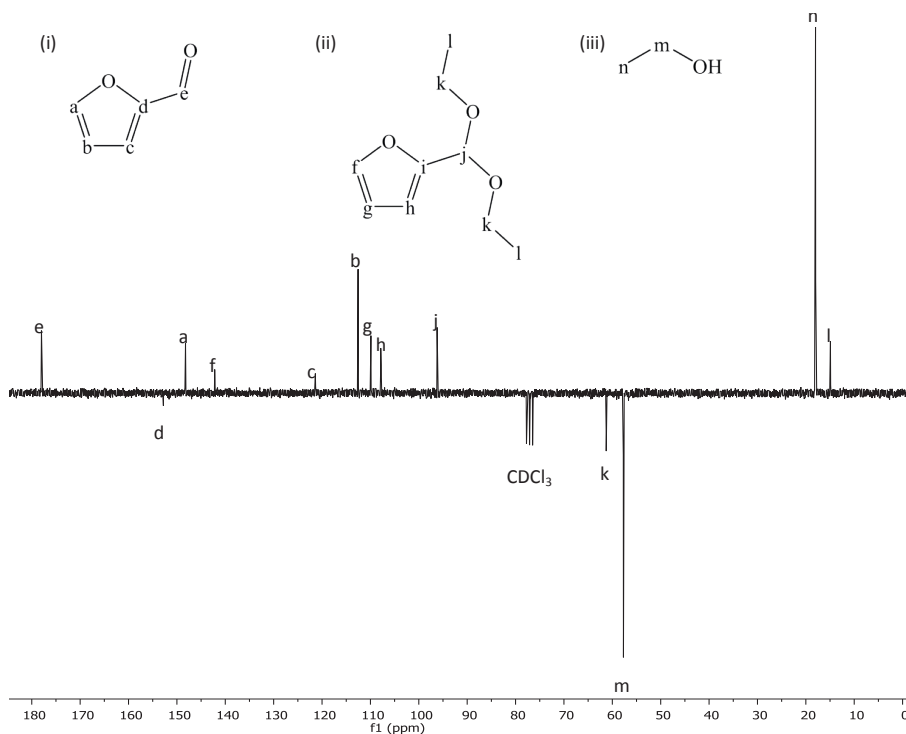


Figure S4. APT ^{13}C -NMR spectra of FF in 100% ethanol and H_2SO_4 catalyst with peak identification for (i) FF, (ii) 2-furaldehyde-diethyl-acetal and (iii) ethanol

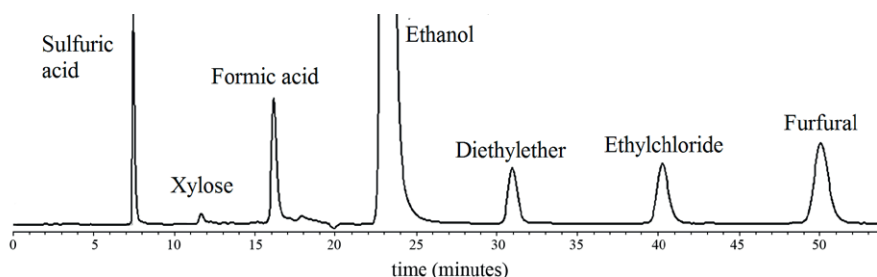


Figure S5. Typical chromatogram (RID detector) using an Aminex HPX-87H column for the reaction of xylose using HCl as the catalyst

Table S1. Acid capacity (meq H⁺/g cat) of the solid catalysts

No	Name	meq H ⁺ per g catalyst	catalyst intake (mg)	Water content (%)	Ref.
1.	Amberlyst® 15	4.7	42.6	< 0.1	1
2.	Nafion® SAC-13	0.8	250	< 0.1	2
3.	Dowex® 50WX8	1.7 ^a	94.2	50–58	3

^a The acid capacity of Dowex® 50WX8 is 1.7 meq/mL (wetted bed volume) with water content of 50–58% and density of 50 lbs/ft³ or 0.8 g/mL

REFERENCES FOR APPENDIX

1. Company, T. D. C. *AMBERLYST™ 15 Dry Industrial Grade Strongly Acidic Catalyst*; Product Data Sheet; Rohm and Haas: Philadelphia, August 2006.
2. Inc., S. A. *Nafion® SAC-13*; Product Data Sheet; Dupont Chemicals, 1972.
3. Company, T. D. C. *DOWEX™ Fine Mesh Spherical Ion Exchange Resin*; Form; Dow Water Solution.

The background of the page is a complex collage. The upper portion features a dense, textured pattern of crumpled, translucent paper in various shades of grey and white. Overlaid on this are several thin, white, curved lines that sweep across the frame. The lower portion of the page is filled with a repeating pattern of small, faint chemical structures. These structures appear to be a combination of furan rings and carboxylic acid derivatives, rendered in a light grey color that blends into the overall design.

SUMMARY

SAMENVATTING

ACKNOWLEDGEMENTS

LIST OF PUBLICATIONS

SUMMARY

The conversion of biomass to biobased chemicals has received major interest in the last decades. Particularly the use of lignocellulosic biomass is of high interest due to its high abundance and sustainable availability, for instance lignocellulosic biomass with a low economic value. To valorise biomass effectively, the biorefinery concept has been introduced and is advocated widely. It involves sustainable and integrated processes to convert low-value biomass into industrial intermediates or final products (energy, fuels, chemicals, materials) using optimum resources with minimum use of energy and low amounts of waste. An important product class of biorefineries is the platform chemicals, which are defined as green building blocks that can be converted to a wide range of chemicals or materials. An important class of platform chemicals from the carbohydrate fraction of biomass are furanics. In fact, two important biobased furanics that can be obtained using chemo-catalytic methodologies have been identified, *viz.* furfural (FF) and 5-hydroxymethylfurfural (5-HMF).

The major issue when converting biomass to biobased furanics is the low product yield, amongst others, due to the relatively low thermal stability of the furanics at reaction conditions. The aim of the research described in this thesis is to develop efficient synthetic methodology for the conversion of sugars to HMF and FF by exploring the effects of i) process conditions (temperature, concentrations, type of solvent), ii) type of sugar feedstocks and iii) the use of catalysts.

In **Chapter 2**, experimental and kinetic modeling studies on the conversion of sucrose to HMF and levulinic acid (LA) in water using sulphuric acid as the catalyst are reported. Several reaction networks are proposed based on earlier studies for the individual sugars (glucose and fructose). A total of 24 experiments were performed in a temperature window of 80–180 °C, a sulphuric acid concentration between 0.005 and 0.5 M, and an initial sucrose concentration between 0.05 and 0.5 M. Glucose, fructose and HMF were detected as the intermediate products. The experimental data were modeled using a number of possible reaction networks. The kinetic parameters and their standard deviations were determined using a MATLAB optimization routine. The best model was obtained when using a first order approach in substrates (except for the reversion of glucose) and agreement between experiment and model was satisfactorily. The best fit kinetic model was then used to determine the optimum reaction conditions for HMF and LA production from sucrose in a batch reactor set-up. The model predicts that the LA yield is highest

at the lowest temperature in the range, viz. 70 mol% at 100 °C due to less humins formation. However, the batch times at lower temperatures are excessively longer than at the highest temperature (up to 70,000 min for maximum LA yield at 100 °C), leading to very unrealistically low reactor productivities ($\text{mol LA} \cdot \text{m}^{-3} \cdot \text{reactor} \cdot \text{h}^{-1}$). As such, the optimum temperature for LA synthesis will be a compromise between LA yield and batch time. The highest experimental value for the yield of LA was 61 mol%, obtained at a relatively high temperature (160 °C) low initial sucrose concentration (0.05 M) using a moderate acid concentration (0.2 M). The highest modeled HMF yield is 21 mol%, obtained at the highest temperature in the range. The maximum experimental yield for HMF was 22 mol%, obtained at a temperature of 140 °C, an initial sucrose concentration of 0.05 M and an acid concentration of 0.05 M.

In **Chapter 3**, the use of four ketohexoses i.e. fructose, tagatose, sorbose and psicose for HMF synthesis in water using sulphuric acid as the catalyst is reported (sugar concentration of 65 g/L or 0.36 M, 137 °C, acid concentration between 33 and 300 mM). Significant differences in reactivity were observed and tagatose and psicose were by far more reactive and were converted at a higher rate than fructose and sorbose. Furthermore, the selectivity for HMF formation was higher for psicose and fructose than for sorbose and tagatose. For psicose, the highest HMF yield at 137 °C was about 50% at a sugar conversion of 80-90%. Further kinetic studies for psicose (9 experiments, using an initial psicose concentration of 65 g/L or 0.36 M, temperatures of 100, 120 and 137 °C with acid concentrations between 33 and 300 mM) reveal that the conversion versus time curves for the batch experiments are well described with a first order dependency in both psicose and acid with an activation energy of $158 \pm 9 \text{ kJ/mol}$ which is much higher than for fructose ($117 \pm 3 \text{ kJ/mol}$). Thus, psicose appears to be the best substrate for HMF production in water, as it has a higher selectivity for HMF formation than sorbose and tagatose, and a higher reactivity than fructose. However, psicose is a rare sugar, present in only small amounts in some biomass sources like wheat, Itca plants, processed sugar cane and beet molasses. As such either a psicose producing organism or an isomerisation process to obtain psicose from readily accessible sugars would be required to develop a techno-economically viable process for HMF production from psicose. Together with HMF, significant amounts of 2-hydroxyacetylfruran (2-HAF) were formed, particularly when using sorbose and psicose as the reactants.

For optimization of the HAF yields from C6-sugars, information about the stability of HAF in the reaction medium at relevant conditions is required. In

Chapter 4, studies on the stability of 2-HAF in the presence of Brønsted acid catalysts are reported. The main goals of this study were i) to determine the rate of decomposition of 2-HAF and ii) its possible involvement in LA formation. A total of 12 experiments were performed (batch set-up) in water with sulphuric acid as the catalyst (100–170 °C, $C_{\text{H}_2\text{SO}_4}$ ranging between 0.033 and 1.37 M and an initial HAF concentration between 0.04 and 0.26 M). Good agreement between model and experimental data ($R^2 = 99.57\%$) was obtained when using a first order approach in both HAF and H^+ . The activation energy was found to be $98.7 (+ 2.2) \text{ kJ}\cdot\text{mol}^{-1}$, which is far less than for the decomposition reaction of HMF to humins ($138 \text{ kJ}\cdot\text{mol}^{-1}$). At 170 °C, the kinetic constant for HCl was found to be 0.32 min^{-1} which is 1.5 higher than H_2SO_4 (0.21 min^{-1}), implying an anion effect on the rate of decomposition. The reaction does not lead to the formation of a single reaction product; instead a large number of soluble, non-identified products was observed (HPLC) and solids formation was also inevitable. The only exceptions are LA and FA, which were present in significant amounts when using HCl as the catalyst ($Y_{\text{LA}} = 10 \text{ mol}\%$ and $Y_{\text{FA}} = 24 \text{ mol}\%$). In contrast, both LA and FA were formed in minor amounts when using H_2SO_4 as the catalyst, again indicating a significant anion effect. The findings described in this chapter will be of relevance for the development of an efficient route for HAF from C6 sugars and allow selection of optimum reaction conditions to reduce the rate of HAF decomposition.

In the last chapter, **Chapter 5**, experimental studies in a batch set-up on solvent effects for the conversion of xylose to furfural in ethanol/water mixtures both using homogeneous and heterogeneous Brønsted acid catalysts are provided. The best results when using sulphuric acid as the catalyst were obtained in solvent mixtures with 70–90% ethanol, giving furfural yields up to 73 mol%. This is a considerable improvement compared to experiments in water only at similar reaction conditions, giving a maximum furfural yield of 59 mol%. Individual reactions with furfural showed that the rate of furfural decomposition is a function of the ethanol content and shows the lowest degradation rate at ethanol concentrations between 40 and 60%. Comparable maximum FF yields (71 mol%) were obtained using HCl. The results were rationalised by considering a reaction network involving ethylxylosides (from xylose) and furfuralacetal (from FF) as intermediates. It is postulated that the rate of byproduct formation from ethylxylosides is lower than for xylose whereas the decomposition rate for furfuralacetal is higher than for FF. Ethylxyloside and acetal formation are both favoured in media with high ethanol contents due to equilibrium considerations. To maximise FF yields, it

is thus best to operate the reaction using an intermediate ethanol to water ratio. Further kinetic studies will be required to quantify the rate of the individual reactions and to proof the proposed reaction network. Humins, the oligomeric/polymeric byproducts formed during most of the reactions, were isolated from reactions involving furfural and characterised using elemental analysis and TEM. It was found that the morphology of the soluble and insoluble humins is a function of reaction conditions and the acid catalyst used. One of the possible causes for these differences is the incorporation of S in the structure, likely in the form of sulphonate groups, when using sulphuric acid as the catalyst. The research was extended using heterogeneous catalysts in water-ethanol mixtures and Dowex® 50WX8 showed comparable performance as found for the homogeneous Brønsted acids with FF yields up to 68% at 96% xylose conversion in a mixture with 90 wt% ethanol, demonstrating the potential of heterogeneous Brønsted acid catalysts for FF formation from xylose.

SAMENVATTING

De omzetting van biomassa naar chemicaliën heeft de afgelopen decennia veel aandacht gekregen. Vooral het gebruik van lignocellulose rijke biomassa is erg interessant omdat het in grote hoeveelheden en duurzaam beschikbaar is op aarde. Voor de efficiënte valorisatie van biomassa wordt het bio-raffinage concept veelvuldig toegepast. In een bioraffinaderij wordt laagwaardige biomassa omgezet naar tussen- of eindproducten (zoals energie, brandstoffen, chemicaliën en materialen) met een minimale hoeveelheid aan energie en met zo weinig mogelijk afval. Belangrijke producten van een bioraffinaderij zijn zogenaamde platform chemicaliën, dit zijn groene bouwstenen die kunnen worden omgezet in een breed scala aan chemicaliën en materialen. Furanen uit biomassa zijn belangrijke platform chemicaliën, voorbeelden zijn furfural (FF) en 5-hydroxymethylfurfural (5-HMF).

Het grootste probleem bij het omzetten van lignocellulosische biomassa naar furanen is de lage product opbrengst. Dit komt door de relatief lage thermische stabiliteit van de furanen bij de reactie condities. Het doel van het onderzoek beschreven in dit proefschrift is de ontwikkeling van efficiënte routes voor de omzetting van de suikers in lignocellulosische biomassa naar HMF en FF door optimalisatie van i) de proces condities (temperatuur, concentratie, type oplosmiddel), ii) de gebruikte biomassa en iii) de toepassing van katalysatoren.

In **Hoofdstuk 2** wordt kinetisch onderzoek beschreven naar de omzetting van sucrose naar HMF en levulinic acid (LA) in water met zwavelzuur als katalysator. Er zijn in totaal 24 experimenten uitgevoerd bij verschillende temperaturen (80–180 °C), zwavelzuur concentraties (0.05–0.5 M) en initiële sucrose concentraties (0.05–0.5 M). In alle reactie mengsels werden glucose, fructose en HMF aangetoond. De concentraties van deze producten gaven een optimum te zien, een indicatie dat het intermediaire producten zijn. De experimentele data zijn gebruikt voor de ontwikkeling van een reactie netwerk. Kinetiek parameters en de bijbehorende standaard deviaties zijn bepaald door gebruik te maken van een MATLAB optimalisatie methode. Een model met de aanname van een eerste orde reactie in uitgangsstoffen (behalve voor de reactie van glucose naar glucose oligomeren) gaf de beste resultaten. Met dit kinetiek model zijn de optimale reactie condities voor HMF en LA productie uit sucrose in een batch reactor bepaald. Het model voorspelt de hoogste LA opbrengst (70 mol%) bij de laagste temperatuur (100 °C) omdat bij deze condities de vorming van vaste stoffen (humines) onderdrukt

wordt. Een nadeel van het uitvoeren van de reactie bij lage temperatuur is dat dit leidt tot veel langere reactietijden voor maximale LA opbrengst (tot wel 70,000 min bij 100 °C) wat resulteert in een onrealistisch lage reactor productiviteit. De optimale temperatuur voor LA synthese is daarom een compromis tussen LA opbrengst en batch tijd. De hoogste experimentele opbrengst van LA was 61 mol%, verkregen bij een relatief hoge temperatuur (160 °C), een lage initiële sucrose concentratie (0.05 M) en een intermediaire zuur concentratie (0.2 M). De hoogste gemodelleerde HMF opbrengst was 21 mol%, de maximale experimentele opbrengst voor HMF was 22 mol%, verkregen bij een temperatuur van 140 °C, een initiële sucrose concentratie van 0.05 M en een zuur concentratie van 0.05 M.

In **Hoofdstuk 3** wordt het gebruik van vier ketohexoses (fructose, tagatose, sorbose en psicose) voor HMF synthese in water met zwavelzuur als katalysator beschreven (initiële suiker concentratie van 65 g/L (0.36 M), 137 °C, zuurconcentratie tussen de 33 en 300 mM). De 4 suikers laten grote verschillen zien in reactiviteit. Tagatose en psicose zijn verreweg het meest reactief. De selectiviteit voor HMF vorming is beter voor psicose en fructose. Naast HMF wordt een significante hoeveelheid aan 2-hydroxyacetylfuraan (2-HAF) gevormd, vooral voor sorbose en psicose. Voor psicose is de hoogste HMF opbrengst ongeveer 50% bij een suiker conversie van 80–90%. Kinetiek studies voor psicose (9 experimenten; initiële psicose concentratie van 65 g/L (0.36 M), 100, 120 en 137 °C en zuurconcentraties tussen de 33 en 300 mM) laten zien dat de conversie-tijd grafieken voor de batch experimenten goed te beschrijven zijn met een eerste orde afhankelijkheid in zowel psicose als zuur. De activeringsenergie (158 ± 9 kJ/mol) is hoger dan voor fructose (117 ± 3 kJ/mol). Concluderend lijkt psicose het beste substraat voor HMF productie in water omdat het een hogere selectiviteit geeft voor HMF vormig dan sorbose en tagatose. Tevens heeft psicose een hogere reactiviteit dan fructose. Echter psicose is een suiker die niet veel voorkomt in de natuur en alleen in kleine hoeveelheden aanwezig is graan, Itrea planten, geraffineerde suikerriet en suikerbiet molasse. Mogelijke opties om de psicose op grotere schaal en goedkoper te produceren zijn biotechnologische processen of de isomerisatie van goedkopere suikers naar psicose.

Voor de optimalisatie van de HAF opbrengst uit C6-suikers is informatie over de stabiliteit van HAF in het reactie medium bij relevante condities nodig. In **hoofdstuk 4** worden studies beschreven om de stabiliteit van 2-HAF in water te bepalen in de aanwezigheid van Brønsted zure katalysatoren (HCl en H₂SO₄). De belangrijkste doelen van deze studie waren i) het bepalen van

de reactiesnelheid van de ontleding van 2-HAF en ii) inzicht te krijgen in producten en vooral de vorming van LA. Er zijn 12 experimenten uitgevoerd in een batch reactor in water met zwavelzuur als katalysator (100–170 °C, H₂SO₄ concentraties tussen 0.033 en 1.37 M en een initiële HAF concentratie tussen 0.04 en 0.26 M). De experimenten zijn het beste te beschrijven met een model waarbij eerste orde reacties aangenomen worden in HAF en H⁺ (R² = 99.57%). De activeringsenergie voor de hoofdreactie was 98.7 (± 2.2) kJ.mol⁻¹; wat veel lager is dan voor de ontledingsreactie van HMF naar humines (138 kJ.mol⁻¹). Experimenten met HCl geven aan dat de reactiesnelheden voor dit zuur een factor 1.5 hoger liggen dan voor H₂SO₄. Dit suggereert een anion effect op de ontledingssnelheid. De ontleding van HAF resulteert niet in de selectieve vorming van één product, maar een groot aantal oplosbare, niet geïdentificeerde producten (HPLC) naast de vorming van vaste stoffen (humines). LA en FA waren aanwezig in significante hoeveelheden bij het gebruik van HCl als katalysator (Y_{LA} = 10 mol% en Y_{FA} = 24 mol%). De resultaten behaalt in deze studie kunnen gebruikt worden voor de ontwikkeling van een efficiënte route voor HAF uit C6 suikers en vooral tot de selectie van de optimale reactie condities om de HAF ontledingssnelheid te minimaliseren.

In het laatste hoofdstuk, **hoofdstuk 5**, worden experimentele studies beschreven naar oplosmiddel effecten (ethanol-water combinaties) op de omzetting van xylose naar FF met homogene- en heterogene Brønsted zure katalysatoren. De beste resultaten met zwavelzuur als katalysator zijn behaald in oplosmiddel mengsels met 70–90% ethanol, resulterend in FF opbrengsten tot wel 73 mol%. Dit is een grote verbetering ten opzichte van experimenten in water waarbij onder vergelijkbare reactie condities een maximale furfural opbrengst van 59 mol% behaald werd. Individuele reacties met furfural laten zien dat de reactiesnelheid van de ontleding van furfural een functie is van het ethanol gehalte, waarbij de minimale ontledingssnelheid bij ethanol concentraties tussen 40 en 60% werden waargenomen. Op basis van de resultaten is een reactie netwerk opgesteld met ethylxylosides (van xylose) en furfural-acetal (van FF) als tussenproducten. Om de product samenstelling als functie van de oplosmiddel samenstelling te verklaren is aangenomen dat de reactiesnelheid voor bijproduct vorming vanuit ethylxylosides lager is dan vanuit xylose en de ontledingssnelheid van furfuralacetalen hoger is dan voor FF. Voor het verkrijgen van een zo hoog mogelijke FF opbrengst, is het daarom het beste om de reactie uit te voeren bij een intermediaire ethanol-water verhoudingen. Aanvullende kinetiek studies zijn nodig om de reactiesnelheid van de individuele reacties te kwantificeren en de voorgestelde reactie schema's te

verifiëren. Humines, de oligomere/polymere bijproducten die gevormd worden gedurende de meeste reacties, zijn geïsoleerd voor reacties met furfural en gekarakteriseerd met element analyse en TEM. Hieruit bleek dat de morfologie van de oplosbare en niet oplosbare humines een functie is van de reactie condities en de gebruikte zure katalysator. Eén van de mogelijke oorzaken voor deze verschillen is de aanwezigheid van S in de humine structuur (waarschijnlijk in de vorm van sulfonaat groepen) wanneer zwavelzuur als zure katalysator wordt gebruikt. Het onderzoek is uitgebreid met het gebruik van heterogene katalysatoren in water-ethanol mengsels in plaats van homogene zuren. Dowex® 50WX8 gaf vergelijkbare resultaten met FF opbrengsten tot 68% bij een xylose conversie van 96% in een mengsel met 90% ethanol. Dit laat zien dat heterogene Brønsted zure katalysatoren potentie hebben om gebruikt te worden voor FF vorming uit xylose.

ACKNOWLEDGEMENTS

Finally the long journey has come to the end. The long quest has been completed, opening the gate to another quest, awaiting in front of me to be explored. Honestly being able to accomplish this book is a miracle for me and I know exactly that none of this would have been possible without the countless precious supports and contributions from many people that I have received during my doctoral study, both in the Netherlands and in Indonesia. Therefore I would like to express my sincere gratitude to those who have supported me along the way to completion of this thesis.

Firstly, I would like to express my deep gratitude to my promotor, Prof. dr. ir. H. J. Heeres. Erik, your support and guidance was precious for me. Thank you for the opportunity, efforts and time you have given me during my PhD time. Thank you for your kind support, encouragement and patience which enabled me to finalize the thesis. I really enjoyed our discussions and I learned so much from you in terms of experimental methods and critical insights in writing as well as in life philosophy. Your perseverance has impressed me so much and I feel very lucky and honored to have you as my supervisor, tutor and friend. I deeply appreciate your expertise and I believe this is not the end but the beginning for another scientific journey with you. In fact, I am looking forward for it in the near future.

I would like to thank the members of the reading committee: Prof. dr. F. Picchioni, Prof. dr. A.A. Broekhuis and Prof. dr. A.M. Raspolli Galletti for their valuable comments and suggestions to improve this dissertation.

I would like to express my deep gratitude to DIKTI (Directorate General for Higher Education Indonesia) and UNPAR (Parahyangan Catholic University) for the financial support during my doctoral study. My sincere gratitude to Dr. Cecilia Lauw Giok Swan, Ir., M.Sc., the ex-rector of UNPAR who granted me permission to continue my study in the Netherlands; *Prof. Ir. Robertus Wahyudi Triweko*, M.Eng., *Ph.D*, the ex-rector of UNPAR who has approved the financial support for my last year doctoral study in the Netherlands; Dr. Paulus Sukapto, Ir., M. B. A., the ex-dean of Faculty of Industrial Technology and the vice rector for Human Capital and Student Affairs of UNPAR; Dr. *Thedy Yogasara*, S.T., M.Eng.Sc., the dean of Faculty of Industrial Technology, UNPAR; Dr. Henky Muljana, S.T., M.T. and Dr. Buana Girisuta, S.T., M.T., the ex-head of the Chemical Engineering Department of UNPAR as well as Dr. Ratna Frida Susanti, S.T., Ph.D, the head of the Chemical Engineering Department and Anastasia Prima Kristijati, S.Si, M.T., the ex-secretary of the

Chemical Engineering Department of UNPAR for the enormous support, encouragement and recommendation that enabled me to complete my doctoral study.

I would like to acknowledge the academic, technical and administrative support I have received during my study in the University of Groningen, the Netherlands: Marya van der Duin-de Jonge and Annette Korringa-de Wit for the administrative support, Jan Henk Marsman and Leon Rohrbach for the valuable discussions regarding analytical techniques and instruments; Anne Appeldoorn, Marcel de Vries and Erwin Wilbers for the technical and non-technical support (eq. Labuitjes); Maarten Vervoort for the ampoules and any glass modification support; Vaclav Ocelik for the valuable discussions about SEM and HRTEM including EDAX analysis and interpretation; Gert Alberda van Ekenstein, Hans van der Velde and Theodora Tiemersma-Wegman for supportive analysis during my doctoral study in Groningen. Thanks also to Alphons A. A. Navest for helping me with financial administrative issues and the last but not least, my gratitude for Tim Zwaagstra for the encouragement and cheerfulness he brought me while struggling with the finalization of writing of this thesis.

I am deeply thankful to my paranympths: Henk van de Bovenkamp and Ria Abdilla. You guys have been involved in this research from the beginning and it is an honour for me to have you both as my paranympth. Henk, you are involved in almost in all chapters of this book, either in the analysis or in the writing and I appreciate your contribution so much. You have given me so many valuable inputs and helped me a lot in improving the papers published from this dissertation. Ria, you have been my friend since the beginning of my PhD time. I know you as a master student and now you are already a PhD student. We worked on closely related research topics and I hope that you will get all the fun and will successfully finalize your PhD thesis.

I want to give my special thanks to Dr. Louis Daniel, my friend and my brother. You have given me countless support while finalizing this book. Your insights, support and encouragement is enormous and I value it so much. My deep gratitude for all the time you have spent to make it better.

I want to thank Dr. Buana Girisuta and Dr. C.B. Rasrendra. You both have inspired me a lot while doing this research. Buana, you are the one who encouraged me to conduct this doctoral study and C.B., you are the one who always came with brilliant inspiring ideas for the research. Many of my studies were improved because of our small chit chat during snack time. Thank you for that, C.B and I wish you all the success with your academic career in ITB.

I want to thank all other present and past people working in the chemical engineering department of the University of Groningen: Angela Kumalaputri, Laura Junistia Wirawan, M. Iqbal, Claudio Toncelli, Miftahul Ilmi, Valeria Zarubina, Anna Piskun, Arjan Kloekhorst, Zheng Zhang, Bilal Niazi, Jan Willem Miel, Teddy Buntara, Boy A. Fachri, Susanti, Martijn Beljaars, Joni Arents, Arne Hommes, Agnes Ardiyanti and the other ex-PhD students who shared good memories with me during my five year PhD time in Groningen.

I would like to thank also all friends and colleagues in the chemical engineering department of the Parahyangan Catholic University: Angela Martina, Susiana Prasetyo, Tony Handoko, Asaf Kleopas Sugih, M. T. Judy Retti B. Witono, Yos Triatmojo, Andy Chandra, Yansen Hartanto, Y. I. P. Arry Miryanti, Pandega, Kevin Wanta and Putri Ramadhani, Hans Kristianto for the support as well as the analysts and technicians in the Chemical Engineering Department of UNPAR who were very supportive during my 1st year PhD study: Asep Suherli, Yana Mulyana, Lusiana Silvia, Heni Saptasari and Lisbet W. Simanjorang.

I would like to thank also my second family in Groningen, the GBI's: Pastor Ika W. Hoogland, Pastor Ronald Wakano and his wife Ida Asyura, Pastor Sandi and his wife Sandra Gunawan, Tante Hanna de Jong, Oom Fred and Tante Tini Berg, Tante Naomi, Tante Asyura, Roga Kembaren, Max and Meta Leuven, Rosalina Wisastra (Ocha), Laura Junistia (Lala) and her husband Jerome Wirawan, Yeni Kuncoro, Yanti, Samuel, Ria, Winarto, Fia Fia and Hartono Lie, Claudya Siahaan and many other GBI's members that cheered up my days in Groningen.

I would also like to give my appreciation to my dear family: my beloved husband, Sien Koen Jeffry Tan, for without your countless support and understanding this thesis would not have been completed. I thank both my parents, dr. Abraham K. Soetedjo and dr. Ginding Seruniwati Lingidjojo, both my foster parents, dr. Toni and dr. Wani Kosan who now already peacefully rest in heaven and my other foster parents, Mr. Vada dan Silvie Subanda. All of you have become role models for me, in term of faithfulness, perseverance and kindness. Thank you for all the prayers and guiding you have given me along my life and that has strengthened my feet in any circumstances. I thank also my brother and sister in law, sister, foster sister, nephews: Ir. Eddie Mulyawan Soetedjo and Lisna Liudy, dr. Nanny Natalia M. Soetedjo, SpPD-KEMD., M. Kes., dr. Maria Riastuti Iryaningrum, Sp.PD-KGH, Christopher and Theofilus for all time support and prayers. My deep thanks to all family in Groningen: my mother in law Thelma Oerlemans Schardiyn, Lizzy and Gerard Mulder, Hedwig

Tan, Francis Tan and my lovely nieces: Laura-Ann and Tessa Mulder with big thanks to Rogert Mulder for all the help and advise regarding the tax. I thank also Ferry MacKenzie and Nini Simon, thank you for the fun we had together before going back to Indonesia, to Bert and Nane Berkhof from Utrecht for the nights we spend there during my NIOK exam and to family Tante Dee Schardijn from Amsterdam for the nice friendship and warm welcome during our visit to Amsterdam.

I thank also my dear friends in the Netherlands: Tante Smith, thank you for accepting me and cheering up my first few months in Groningen, family Ha from Hock Sieng, for our precious lovely moments during Chinese new year and Queen/King's day, Henk, Kitty and George Goudsmith from Omhelzing, the best place for Indonesian satay ever in Groningen, friends from the Waterloo bar: Ellen van der Lee, Esther Groeneweg, Cecile and Rob Hendriks, Enne Hovingh, Jack Stijfhoorn, Erik Wieringa, Lajendra van de Waardt for all the wonderful and fun time we had together. I specially thank and Andy Dipoikromo, Barbara and Anton Tems for the genuine everlasting friendship we have built up.

My deep thanks for my lovely friends from Waroeng Le Cordon, the most beautiful restaurant in North Bandung. I will never forget the warm welcome and wonderful service everytime I come. Thank you so much for your prayers and supports during the finalization of my dissertation: Yuli Magelchant, Wendy Chandra, Ridwan Widjaja, Marcella Octaviany, Lilis Novianti, Utami and any others that I cannot mention one by one here.

And above all, I give thanks to the Lord, for Your everlasting countless love in my life, for all the privileged experiences beyond my limit, for Your trust in me that still amazed me until now. For You have made all impossible things possible and made all dreams come true in my life. Praise the Lord!

LIST OF PUBLICATIONS

Chapter 2:

Tan-Soetedjo, J. N. M.; van de Bovenkamp, H. H.; Abdilla, R. M.; Rasrendra, C. B.; van Ginkel, J.; Heeres, H. J., Experimental and Kinetic Modelling Studies on the Conversion of Sucrose to Levulinic Acid and 5-Hydroxymethylfurfural Using Sulfuric Acid in Water, *Ind. Eng. Chem. Res.*, **2017**.
(doi: 10.1021/acs.iecr.7b01611).

Chapter 3:

van Putten, R.J.; Soetedjo, J. N. M.; Pidko, E. A.; van der Waal, J. C.; Hensen, E. J. M.; de Jong, E.; Heeres, H. J., Dehydration of Different Ketoses and Aldoses to 5-Hydroxymethylfurfural, *ChemSusChem* **2013**, 6 (9), pp 1681–1687.
(doi: 10.1002/cssc.201300345).

Chapter 4:

Soetedjo, J. N. M.; van de Bovenkamp, H. H.; Deuss, P. J.; Heeres, H. J., Biobased Furanics: Kinetic Studies on the Acid Catalyzed Decomposition of 2-Hydroxyacetyl Furan in Water Using Brønsted Acid Catalysts, *ACS Sustainable Chem. Eng.*, **2017**, 5(5), pp 3993–4001.
(doi: 10.1021/acssuschemeng.6b03198).